

AD A 040 135

AFAPL-TR-76-80

DEVELOPMENT OF A CATALYTIC COMBUSTOR FOR AIRCRAFT GAS TURBINE ENGINES

GOVERNMENT RESEARCH LABORATORIES
EXXON RESEARCH AND ENGINEERING COMPANY
LINDEN, NEW JERSEY 07036

DDC
RECEIVED
JUN 3 1977
C

SEPTEMBER 1976

TECHNICAL REPORT AFAPL-TR-76-80
FINAL REPORT FOR PERIOD 22 MAY 1975 - 22 SEPTEMBER 1976

Approved for public release; distribution unlimited

DDC FILE COPY

AIR FORCE AERO-PROPULSION LABORATORY
AIR FORCE WRIGHT AERONAUTICAL LABORATORIES
AIR FORCE SYSTEMS COMMAND
WRIGHT-PATTERSON AIR FORCE BASE, OHIO 45433

14 EXXON/GRU. IBFA. 7

UNCLASSIFIED

SECURITY CLASSIFICATION OF THIS PAGE (When Data Entered)

REPORT DOCUMENTATION PAGE		READ INSTRUCTIONS BEFORE COMPLETING FORM	
1. REPORT NUMBER AFAPL TR-76-80	2. GOVT ACCESSION NO.	3. RECIPIENT'S CATALOG NUMBER	
4. TITLE (and Subtitle) Development of a Catalytic Combustor for Aircraft Gas Turbine Engines.		4. TYPE OF REPORT & DATES COVERED Final Technical Report 22 May 75-22 Sep 76	
5. AUTHOR Vincent J. Siminski Henry Shaw		6. PERFORMING ORG. REPORT NUMBER GRU. IBFA. 76	
6. PERFORMING ORGANIZATION NAME AND ADDRESS Exxon Research & Engineering Company P. O. Box 8 Linden, New Jersey 07036		7. CONTRACT OR GRANT NUMBER(s) F33615-75-C-2033	
8. CONTROLLING OFFICE NAME AND ADDRESS Air Force Aero Propulsion Laboratory Wright-Patterson Air Force Base, Ohio 45433		8. PROGRAM ELEMENT, PROJECT, TASK AREA & WORK UNIT NUMBERS 3048 3048 30480560	
9. MONITORING AGENCY NAME & ADDRESS (if different from Controlling Office)		10. SECURITY CLASS. (of this report) Unclassified	
10. DISTRIBUTION STATEMENT (of this Report) Approved for Public Release; Distribution Unlimited.		11. SECURITY CLASS. (of abstract) Unclassified	
11. DISTRIBUTION STATEMENT (of the abstract entered in Block 20, if different from Report)		12. SECURITY CLASS. (of report) Unclassified	
12. SUPPLEMENTARY NOTES		13. DECLASSIFICATION/DOWNGRADING SCHEDULE	
13. KEY WORDS (Continue on reverse side if necessary and identify by block number) Environmental Pollution Turbine Engine Emissions Combustion		14. DISTRIBUTION STATEMENT (of this Report) Approved for Public Release; Distribution Unlimited.	
14. ABSTRACT (Continue on reverse side if necessary and identify by block number) The pollution problems associated with unburned hydrocarbons and carbon monoxide in the idle mode, and NO _x and smoke production in the power mode of aircraft gas turbine operation can be minimized using hybrid catalytic combustion. A hybrid catalytic combustor consists of a fuel-rich pre-combustor, secondary air quenching zone, and monolithic catalyst stage which rapidly oxidizes CO and UHC produced in the pre-combustor. The concentration of thermally-produced NO _x in the pre-combustor is very low		15. DISTRIBUTION STATEMENT (of this Report) Approved for Public Release; Distribution Unlimited.	

391 338 ET

UNCLASSIFIED

SECURITY CLASSIFICATION OF THIS PAGE (When Data Entered)

20. because of the lack of oxygen. However, the formation of NO_x precursors such as HCN and NH_3 produced under fuel rich conditions must be considered. Data showed that nitrogenous species produced in the rich pre-combustion zone were efficiently converted to NO_x by catalysts under the very lean mixture conditions that result from the secondary air quench. The equivalence ratio in the pre-combustor was varied from 0.5 to 1.5, while the overall mixture, after secondary air injection, was in the range of 0.1 to 0.3.

The noble metal catalysts on various monolithic support geometries and compositions were found to be the most active materials for CO and UHC oxidation in the temperature range of 700-1200 K. The combustion efficiency of the hybrid catalytic combustor for JP-4, which contained 535 ppm sulfur, was determined to be 99.5% under realistic operating conditions. The combustor pressure drop was less than 6%. The average emission indices of CO, UHC and NO_x leaving the HCC were on the order of 0.95, 0.43 and 1.8 g/kg of fuel, respectively, for a metal supported Pt catalyst. This catalyst was effective in reducing CO by 86% and UHC by 94%, and increasing NO_x by 68%. Using approximate methods for estimating the EPA emission parameters, it was determined that the hybrid catalytic combustor can meet the 1981 new aircraft emission standards.

Based upon these encouraging results, two 7.6 cm diameter hybrid catalytic combustors were fabricated and delivered to the Air Force for further evaluation.

UNCLASSIFIED

SECURITY CLASSIFICATION OF THIS PAGE (When Data Entered)

TABLE OF CONTENTS

	PAGE
I. SUMMARY	1
II. INTRODUCTION	3
III. EXPERIMENTAL FACILITIES AND PROCEDURES	6
1. Hybrid Catalytic Combustor	6
2. Flow Characteristics of the Pre-Combustor	6
3. Fuel Injection System	10
4. Air Supply System	10
5. Temperature Measurements	12
6. Gas Sample Measurements	13
7. Gas Analysis Instrumentation	15
IV. RESULTS	19
1. Operation in the All-Catalytic Mode	19
2. Combustion Characteristics of the Pre-Combustor	20
3. Description of Candidate Catalyst	29
4. Methods of Preparing Catalysts for Testing	35
5. Pressure Drop Characteristics of Supports	36
6. Effects of S/V on Conversion	39
7. Effects of Substrate Material on CO and UHC Conversions	41
8. Effects of Wash Coat Materials on CO and UHC Conversions	44
9. The Effects of Catalyst Formulation on CO, UHC and NO _x Conversions	45
10. The Temperature Dependency of Catalyst Activity For UHC and CO Conversion and NO _x Production	48
11. The Effect of Bed Length and Temperature on Conversions	70
12. The Results of a 20 Hour Durability Test of Catalysts QF and KQ	73
13. Methods for Determining Combustion Efficiency and The Emission Index of Exhaust Products	77
a. Emission Index of CO, UHC and NO _x	77
b. Combustion Efficiency	78
c. Material Balance Calculations	78
V. DISCUSSION	80
VI. DESIGN OF 7.6 CM DIAMETER COMBUSTORS	86
1. Design and Fabrication of Combustors for Large Scale Testing	86
2. Preliminary Hazards List	89
a. System Environmental Constraints	89
b. Pressure Vessels and Plumbing	90
c. Safe Operation and Maintenance of the System	90
d. Fire Ignition and Propagation Sources	90
e. Resistance to Shock Damage	90

TABLE OF CONTENTS (CONT'D)

	PAGE
VII. CONCLUSIONS AND RECOMMENDATIONS	92
APPENDIX I - DESCRIPTION OF SUPPORT GEOMETRY AND MATERIALS	94
APPENDIX II - CATALYST DESCRIPTION	98
APPENDIX III - SUMMARY OF EMISSION INDEXES AND COMBUSTION EFFICIENCIES125
REFERENCES152

LIST OF ILLUSTRATIONS

FIGURE		PAGE
1	Schematic Drawing of the Hybrid Catalytic Combustor . . .	7
2	Photograph of the Assembled Combustor	8
3	Compressed Air and Fuel Supply	11
4	Combination Gas Sample and Temperature Probe	14
5	Portable Gas Analysis System	16
6	Piping Schematic of the Gas Sample System	17
7	Axial Concentration Profiles of NO _x and Hydrocarbons in an Empty Catalyst Chamber	25
8	Varying Secondary Air Split on Temperature and Unburned Hydrocarbons at the Catalyst Bed Inlet (ϕ Overall = 0.3)	26
9	Axial Centerline Temperature of Catalyst for Overall ϕ = 0.3	27
10	Isothermal Pressure Drop Characteristics of Monoliths . .	37
11	The Effect of Support Surface/Volume Ratio on Conversion With a Constant Noble Metal Loading in the Reactor	40
12	Arrhenius Plot of CO and UHC Oxidation on Pt/Pd (1/1) Catalysts of Different Geometries	42
13	Comparison of CO Conversion with UHC Conversion	47
14	Effects of Catalyst Inlet Temperature on CO, UHC and NO _x Conversion Over Catalyst GH	49
15	Effects of Catalyst Inlet Temperature on CO, UHC and NO _x Conversion Over Catalyst JH	50
16	Effects of Catalyst Inlet Temperature on CO, UHC and NO _x Conversion Over Catalyst FH	51
17	Effects of Catalyst Inlet Temperature on CO, UHC and NO _x Conversion Over Catalyst KQ	52

LIST OF ILLUSTRATIONS (CONT'D.)

FIGURE		PAGE
18	Effects of Catalyst Inlet Temperature on CO, UHC and NO _x Conversion Over Catalyst KQ	53
19	Effects of Catalyst Inlet Temperature on CO, UHC and NO _x Conversion Over Catalyst KR	54
20	Effects of Catalyst Inlet Temperature on CO, UHC and NO _x Conversion Over Catalyst RA	55
21	Effects of Catalyst Bed Inlet Temperature on CO, UHC and NO _x Conversion Over Catalyst KU	56
22	Effects of Catalyst Inlet Temperature on CO, UHC and NO _x Conversion Over Catalyst MQ (1/2 length)	57
23	Effects of Catalyst Inlet Temperature on CO, UHC and NO _x Conversion Over Catalyst KQ & MQ in Series	58
24	Effects of Catalyst Inlet Temperature on CO, UHC and NO _x Conversion Over Catalyst KQ & FH in Series	59
25	Effects of Catalyst Inlet Temperature on CO, UHC and NO _x Conversion Over Catalyst FZ	60
26	Effects of Catalyst Inlet Temperature on CO, UHC and NO _x Conversion Over Catalyst FV	61
27	Effects of Catalyst Inlet Temperature on CO, UHC and NO _x Conversion Over Catalyst JG	62
28	Effects of Catalyst Inlet Temperature on CO, UHC and NO _x Conversion Over Catalyst FG	63
29	Effects of Catalyst Inlet Temperature on CO, UHC and NO _x Conversion Over Catalyst FY	64
30	Effects of Catalyst Inlet Temperature on CO, UHC and NO _x Conversion Over Catalyst QF (13.25 cm Length)	65
31	Effects of Catalyst Inlet Temperature on CO, UHC and NO _x Conversion Over Catalyst PC & FL in Series	66
32	Effects of Catalyst Inlet Temperature on CO, UHC and NO _x Conversion Over Catalyst FD & FE in Series	67
33	Effects of Catalyst KQ Length and Inlet Temperature on CO Conversion	71

GPO : 1968 O - 348-000

LIST OF ILLUSTRATIONS (CONT'D.)

FIGURE		PAGE
34	Effects of Catalyst KQ Length and Temperature on UHC and NO _x Conversion	72
35	Twenty-Hour Test of Catalyst QF at 1200 K	74
36	Twenty-Hour Test of Catalyst KQ at 1200 K	75
37	Effects of Catalyst Aging at 1200 K on NO _x Concentration Change	76
38	NO _x Equilibrium in JP-4 Combustion	82
39	Schematic of a 7.6 cm Diameter Hybrid Catalytic Combustor	87
40	Photograph of HCC Components	88

LIST OF TABLES

TABLE	PAGE
I Instruments Used for Gas Analysis	15
II Aircraft Operating Parameters and Equilibrium Gas Composition	20
III Flow Characteristics in the Hybrid Catalytic Combustor . .	22
IV Axial Temperature and Combustion Products Distribution in Empty Catalyst Combustion Chamber (Dry Basis)	24
V Equilibrium Composition of Products From JP-4 Combustion With Air at 300 kPa	28
VI Relationship Between Combustion Mixtures and Temperature in the Pre-Combustor	29
VII Relative Catalyst Activities for Overall $\phi = 0.28-0.30$ at 376 kPa and 25.8 m/s Reference Velocity (Catalyst Length = 20.3 cm)	32
VIII The Effects of Catalyst Loading and Support Surface Area on UHC and CO Conversion	39
IX Wash Coat Compositions	44
X Effect of Noble Metal Composition on Oxidation Activity . .	46
XI Comparison of HCC Effluents with EPA 1981 New Aircraft Limitations	81
XII Emissions from Hybrid Combustor	84
XIII General Refractories Supports	94
XIV W. R. Grace Supports	95
XV Norton Supports	95
XVI Nippon Sealol Supports	96
XVII DuPont Supports	96
XVIII Johnson-Matthey Supports	97
XIX Matthey-Bishop Supports	97

CONVERSION FACTORS - SI TO ENGLISH UNITS

	<u>SI (metric)</u>	<u>English System</u>
Length	m	3.28 ft
Area	m ²	10.76 ft ²
	ha	2.47 acres
Volume	m ³	6.29 bbl (42 gal)
	m ³	35.31 ft ³
Mass	kg	2.20 lb
	t	1.10 US ton
Pressure	kPa = kN/m ²	0.145 lb/in ²
	kPa	4.02 in H ₂ O (60°F)
	kPa	0.296 in Hg (60°F)
Temperature	°C	1.8 (°C + 32)°F
	K	1.8 °F
Energy	kJ	0.948 Btu
	MJ	0.373 hp·h
Power	W	3.41 Btu/h
	kW	1.34 hp

SI Prefixes

<u>Factor</u>	<u>Symbol</u>
10 ¹²	T
10 ⁹	G
10 ⁶	M
10 ³	k
10 ²	h
10 ⁻¹	da
10 ⁻²	d
10 ⁻³	c
10 ⁻⁶	m
10 ⁻⁹	μ

LIST OF ABBREVIATIONS AND SYMBOLS

- $(A/F)_g$ = Stoichiometric air to fuel ratio by weight.
- $(A/F)_o$ = Operating air to fuel ratio by weight.
- Cycle = LTO Cycle.
- Ei_1 = Emission index of component i in g of i /kg fuel.
- $$= X_i \frac{(MW)_i}{(MW)_{flue}} (1 + \frac{(A)}{(F)}_o) 1000.$$
- $EPAP_1$ = EPA emissions parameter of component i = mg/N.h.cycle.
- LTO
- $$= \sum_{mode} EI_{i, mode} \times SFC_{mode}$$
- = Sum of mass of i per mode for each mode
Sum of the work output of each mode
- L/D = Length to diameter ratio.
- LTO = Landing and Take-Off Cycle.
- $(MW)_i$ = Molecular weight of component i .
- Mode = Part of LTO Cycle i.e., taxi/idle (out), take-off, climbout, approach, or taxi/idle (in).
- N = Newton = 1 kg m/s².
- P = Pressure in kPa.
- SFC = Specific fuel consumption in g fuel/h.N thrust.
- S/V = Surface to volume ratio in m⁻¹.
- V_R = Reference velocity at 400 K and 375 kPa in m/s.
- V_S = Space velocity = volumetric flow/volume of catalyst = V/V/h.
- t = Time in seconds.
- T = Temperature in K.
- X_i = Mole fraction of component i .
- ϕ = Equivalence Ratio = $(A/F)_g / (A/F)_o$.

SECTION I

SUMMARY

The Environmental Protection Agency emissions standards for subsonic turbofan or turbojet aircraft engines manufactured on or after January 1, 1981 of 35.6 kN thrust or greater cannot be satisfied by current designs. NO_x emissions are difficult to control during high power operation when the near stoichiometric flame conditions in the combustor produce copious quantities of nitrogen oxides from the oxidation of atmospheric nitrogen. CO and UHC emissions are low because of the high combustion efficiency obtained during the high power condition. During engine idle conditions, the production of nitrogen oxides is generally no problem, but because of lowered combustion efficiencies, the CO and UHC emissions become unacceptable.

Of the numerous combustion schemes proposed during the past few years, one of the most promising techniques demonstrated to be effective in reducing NO_x , CO and UHC emissions is catalytic combustion. The Air Force recently showed that very high combustion efficiencies, in the order of 99.5% without the concomitant production of nitrogen oxides, were feasible under high power conditions. It should be pointed out that methods which may not be applicable to actual aircraft combustors were used to mix the air and fuel, and bring the catalyst to operating temperature. Special equipment would be needed in an aircraft engine to bring the catalyst to operating temperature prior to engine start-up. Also, the successful utilization of catalytic combustion techniques under low power or idle conditions has not been demonstrated.

In order to overcome the apparent difficulties with the "all catalytic" combustion of premixed fuel and air and not significantly increase the emissions of pollutants, a new technique was tested in which less than 75% stoichiometric air is used to oxidize the fuel in a conventional pre-burner and the rest of the air is rapidly mixed in after combustion to quench the reaction and reduce the gas temperature to a level that can be tolerated in the gas turbine. This technique has the theoretical potential of oxidizing the unburned hydrocarbons and CO in the post-combustion zone without adding significant quantities of NO_x . Since it may be difficult to control the oxidation of reducing species in the quench zone, a catalyst could be used to accelerate the oxidation of these species. Thus, such a technique may be considered to operate in a hybrid mode i.e., homogeneous combustion followed by catalytic combustion. Hybrid catalytic combustion thus provides a method of fulfilling the pollution control requirements without the need of special equipment to heat the catalyst or premix liquid fuel with hot air.

The feasibility of the hybrid catalytic combustion concept, as applied to aircraft gas turbine combustors operating over the entire landing and take-off cycle air-fuel ratios, was demonstrated in this laboratory program. The air temperature was maintained at 400 K in the experimental work presented here and is thus representative of idle operation. An air temperature of 775 K would have been required to simulate full power operation (takeoff).

The hybrid catalytic combustion technique tested in this program consisted of pre-burning JP-4 in a conventional can-type combustor under rich conditions, followed by the injection of secondary air to quench the chemical reactions and lower the temperature. The unburned CO and UHC were then completely oxidized over a monolithic catalyst located at the exit of the combustor.

Of the more than 35 different catalysts obtained from manufacturers that were evaluated, the noble metals supported on honeycomb structures were found to be the most active for converting CO and UHC. Conversions in the range of 90-95 percent were achieved at catalyst temperature of 1200 K, overall equivalence ratios of 0.3 and air preheat temperatures of 400 K. Base metal oxides and rare earth oxides on cordierite supports were much less active than the noble metals on the same supported geometry.

The most satisfactory catalyst evaluated consisted of a corrugated and rolled metal support, washcoated with stabilized Al_2O_3 , and impregnated with 5.3 kg/m^3 platinum. This catalyst achieved combustion efficiencies of 99.8 percent over the temperature range of 1000-1200 K. The reference velocity at the catalyst inlet was 25 m/s. During a 20-hour test at 1200 K, the metal supported catalyst did not show any indications of activity loss for CO or UHC conversions. Under the same circumstances, a cordierite supported palladium catalyst lost a substantial amount of its initial activity after 10 hours of operation.

As a result of this research, it appears that an efficient, low emissions hybrid catalytic combustor can be developed to operate over the entire range of gas turbine power settings from idle to full power. It should be noted that the hybrid catalytic combustor approach is not limited to idle operation, but can indeed operate effectively at full power, as demonstrated by operating the combustor at $\phi = 0.3$. No attempt was made to determine how an engine using a hybrid catalytic combustor system would operate over the LTO cycle. The feasibility of using the hybrid catalytic combustor for idle operation followed by an all catalytic high power mode is currently being considered by the Air Force. It must be emphasized that actual engine tests must be conducted to fully assess the feasibility of the hybrid catalytic combustor concept.

Based upon the results of the catalyst screening program, two complete hybrid catalytic combustors capable of 300 g/s air flow were designed and fabricated for delivery to the Air Force for testing. It is estimated that these slightly scaled-up versions of our laboratory test combustor will achieve a minimum combustion efficiency of 99.5% at idle, and NO_x , CO, and UHC emissions that will probably meet the 1981 EPA aircraft emission standards.

Although the results presented here support the technical feasibility of catalytic combustion for aircraft turbine engines, there remain many practical problems which must be considered. The most significant problems involve the physical durability of the catalyst and the transient response in flight. Clearly, a catalyst that could fracture or spall in flight could damage the turbine and endanger those on-board. Other considerations associated with engine response and operability in flight must be carefully analyzed.

SECTION II

INTRODUCTION

Current aircraft engine designs are not expected to meet the EPA emissions specifications for subsonic turbofan or turbojet aircraft engines manufactured on or after January 1, 1981 of 35.6 kN thrust or greater (1). These designs produce excessive concentrations of CO (carbon monoxide) and UHC (unburned hydrocarbons) during the idle mode, and NO_x (nitrogen oxides) and possibly smoke during the high power mode (2). Poor combustion efficiency under idle conditions due to poor air-fuel mixing is the source of CO and UHC, while very high flame temperatures generated near stoichiometric combustion during the high-power mode give rise to high concentrations of thermally produced NO_x and smoke. In all existing gas turbine combustors, a portion of the air supply is utilized in the primary combustion zone with a near-stoichiometric quantity of fuel. Successive addition of combustion air in the secondary and quench zones of the combustor reduces the gas temperature to acceptable turbine inlet values. The turbine firing temperature limitation is dictated by structural considerations. The equivalence ratio (ϕ)¹ of the turbine inlet mixture is in the range of 0.25-0.35 in the high power mode. In the idle mode, the ϕ at the turbine inlet mixture is approximately 0.15.

Most proposed solutions for the reduction of gas turbine emissions of pollutants retain the basic gas turbine multi-combustion zone concepts, but alter the methods in which the fuel and air, or both, are introduced into the primary combustion zone. More efficient fuel atomization and primary zone mixing have been shown to effectively reduce CO and UHC emissions under idle conditions, but have not substantially affected the NO_x problem at high-power conditions. The most promising combustor modifications for high-power operation consist of pre-vaporizing and premixing the fuel so that stable and efficient fuel-lean combustion occurs at somewhat lower adiabatic flame temperatures, thus producing lower concentrations of thermal NO_x. Problems that must be solved before the pre-vaporization and premixing technique can be introduced into production engines include:

1. The premature autoignition of the mixture during the high-power mode where air compressor discharge temperatures and pressures may be 900 K and 3.0 MPa, respectively.
2. The thermal decomposition of the fuel in the vaporization system may lead to the formation of carbonaceous deposits on the walls which would alter the heat transfer properties of the metal, and possibly cause thermal failure of the vaporizer.
3. The satisfactory operation of the vaporizer may be interrupted by flashback where high flame temperatures could damage the vaporizer-mixing section of the combustor.

¹ See Nomenclature pg. x for definition.

In order to explore the feasibility of catalytic combustion in aircraft gas turbine combustors, the Air Force initiated a program at the AFAPL (Air Force Aero Propulsion Laboratory). It determined the combustion efficiency to be in excess of 99.5% and the production of NO_x to be well below that required to meet the 1981 EPA specifications for new aircraft under test conditions which simulated high-power operation (3). Similar data were obtained by others working with gaseous fuels (4). These initial studies did not investigate catalytic combustion under simulated idle operation. The lack of data for idle conditions prompted the Air Force to award Exxon Research and Engineering Company a research program to obtain the experimental data necessary to evaluate catalytic combustion at gas turbine idle conditions. The general criteria for developing an acceptable combustor were:

1. The total pressure drop through the combustor should not exceed 6% of the operating pressure of 0.3 MPa at a reference velocity of about 25 m/s.
2. The minimum combustion efficiency at gas turbine idle should be 99.5%.
3. The CO, UHC and NO_x emissions should be within the EPA emission specifications for subsonic turbofan or turbojet aircraft engines manufactured on or after January 1, 1981 of 35.6 kN thrust or greater (1).
4. The heat release rate of the combustor should be on the order of $1 \text{ kJ/Pa}\cdot\text{s}\cdot\text{m}^3$.
5. The total volume of the catalytic combustor and associated premixing, pre-vaporization or pre-combustion components should not exceed the volume of a conventional aircraft turbine engine having a comparable heat release rate.

The program was divided into three phases. Phase I consisted of a thorough review of the literature concerning catalytic oxidation of hydrocarbons and an assessment of the state-of-the-art in catalyst preparation on monolithic ceramic, refractory material, or metallic supports capable of high temperature operation.

The second phase was concerned with the experimental determination of the effectiveness of commercially available catalysts in promoting JP-4 ignition with 400 K preheated air to simulate idle operation in the absence of any pre-combustion scheme. If, as was expected, no catalysts were found that had sufficient activity at 400 K to initiate the combustion reactions, then the remainder of the second phase would be concerned with the design and characterization of a pre-burner which, when coupled to a fixed catalyst bed, would make up the HCC (hybrid catalytic combustor). After the operating characteristics of the combustors were determined, a three-part catalyst screening program started. Part One ranked catalyst activity as a function of temperature and surface/volume ratio of seven different Pt/Pd catalysts deposited on a single substrate composition of varying geometry. Part Two evaluated various substrates and high surface

area wash coat materials on which noble metals, base metals, rare earths, etc., had been deposited. The most promising catalysts were studied in greater detail in Part Three in order to choose the catalysts most applicable in the hybrid mode of operation. The total number of experimental test hours exceeded 100, and the number of catalyst-substrate combinations tested was in excess of 35. The two best catalysts were subjected to a 20-hour durability test at 1200 K to determine the extent of catalyst deactivation under high velocity and high temperature operation.

The third phase of the program was directed at the design and fabrication of a set of 7.6 cm diameter catalytic hybrid combustors containing the best catalysts found in Phase Two for delivery to AFAPL. Extensive testing of the catalytic hybrid combustors under simulated idle and high-power conditions are planned by AFAPL.

SECTION III

EXPERIMENTAL FACILITIES AND PROCEDURES

The experimental equipment used in this study included a specially designed combustor, fuel injection system, air supply system, sampling and analytical system, and temperature and pressure instrumentation. Information on the design and calibration of this equipment is provided in this section.

1. HYBRID CATALYTIC COMBUSTOR

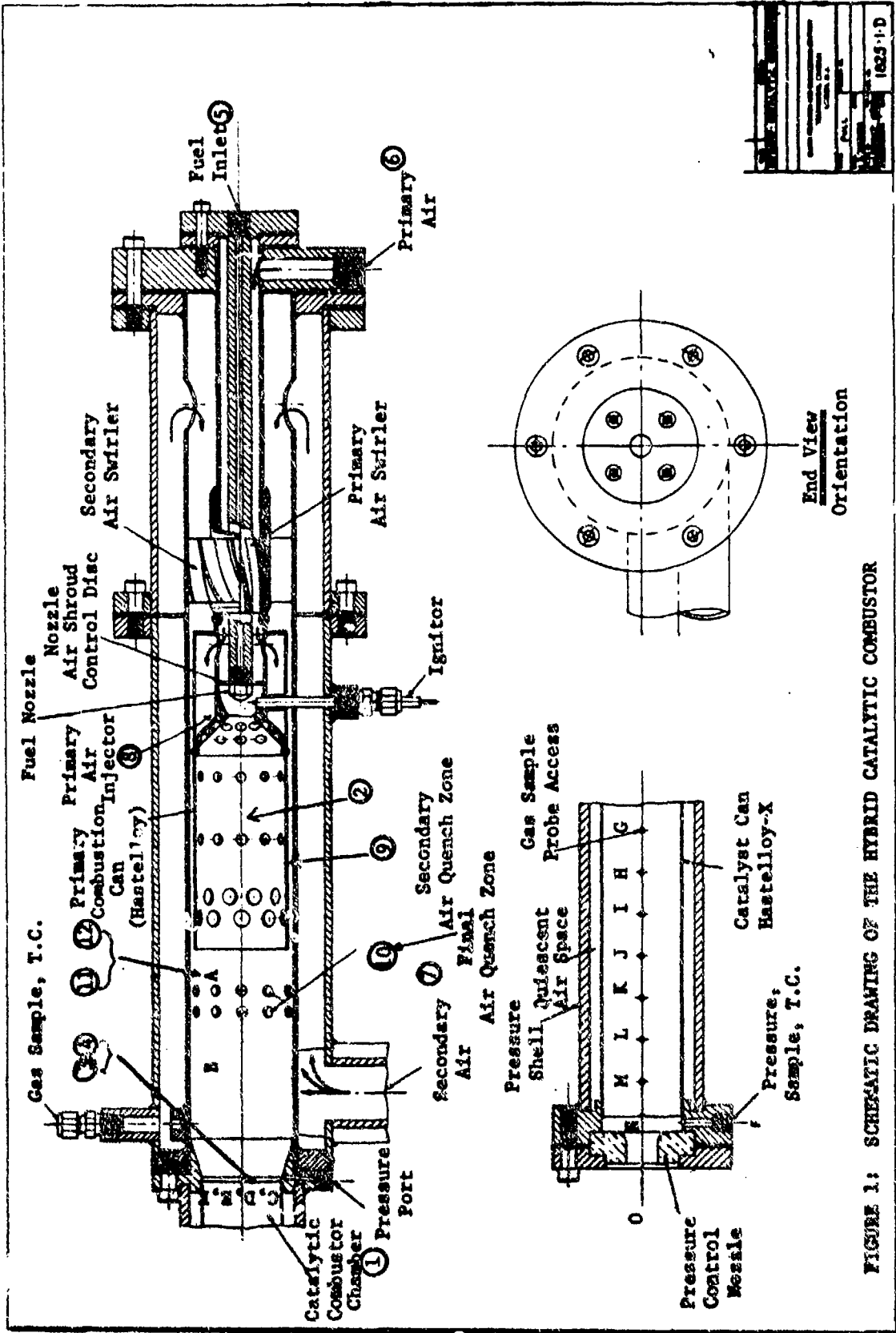
A schematic diagram of the hybrid catalytic combustor is shown in Figure 1, and a photograph of the experimental arrangement is shown in Figure 2. The combustor consisted of a conventional cannular pre-combustor followed by a catalytic combustion chamber. The components which made up the pre-combustion section consisted of a primary combustion air swirler, secondary air swirler, pressure atomizing fuel nozzle, ignition electrode, and primary, secondary and quench air injection orifices. The pre-burner components were constructed out of type 304 stainless steel, except for the combustor can which was fabricated from 0.033 cm Hastalloy-X sheet. The can was rolled into a cylinder 5.08 cm in diameter by 11. cm long.

The catalytic combustor chamber which was fabricated from type 304 stainless steel, was bolted onto the pre-burner section so that it could be easily and quickly disassembled without disturbing the pre-combustion section of the combustor. The catalyst candidates were contained in a Hastalloy-X thin wall cartridge (0.033 cm thick x 21.6 cm long x 5.08 cm diameter) which was inserted into the heavy wall catalyst combustion chamber. Channeling of the hot gas flow in the catalyst combustion chamber was prevented by metal to metal pressure seals located at both ends of the thin wall catalyst cartridge. An annular space between the Hastalloy-X cartridge and the heavy pressure-bearing wall of the catalyst combustion chamber, reduced the conductive heat losses in this section of the hybrid combustor.

The combustor pressure was controlled by the combination of a 3.8 cm diameter, type 310 stainless steel, square edge orifice located at the discharge end of the catalyst combustion chamber, and a remotely operated, eccentric plug valve located at the discharge end of a multi-tube countercurrent heat exchanger which cooled the hot combustion gases to 530 K. The HCC exhaust temperatures were typically in the range of 800-1300 K.

2. FLOW CHARACTERISTICS OF THE PRE-COMBUSTOR

Figure 1 shows that the combustion air supply to the HCC was split into three different paths. The total air flow rate through the combustor was maintained at 133 g/s. Of this total flow rate, 27 g/s went to the primary zone (location 8), 66 g/s were used in the secondary zone (location 9), and the remaining 40 g/s (location 1) were used in the final quench. The reference velocity at the catalyst chamber inlet was 25.8 m/s (400 K and 379 kPa).



BEST AVAILABLE COPY



FIGURE 2: PHOTOGRAPH OF THE ASSEMBLED COMBUSTOR

The percent of the total air-flow area in each of the three flow streams which determined the air flow rates were:

<u>Primary Air</u>	<u>% Distribution of Air Flow Area (21.9 cm²)</u>
25 holes, 0.254 cm diameter	5.8
0.0762 cm annular gap around fuel injector	3.2
<u>Secondary Air</u>	
0.635 cm annular gap around can	53.0
26 quench holes, 0.635 cm diameter	<u>38.0</u>
Total	100.0

The secondary air distribution holes in the 5.08 cm diameter Hastelloy-X can attached to the primary air injector consisted of four rows of different diameter holes located at various axial distances from the primary air injector. The hole sizes, axial locations measured in L/D (length to diameter) and their relative areas were:

<u>L/D (location)</u>	<u>No. of Holes</u>	<u>Hole Diameter (cm)</u>	<u>% Total Hole Area of Can</u>
0.168	12	0.553	13.8
0.484	12	0.635	18.2
0.754	10	0.952	34.0
0.846	10	0.952	<u>34.0</u>
Total			100.0

The gas velocities in each of the three air flow paths were calculated from the air flow rates at operating conditions (P = 379 kPa, T = 400 K)

<u>LOCATION IN COMBUSTOR</u>	<u>VELOCITY (m/s)</u>
<u>Primary Air Zones</u>	
0.076 cm annular gap around fuel nozzle air shroud	22.5
0.254 cm diameter primary injector hole	65.7
<u>Secondary Air Zones</u>	
0.635 cm annular gap around primary combustion can	22.5
0.635 cm diameter quench air hole	17.0
<u>Reference Velocity at Catalyst Chamber Inlet</u>	
5.08 cm diameter catalyst	25.8

3. FUEL INJECTION SYSTEM

JP-4 was injected at ambient temperature into the pre-combustor through a $3.15 \text{ cm}^3/\text{s}$ pressure atomizing swirl nozzle that had a 1.4 rad (80 degree) solid spray angle. The flow of a fraction of the primary air around the air shroud control disc provided a suitable fuel-air mixture in the area of the ignition electrode that was conducive to good ignition characteristics. The flow of air around the fuel injector tip also provided nozzle cooling. The electrical breakdown of the gap between the fuel nozzle and the ignition electrode tip by a 10 kV alternating current transformer initiated the combustion of the fuel in the pre-combustor. A 1.4 rad (80 degree) spray nozzle was chosen so that the spray fan would not impinge upon the central orifice walls of the primary air injector.

Efficient mixing and flame stabilization of the fuel-air mixture was assured by the high velocity swirling motion imparted to the air flow by virtue of the 0.7 rad (40 degree) angle (with respect to the longitudinal axis) at which the holes were drilled into the face of the air injector.

The fuel was pumped from a shipping container into two 0.019 m^3 pyrex containers. The volumes of the glass containers were calibrated and divided into 500 cm^3 graduations on the outside of containers. A suction-pressure gear pump was used to withdraw the fuel from the containers and expel it through the pressure atomizing nozzle. Approximately 90% of the fuel was recirculated to the glass containers. The pump pressure could be varied to 3.1 MPa, but for the purposes of this study the pressure was maintained at 1.3 MPa. A rotameter in the stainless steel fuel system located between the gear pump and the pressure atomizing nozzle was utilized to monitor the fuel flow rate. Appropriate metering valves were located upstream and downstream of the rotameter to provide constant pressure and fuel flow. A 20-micron sintered bronze filter was located in the fuel line. The Δp across the atomizing fuel nozzle was always maintained at 1.1 MPa to assure critical flow conditions which prevented any fluctuations in the fuel flow due to combustion chamber pressure fluctuations.

The fuel rotameter and pressure atomizing nozzle were calibrated by weighing the amount of fuel collected over a specified period of time at each rotameter setting. Periodically, the calibration of the fuel system was checked by observing the volume of fuel displaced from the gas reservoirs during a test firing for a given fuel rotameter setting and time interval.

4. AIR SUPPLY SYSTEM

A schematic diagram of the rate of air input to the combustor is given in Figure 3. Compressed air was supplied at a $70.8 \text{ dm}^3/\text{s}$ with a 1.034 MPa air compressor which was equipped with oil, water and particulate filters.

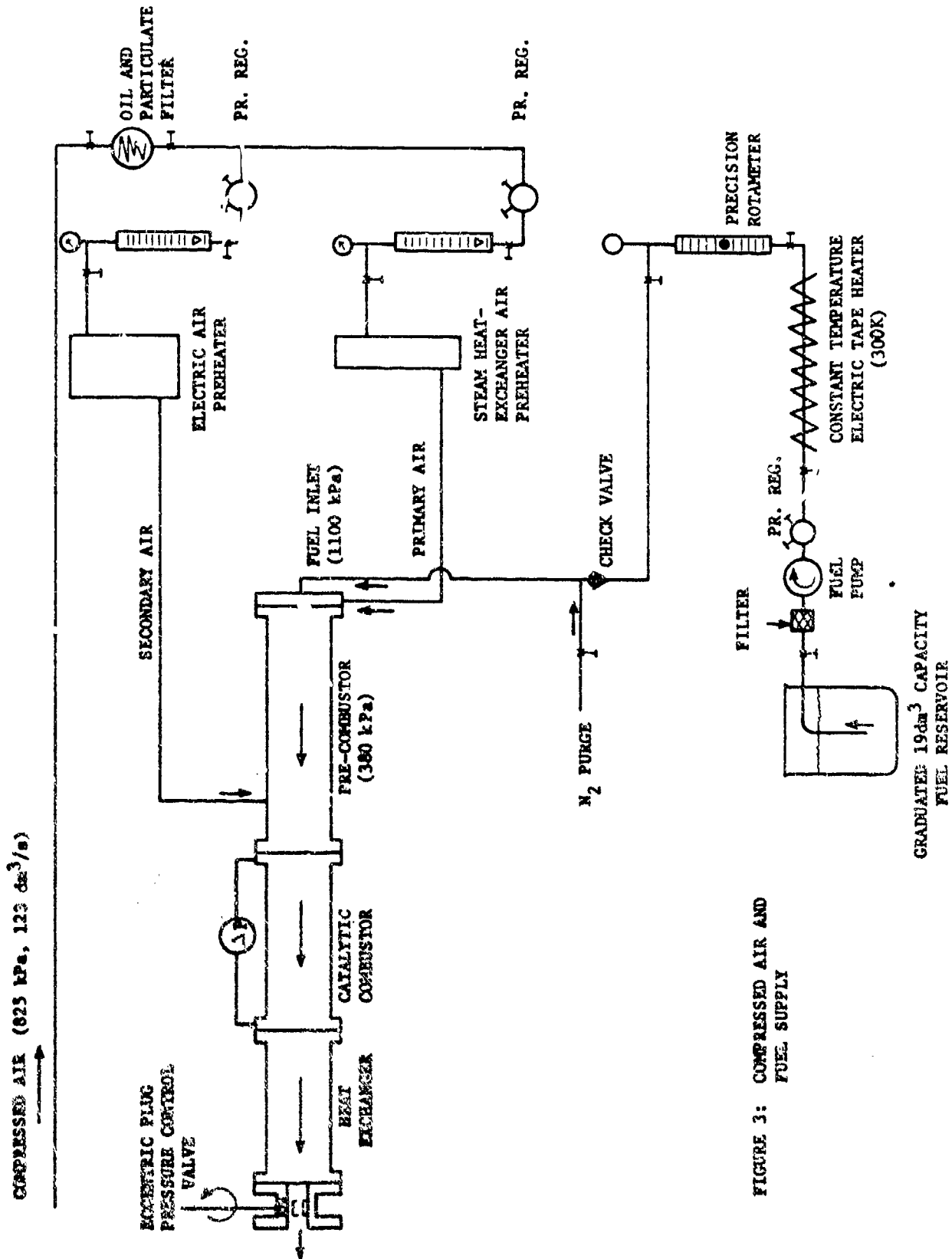


FIGURE 3: COMPRESSED AIR AND FUEL SUPPLY

The main air supply was divided into primary and secondary air systems. Each air system had its own pressure regulator, preheater and rotameter. The flow of air through each system was controlled by globe valves located in the air line at either end of the rotameters. Bourdon-tube pressure gauges and iron-constantan thermocouples were located in the air system lines downstream of the rotameters. A 30 kW electrical heater was used to preheat the secondary air to a maximum of 560 K, and a high pressure steam heat exchanger was used to preheat the primary air to a maximum of 420 K. The rotameters used to measure the air flow rate were calibrated with wet and dry test meters, depending upon the magnitude of the air flow rates. The calibrations were periodically checked to assure the accuracy of the rotameters. The temperature and pressure of the air in the metering system were continuously recorded and utilized in the calculation of the total air flow rates. The pressure of the primary and secondary air rotameters was maintained at 450 kPa, while the combustion chamber pressure was 379 kPa.

5. TEMPERATURE MEASUREMENTS

The determination of the axial and radial temperature profiles, and chemical concentrations throughout the hybrid combustor was accomplished with a specifically designed analytical gas sampling train and multi-probe thermocouple and gas sample rakes. The equipment and procedures utilized in the course of the study for temperature measurement are described below.

The gas temperatures in the pre-combustion and catalytic sections of the hybrid combustor were taken at various locations identified in Figure 1. Chromel-alumel dual-junction thermocouples with either 0.317 cm or 0.157 cm diameter stainless steel sheaths were located at positions A, B and C in the pre-burner section. Temperatures within the catalyst (locations G-M) were determined with 0.063 cm diameter inconel sheathed chromel-alumel thermocouples located at 2.54 cm intervals along the length of the 20.32 cm long catalyst section. The tips of all the thermocouples in the pre-combustion stage and the catalyst stage were positioned on the centerline of the hybrid combustor.

When radial gas temperature distributions were obtained in the pre-combustion section, the single thermocouple located at position C was removed and replaced with four 0.157 cm diameter thermocouples which were mounted in a 0.635 cm diameter stainless steel tube. The 0.635 cm tube provided a pressure seal at the outside wall of the pre-combustor. The tips of the four parallel thermocouples were separated from each other by 1.27 cm. The tips of the longest thermocouple and shortest thermocouple were 0.635 cm from the inside walls of the pre-combustion chamber. The four gas temperatures measured simultaneously by the thermocouples were recorded on a multi-point strip chart recorder.

6. GAS SAMPLE MEASUREMENTS

The gas sample and temperature probes utilized in the catalyst section of the hybrid combustor were designed so that simultaneous determinations of gas temperature and composition could be obtained with a minimum of interference to the gas flow within the cellular catalysts. A schematic drawing of the probe is shown in Figure 4. A 0.063 cm diameter thermocouple was concentrically located within the 0.157 cm internal diameter inconel tube with the tip of the thermocouple just slightly below the end of the inconel tube. This configuration provided protection for the fragile thermocouple, and simultaneously allowed the gas sample to be taken through the annular gap between the thermocouple and the inconel tube. The tips of the inconel tubes were located on the centerline of the catalyst and were spaced at 2.54 cm intervals along the longitudinal axis. Seven 0.203 cm diameter holes were carefully drilled into the catalyst substrate after the catalysts were installed within the Hastelloy-X catalyst container. Mating holes in the Hastelloy-X catalyst container and the catalyst chamber wall allowed the gas sampling probes to be inserted into the catalyst combustion chamber in locations G through M as shown in Figure 1. The insertion of the probes into the catalysts in this manner assured that the measured temperature was the gas stream temperature and not the surface temperature of the substrate material. The walls of the gas sample tube shielded the thermocouple from the radiation emitted from the solids, thereby eliminating the need for a radiation correction on the measured temperatures. The gas sample obtained by each probe was, because of the parallel wall nature of cellular catalyst substrate materials, representative of the particular cell from which the sample was obtained.

Radial profiles of combustion product concentrations were obtained at the inlet and outlet of the catalyst combustion chamber with gas sample rakes, each of which had four separate probes. The 4 parallel probes on each rake were 0.152 cm outside diameter thin-wall stainless steel tubes. The four tubes were soldered together into a 0.635 cm diameter thin-wall tube in a manner so that the pressure seal at the wall of the combustor could be made around the 0.635 cm tube. As in the design of the multi-thermocouple rake discussed previously, the tips of the gas sample tubes were staggered so that the four parallel probe tips were evenly distributed across the diameter of the combustion chamber at the inlet end and the discharge end of the catalyst.

The gas samples from each of the four probes in a rake could be examined separately, or as was the case in determining combustion efficiencies of the catalysts, combined in a manifold located in the gas sample train so that an average concentration would be obtained. The radial concentration distribution of combustion products was determined by analyzing the gas sample from each of the four probes during a test where the combustion conditions were maintained at fixed air and fuel flow rates.

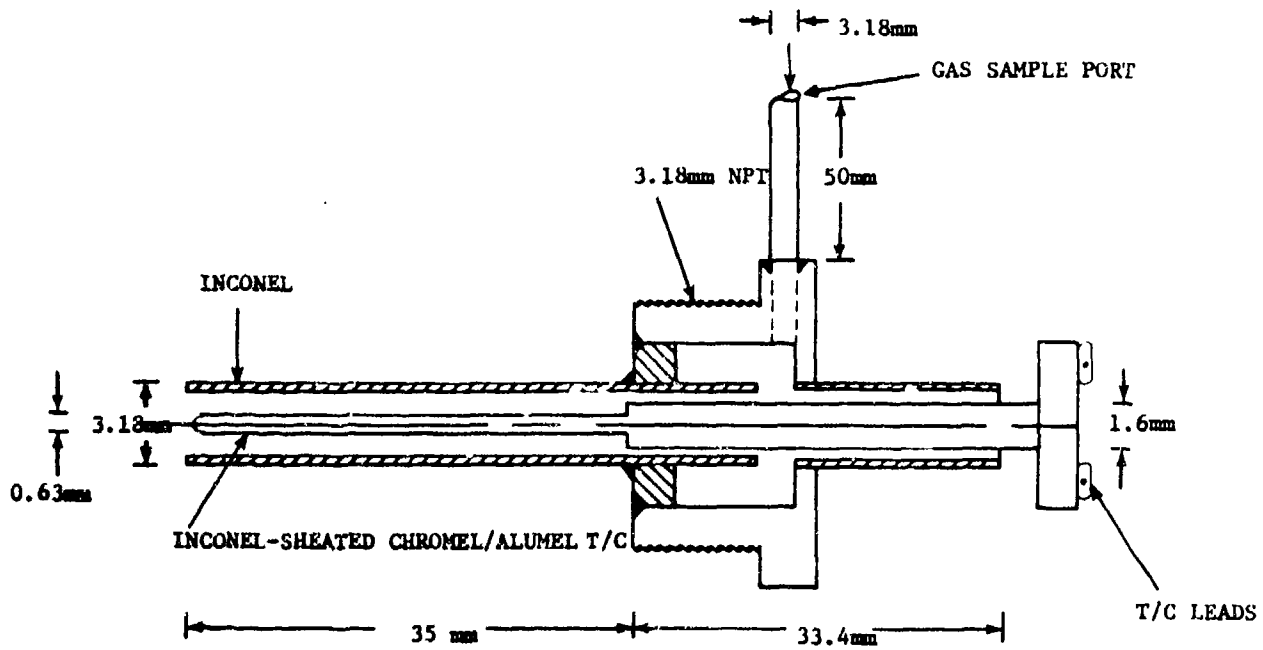


FIGURE 4: COMBINATION GAS SAMPLE AND TEMPERATURE PROBE

7. GAS ANALYSIS INSTRUMENTATION

A photograph of the gas analysis system utilized in this program is shown in Figure 5. A schematic piping diagram showing the location of sample probes, valves, instruments and the calibration gas system is shown in Figure 6. Adequate quenching of CO oxidation was assumed, based on Shaw's results in essentially the same equipment, which showed no change in CO concentration as a function of probe materials of construction (stainless steel or quartz) and filter elements (stainless steel or glass) (5). The sampling and analytical system for measuring exhaust emissions was designed to generally conform to the EPA requirements for determining compliance with the aircraft emission standards(1), with the exception that a water removal device, i.e., a condenser, was used prior to the NO_x analyzer.

Nine electrically heated stainless steel sample lines were used to direct the flow of gas from the sample probes in the hybrid combustor to a heated manifold located near the instrument train. Each sample line contained a high temperature bellows shut-off valve which was used to select the sample line or lines which would be diverted to the gas analyzer train. A single stainless steel heated tube connected the 9 valve manifold to the instrument train. The gas sample lines were bundled together and covered with electrical tape heaters. Iron-constantan thermocouples imbedded into the heated bundle were used to monitor the line temperature. An automatic temperature controller was utilized to maintain the bundle of gas sample lines at 420 K. The pressure of the gas sample up to the instrument train input corresponded to the pressure of the combustion chamber. The gas sample pressure was reduced to 110 kPa by a pressure regulator located just upstream of a dry ice-acetone bath which was used to freeze out the water in the gas sample. The hydrocarbon sample line bypassed the water knock-out and was fed directly to the Beckman model #402 high temperature FID hydrocarbon analyzer which was maintained at 474 K. The CO, CO₂, NO_x and O₂ instruments were connected in parallel to the gas sample line. A sample flow of 17 cm³/m was maintained through each instrument during the measurements.

Table 1 summarizes the key gas analysis parameters associated with the instruments used in this study.

TABLE I

INSTRUMENTS USED FOR GAS ANALYSIS

- Carbon monoxide. Beckman model 315A (NDIR) with 0-5000 ppmv and 0-2500 ppmv range. Maximum sensitivity was 12 ppmv. Calibrated with 2000 ppm CO in N₂.
- Carbon dioxide. Beckman model 864 (NDIR) with 0-25 and 0-5% range selectors. Maximum sensitivity was .05%. Calibrated with 7% CO₂ in N₂.
- Hydrocarbons. Beckman model 402 (FID) with 0-0.2% range with a 10 position range selector switch. Maximum sensitivity was 1 ppmv. Calibrated with 500 ppm CH₄ in N₂.
- Oxygen. Beckman model 742 with 0-25% range with a 3 position range selector switch for 0-1%, 0-5% and 0-25% ranges. Maximum sensitivity was 0.01%. Calibrated with 10% O₂ in N₂ or ambient air.
- Oxides of Nitrogen. Thermo Electron Corp. model 10A Chemiluminescent Analyzer with 10,000 ppmv range with an 8 position range switch. Maximum sensitivity was 0.25 ppmv. Calibrated with 100 ppm NO in N₂.



FIGURE 5: PORTABLE GAS ANALYSIS SYSTEM

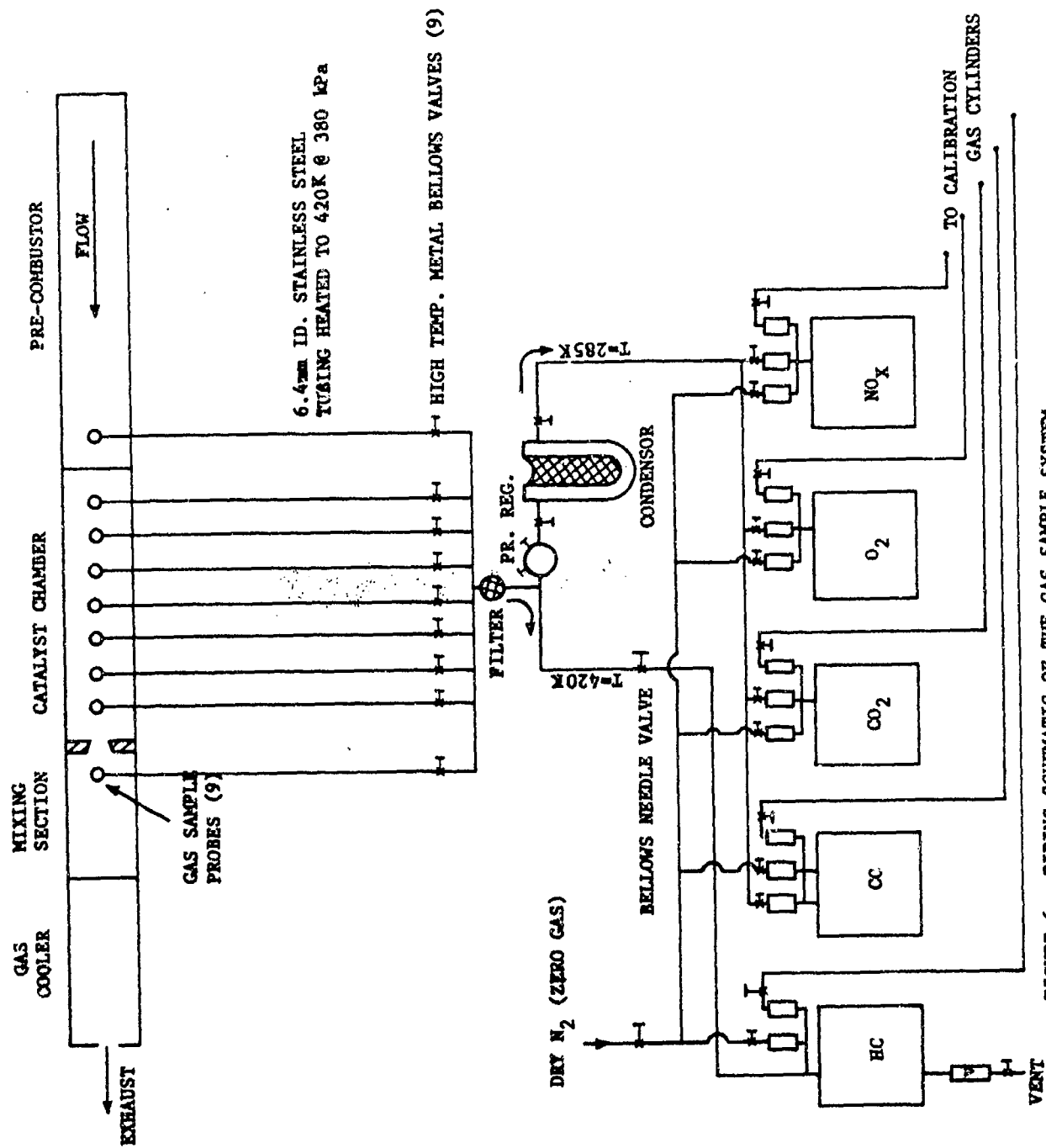


FIGURE 6: PIPING SCHEMATIC OF THE GAS SAMPLE SYSTEM

The instruments in the gas analysis system were calibrated with certified standard gas mixtures in nitrogen. The calibration gases were supplied by the Scientific Gas Co. of S. Plainfield, New Jersey. Dry nitrogen supplied from a cryosphere was used as the zero gas for all the instruments. When the instrument train was idle, a constant nitrogen purge was maintained. The instruments were calibrated before a run and checked at the conclusion of the run. The cylinders of hydrogen and air used to operate the hydrocarbon FID analyzer were certified to contain less than 1 ppmv hydrocarbons.

The effect of the dry ice-acetone bath temperature on CO₂ concentration in the gas sample was checked and found to be unimportant by passing a calibration gas containing 7% CO₂ in nitrogen through the cold trap and observing any loss in CO₂ concentration. The referenced temperature of the bath was 196 K and the sublimation point of CO₂ is 194.5 K (6). The magnitude of the potential reaction of nitrogen oxides with reducing species in the sample gases catalyzed by the heated stainless steel walls of the gas sample lines was assessed. Known NO and NO_x concentrations in combustion gas samples containing CO were passed through heated teflon or stainless steel lines. No difference in either NO or NO_x concentrations were found as a result of contact with the stainless steel or teflon lines. Similarly, no CO loss was detected as a result of oxidation by contact with the transfer lines of the analytical train. These experiments also demonstrated that no significant loss of NO₂ in the condensed water occurred.

Because of the possible production of HCN and NH₃ in the fuel-rich pre-combustion zone of the hybrid combustor, a wet-chemical sampling technique was utilized to obtain some representative gas samples at the inlet and outlet of the catalyst combustor section of the hybrid combustor. This sampling technique consisted of bubbling the sample gas for a known time period at constant flow, through aqueous solutions of NaOH for HCN determinations, and H₂SO₄ for NH₃ determinations. The nitrogen content of the samples was then determined by a specific ion-electrode technique, which has a sensitivity of about 1 ppmv for both nitrogenous compounds (7).

SECTION IV

RESULTS

This section of the report describes the operation of the combustor rig in two different catalytic modes under conditions which simulate aircraft gas turbine idle. First, the combustor was tested in the all-catalytic mode. In this mode, the pre-combustor was inoperative, and all of the combustion reactions were carried out in the catalytic section of the combustor. The fuel was partially vaporized and premixed at 400 K and 379 kPa in the pre-combustor section. In the second or hybrid mode of operation, the pre-combustor was utilized. The hot gas products from the pre-combustor contained approximately 300-800 ppm CO and UHC which were further oxidized in the catalytic section of the combustor. No temperature rise was measured across the catalyst from the oxidation of CO and UHC because their concentration was so low.

All of the tests performed in the all-catalytic mode were unsuccessful because little oxidation of the fuel occurred at 400 K and 25 m/s reference velocity. This was due to the fact that the fuel to air ratio and the inlet temperature were too low at simulated idle to achieve ignition (light-off). For this reason the majority of test results reported involve operation of the hybrid catalytic combustor where most of the fuel was oxidized homogeneously and the remaining UHC and CO were further oxidized in the catalyst chamber.

1. OPERATION IN THE ALL-CATALYTIC MODE

During the past few years, many investigators have shown that the minimum autoignition temperature of hydrocarbon fuel-air mixtures over a high surface area noble metal catalyst (Pt or Pt/Pd) was in the order of 525 K in the pressure range of 100 to 500 kPa (8, 9, 10, 11). These investigators concluded that the most critical test parameters were average residence time (i.e., inverse of space velocity), fuel concentration (equivalence ratio), mixture temperature and catalyst temperature.

During attempts to achieve combustion in the all-catalytic mode, the overall equivalence ratio was varied up to 0.35, the reference velocity at the catalyst inlet was maintained at 25 m/s and the combustion air was preheated to 400 K. Under these conditions, a very small fraction of the JP-4 was being converted, as evidenced by measured CO concentrations at the catalyst exit of about 20 ppm. No temperature rise in the catalyst bed was observed. The catalyst was a combination of 1.2 kg/m³ of (1/1) Pt/Pd on General Refractory Cordierite (0.31 cm hole monolith). From these results, it appeared that if the air preheat temperature was increased or the fuel-air mixture was made richer, an increase in catalyst bed temperature would have resulted and more of the fuel would have been converted. However, because the test facility cell began to fill rapidly with a potentially

explosive mixture of unreacted fuel no further attempts were made to increase the fuel concentration within the combustor. The air preheat temperature was not increased above 400 K because the goal of these tests was to develop a catalytic combustor to operate at simulated idle (see Table II).

Table II summarizes the parameters required to simulate the various aircraft gas turbine operating modes, as well as the equilibrium composition of the combustion products (12).

TABLE II

AIRCRAFT OPERATING PARAMETERS AND EQUILIBRIUM GAS COMPOSITION

	<u>Idle</u>	<u>Approach</u>	<u>Climbout</u>	<u>Takeoff</u>
P, MPa	0.3	1.0	2.0	2.5
Air Inlet T, K	400	600	720	775
Overall ϕ	0.147	0.264	0.338	0.367
V, m/s	24	30	33	34
Flame T, K	768	1,228	1,488	1,596
Gas Composition				
Ar, %	0.93	0.92	0.92	0.91
CO, ppm	< 0.05	< 0.05	0.12	0.54
CO ₂ , %	2.18	3.83	4.83	5.24
HNO ₂ , ppm	< 0.05	0.03	0.13	0.20
HO ₂ , ppm	< 0.05	< 0.05	0.08	0.18
H ₂ , ppm	< 0.05	< 0.05	0.04	0.17
H ₂ O, %	1.81	3.39	4.35	4.74
NO, ppm	1.20	223.32	990.85	1,580.
NO ₂ , ppm	2.46	8.65	18.99	24.08
N ₂ , %	77.17	76.54	76.13	75.94
N ₂ O, ppm	< 0.05	0.04	0.24	0.41
O, ppm	< 0.05	< 0.05	0.24	0.99
OH, ppm	< 0.05	1.26	19.14	45.43
O ₂ , %	17.91	15.30	13.67	12.99

2. COMBUSTION CHARACTERISTICS OF THE PRE-COMBUSTOR

In this study, two different pre-combustor can designs were tested. The first pre-combustor can consisted of a 2.5 cm diameter Hastelloy-X, closed-end tube which was perforated with symmetrically located 6.3 cm diameter holes. A 1.4 rad (80°) angle pressure atomizing fuel nozzle and primary air swirler were attached to the open end of the 20 cm long tube.

The annular gap between the can and the outer combustion chamber wall was purged with low velocity secondary air. Inadequate cooling of the Hastelloy-X can by the secondary air stream resulted in the destruction of the pre-combustion can. Heavy carbonaceous deposits were observed to accumulate at the closed end of the can which ultimately affected the heat transfer properties of the metal, such that the hemispherical end of the can overheated and was badly deformed. After several attempts were made, without success, to improve the durability and combustion efficiency of the pre-combustor can, the design was abandoned and a 5 cm diameter open-ended can-type pre-combustor was devised. The operating characteristics of the pre-combustor that was utilized throughout the program are described below.

Gas temperature and combustion species distributions at the entrance to the catalyst chamber were determined for a set of operating conditions which simulated idle (see Table II). Data were obtained with an empty catalyst chamber, with an inert monolith in the chamber and with an active catalyst in the chamber.

The data were obtained with temperature and gas species probes located at the entrance to the catalyst chamber, in the catalyst chamber, and at the exit of the catalyst chamber. Details on the probes used are given in Section III. Table III summarizes the flow and combustion characteristics of the HCC for two different operating conditions. Figure 1 identifies the various parts of the combustor referred to in Table III. The results reported in Table III show the effect of altering the ratio of secondary air flow between the pre-combustor annular gap (location 9) and the 26 radial injection holes located near the open end of the can-type combustor (location 10). In both conditions the primary air flow rate remained constant at 20% of the total combustion air flow rate.

In condition 1, 65% of the total secondary air went through the annular gap between the pre-combustor-can and the combustion chamber outer wall (location 9), while 35% went through the 26 radial injection holes (location 10). In condition 2 the split of secondary air going to the quench zone vs. that going through the annular gap was 40 to 60%. It should be noted from the results in Table III that minor changes in the secondary air split greatly affected the radial combustion species distribution. This effect was caused by increased mixing due to the higher air injection velocity through the 26 hole quench zone. The total air flow to the quench zone increased from 35 to 40% of the secondary flow. The gas temperatures measured across the duct diameter by four thermocouple probes (C, D, E, and F) were approximately the same for both conditions. The average CO concentration across the duct at the entrance to the catalyst chamber for condition 2 was about half that for condition 1. The corresponding change in radial air injection velocity was from 17 to 19.5 m/s in going from condition 1 to condition 2.

TABLE III

**FLOW CHARACTERISTICS IN THE
HYBRID CATALYTIC COMBUSTOR**

Design Conditions:

Combustor Pressure: 375 kPa
 Air Preheat Temp: 400 K
 Primary ϕ : 1.5
 Overall ϕ : 0.3
 Reference Velocity: 24.4 m/s

Actual Conditions:

Condition 1	Location in Figure 1		Condition 2
334	(1)	Combustor Pressure (kPa)	334
400		Pri. & Sec. Air Preheat (K)	400
1.5	(2)	Primary, ϕ	1.5
0.3	(3)	Overall, ϕ	0.3
24.4	(4)	Reference Velocity (m/s)	24.4
2.71	(5)	JP-4 Flow Rate (g/s)	2.71
26.6	(6)	Primary Air Flow rate (g/s)	26.6
106.	(7)	Secondary Air Flow rate (g/s)	106.
65.6	(8)	Pri. Injector Velocity (m/s)	65.6
22.5	(9)	Sec. Air Vel. Arcual Pre-burner (m/s)	20.3
17	(10)	Sec. Air Inf. Vel. @ Pre-burner Discharge (m/s) (400 K)	19.5
11.2	(11)	Vel. Upstream of Radial Sec. Inf. (m/s) (400 K)	10.5
46	(12)	Vel. Upstream of Radial Sec. Inf. for 1700 K mix. temp. (m/s)	43

Temp. Profile @ Cat. Bed Inlet (K)

875	T/C (C)	924
1060	T/C (D)	1083
1145	T/C (E)	1153
1180	T/C (F)	1143

Concentration Profile (Dry) @ Cat. Bed Inlet

CO ppm	CO ₂ %	O ₂ %	NO _x ppm	UHC ppm		CO ppm	CO ₂ %	O ₂ %	NO _x ppm	UHC ppm
750	3.8	15.1	16	700	Probe (C)	395	4.5	14.4	32	50
625	3.5	15.2	17	540	Probe (D)	345	4.5	14.4	33	70
697	3.5	15.3	18	320	Probe (E)	350	4.6	14.8	26	120
740	3.4	16.0	19	490	Probe (F)	365	4.2	14.6	29	48

The combustion efficiency and combustion product distribution profiles obtained under condition 2 could possibly have been improved if the amount of secondary air flow through the 16 radial holes was increased beyond 40 percent, but this could have resulted in excessive pre-combustor can temperatures due to inadequate cooling. All of the combustion efficiency data and emission index data discussed in the rest of the report were obtained with the combustor operating at condition 1. It is interesting to note that NO_x concentrations were almost double in the better mixed method of operation, i.e., condition 2.

To further characterize the gas temperature and combustion species distribution, axial temperature and species concentration profile measurements were made on the centerline of the combustor. Table IV and Figures 7, 8 and 9 present the information obtained on the pre-combustor axial and radial temperatures, and UHC and NO_x concentrations at an overall ϕ of 0.3 and a pre-combustor ϕ of 1.5. Table IV presents the data obtained from the measurement of the centerline CO , UHC and NO_x concentrations, as well as the gas temperatures in the pre-combustor secondary mixing section and in the empty catalyst chamber. The gas temperature leaving the pre-combustor can, before the secondary quench air was mixed in was on the order of 1570 K. Thermodynamic calculations (presented in Table V) predict that if the system were adiabatic, this temperature would be about 2050 K at a ϕ of 1.5 (12). The difference in temperature is probably due to heat losses from the system to the quench air. The rapid addition of secondary air through the 26 hole quench zone reduced the gas temperature to about 1120 K, which corresponds to a ϕ of 0.3. The axial temperature profile through the rest of the sampling points, identified as locations G through O, remained relatively unchanged. The measured CO_2 and O_2 concentrations at the catalyst chamber inlet agree quite well with the thermodynamic calculations for $\phi = 0.3$ as summarized in Tables III and V. The axial concentrations of CO , UHC and NO_x in Table IV illustrate the effectiveness of quenching that was achieved by the 26 high velocity secondary air jets.

Figure 7 shows the axial distribution of UHC and NO_x at an overall $\phi = 0.3$ with an empty catalyst chamber. The measured NO_x and UHC concentrations were constant (with experimental error) over the 20 cm length. The corresponding gas residence time in the 20 cm path length was in the order of 2-3 ms. Figure 8 is a plot of the radial distribution of gas temperature and hydrocarbon concentration at the catalyst chamber inlet for conditions 1 and 2 described previously (see Table III). The effect of increasing mixing by increasing the velocity through the 26 secondary air jets is a minor change in the radial temperature profile, but a significant change in the radial hydrocarbon concentration profile. Although the hydrocarbon and temperature profiles were more uniform for condition 2, it was decided to conduct all the subsequent testing of catalysts under condition 1 because the fate of large concentrations of unreacted CO and UHC would be more easily and more accurately determined in the catalyst chamber where subsequent conversion of these species would occur.

TABLE IV
AXIAL TEMPERATURE AND COMBUSTION PRODUCTS
DISTRIBUTION IN EMPTY CATALYST COMBUSTION CHAMBER (DRY BASIS)

Pre-Burner $\phi = 1.5$

Overall $\phi = 0.3$

Pre-Combustor

<u>Location</u> (See Figure 1)	<u>Temperature</u> (K)	<u>CO</u> (ppm)	<u>HC</u> (ppm)	<u>NO_x</u> (ppm)
A	1573	--	--	--
B	1361	--	--	--
C	1126	480	210	22
<u>Catalytic Chamber</u>				
G	1133	475	200	21
H	1133	475	220	23
I	1133	445	190	19
J	1111	445	200	18
K	1139	475	200	21
L	1122	435	200	19
M	1116	482	180	20
O	1150	425	80	24

PROBE LOCATION ACCORDING TO FIGURE 1

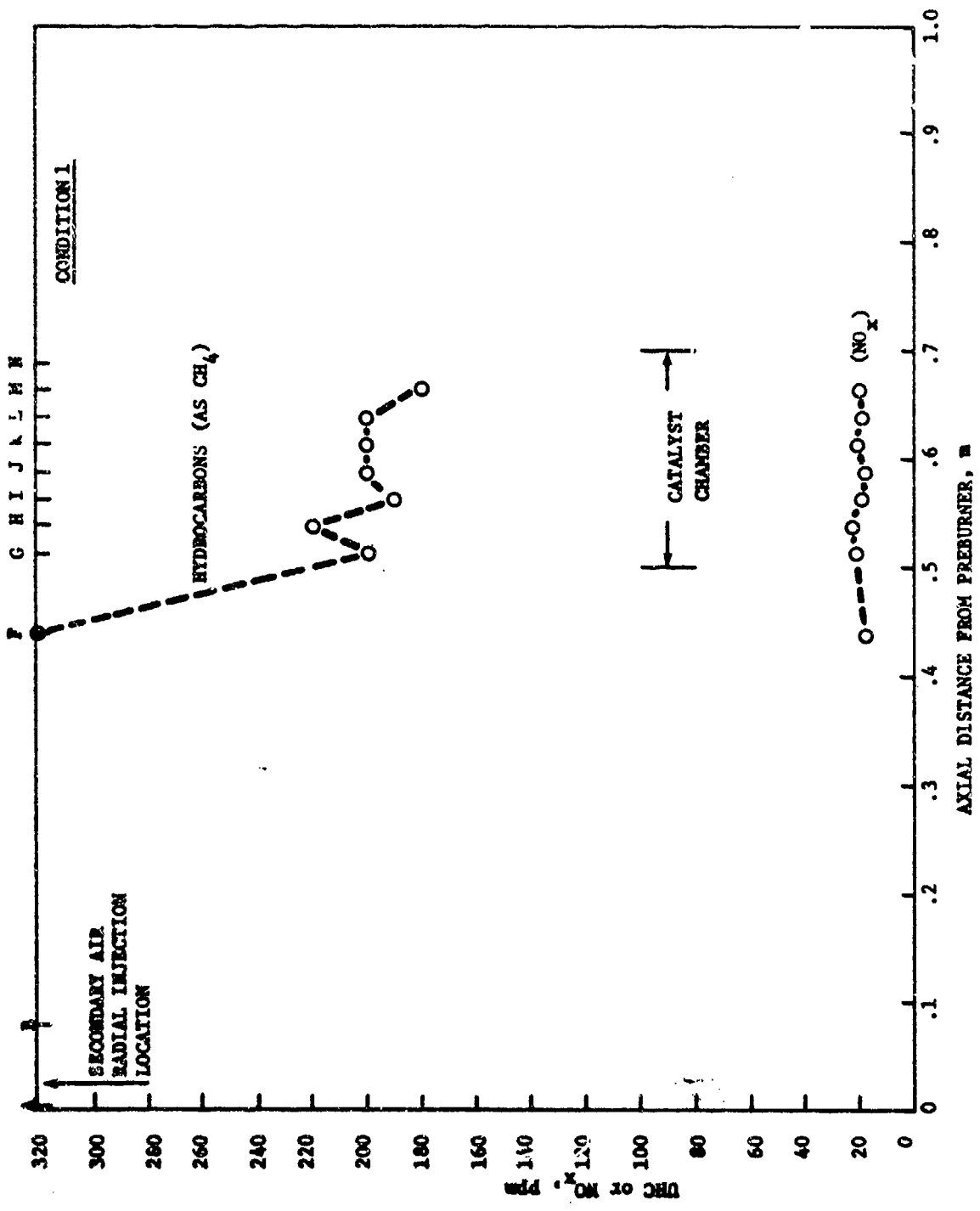


FIGURE 7: AXIAL CONCENTRATION PROFILES OF NO_x AND HYDROCARBONS IN AN EMPTY CATALYST CHAMBER

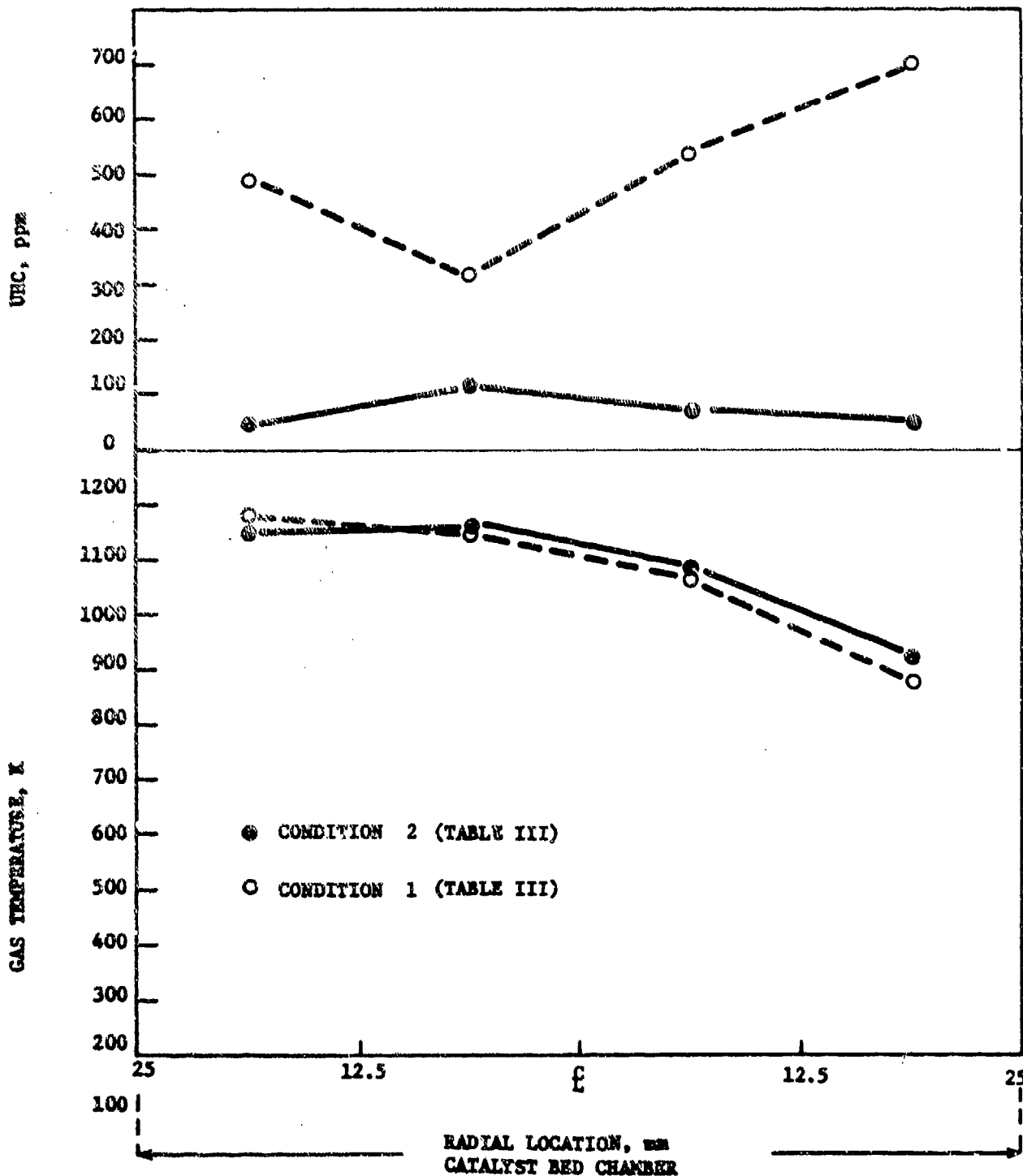


FIGURE 8: VARYING SECONDARY AIR SPLIT ON TEMPERATURE AND UNBURNED HYDROCARBONS AT THE CATALYST BED INLET (ϕ OVERALL = 0.3)

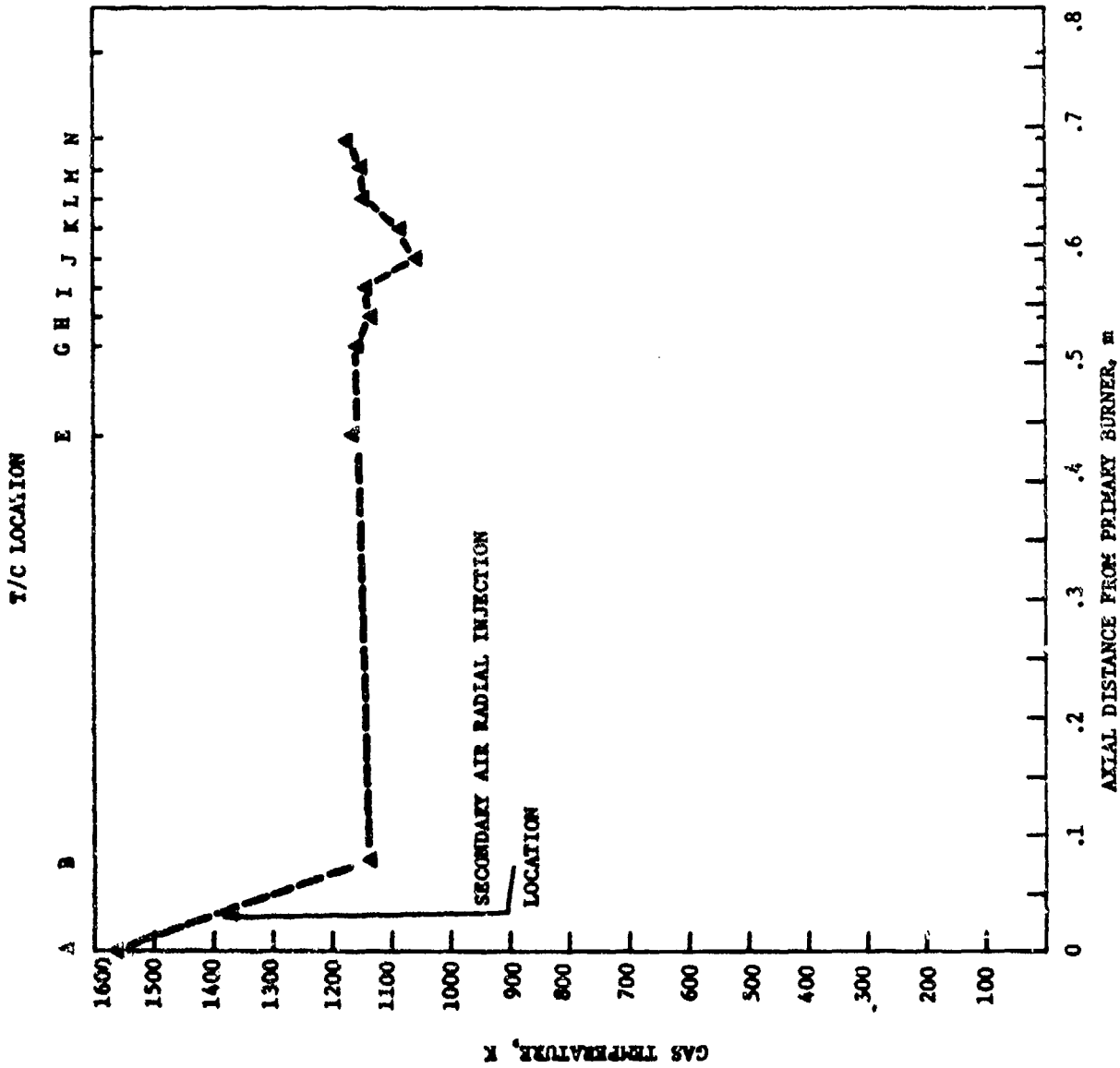


FIGURE 9: AXIAL-CENTERLINE TEMPERATURE OF CATALYST (K) FOR OVERALL $\phi = 0.3$

Figure 9 shows the axial (centerline) gas temperature distribution in a monolithic catalyst at an overall $\phi = 0.3$. A comparison of these temperature data with similar data for an empty catalyst chamber given in Table IV shows that there was no temperature rise across the catalyst. A temperature rise would not be expected for such low concentrations of UHC and CO since the combustion process was better than 98% completed before the gas mixture from the pre-combustor entered the catalyst.

Subsequent tests to determine the effect of an inert monolithic catalyst support on the axial temperature profile within the catalyst chamber were performed with the same results observed for catalyst KN (see Appendix II) shown in Figures 7 and 9.

TABLE V

EQUILIBRIUM COMPOSITION OF PRODUCTS FROM JP-4
COMBUSTION WITH AIR AT 300 kPa

	Mole Percent						Adia- batic Temp. K	Flue Gas Molecular Weight
	O ₂	CO ₂	CO	H ₂	NH ₃	NO		
.05	19.86	.705					539	28.96
.1	18.75	1.39					675	28.96
.2	16.55	2.76				.001	930	28.95
.3	14.37	4.10				.013	1165	28.94
.4	12.21	5.43				.054	1384	28.93
.5	10.06	6.74				.134	1589	28.92
.6	7.92	8.03	.002	.001		.249	1780	28.91
.7	5.79	9.29	.018	.004		.371	1960	28.90
.8	3.74	10.46	.093	.019		.457	2125	28.87
.9	1.89	11.39	.381	.072		.445	2267	28.80
1.0	.547	11.63	1.29	.246		.288	2360	28.64
1.1	.064	10.57	3.36	.739		.096	2356	28.26
1.2	.006	8.95	5.89	1.60		.026	2288	27.77
1.3	.001	7.52	8.18	2.72		.008	2208	27.28
1.4		6.36	10.14	4.04		.003	2128	26.81
1.5		5.45	11.82	5.49		.001	2051	26.35
1.6		4.73	13.28	7.04			1976	25.91
1.7		4.15	14.56	8.62			1903	25.49
1.8		3.68	15.71	10.22			1832	25.09
1.9		3.28	16.75	11.80			1763	24.71
2.0		2.94	17.71	13.36	.001		1696	24.35

The decision to perform all catalyst testing at condition 1 fixed the air distribution mode, as indicated in Table III. Thus, the pre-combustor fuel flow had to be reduced if overall ϕ 's of less than 0.3 were to be studied. Table VI summarizes the required ϕ in the pre-combustor to achieve the indicated overall ϕ , or alternatively, the indicated catalyst inlet temperature. It should be noted that to simulate idle according to Table II, an overall ϕ of about 0.15 would be needed, which would require operating the pre-combustor at $\phi = 0.75$. If, on the other hand, climbout or take-off simulation were desired, then the pre-combustor would have to operate richer than $\phi = 1.55$.

TABLE VI
RELATIONSHIP BETWEEN COMBUSTION MIXTURES
AND TEMPERATURE IN THE PRE-COMBUSTOR

<u>Pre-Combustor</u> <u>ϕ</u>	<u>Catalyst Inlet (Overall)</u>	
	<u>ϕ</u>	<u>Temperature (K)</u>
1.55	0.312	1244
1.5	0.30	1165
1.42	0.285	1144
1.25	0.25	1050
1.11	0.22	990
1.0	0.20	930
0.84	0.169	844
0.75	0.15	810
0.67	0.125	750

3. DESCRIPTION OF CANDIDATE CATALYST

Catalysts and substrate candidates were selected for testing by matching the desirable features of catalysts for HCC application with those of commercially available catalysts (i.e., contractual requirements limited the selection to existing catalyst and substrates). The catalysts were considered to consist of an active material such as Pt, a substrate such as cordierite, and a wash coat such as alumina. Among the factors considered in selecting the catalyst for testing were the maximum operating temperature, potential pressure drop, compressive strength, resistance to thermal shock and capability of retaining a high surface area wash coat. The maximum operating temperature for the catalyst was specified to be the adiabatic flame temperature at the highest overall equivalence ratio

contemplated for this study. Thus, at an overall ϕ of about 0.3, the maximum temperature would be 1165 K according to Table VI. In order to take into account possible experimental deviation from the $\phi = 0.3$ value, the maximum operating temperature of the substrate was limited to 1250 K for specifying catalysts and materials of construction.

One of the most important constraints placed on catalyst selection was that high surface/volume configurations would be required if complete conversions of unreacted CO and UHC were to be achieved under high space velocity operation. This was due to preliminary indications in the literature⁽¹³⁾ as well as in our initial experiments⁽¹⁴⁾ that the kinetics were diffusion limited.

Other considerations in substrate selection included compressive strength in the direction parallel to the gas flow, resistance to thermal shock and magnitude of thermal expansion. The substrates were also required to be resistant to high temperature oxidation, and capable of accepting and retaining high surface area wash coats of refractory oxides such as alumina, zirconia, magnesia, etc. The geometries of the 5.08 cm diameter by 5.08 cm long catalyst supports obtained for this program included round holes of different diameters, squares, rectangles, triangles, and other more complex hollow configurations. The support materials included cordierite, alumina, silicon carbide, metal foils, and screens.

Although the catalyst requirements mentioned above could be satisfactorily met by a number of manufacturers and suppliers, the following suppliers were selected because they were familiar with our requirements. Also, some of these suppliers produced novel materials or geometries which appeared promising for use in a catalytic combustor. Details about each substrate tested are given in Appendix I.

- General Refractories Co., Philadelphia, Pa.
- W. R. Grace & Co., Columbia, Md.
- Norton Industrial Ceramics, Worcester, Mass.
- Nippon Sealol Co., Ltd. (Pure Carbon Co., St. Mary's Pa.)
- DuPont Corp., Wilmington, Del.
- Johnson-Matthey Co., Ltd., Reading, England
- Matthey-Bishop, Inc., Malvern, Pa.

In addition to containing a tabulation of the substrate properties, Appendix I also includes limited experimental data on tests of substrates that either had very high pressure drop characteristics, or low compressive strength which resulted in their destruction at the reference velocities of interest in this program.

Packed nickel alloy screens coated with platinum, manufactured by the Matthey-Bishop Co., were shown to have an isothermal pressure drop at a reference velocity of 25 m/s of 54.6% for a support length of 7.6 cm. Because of the high pressure drop associated with this configuration, no attempts were made to obtain CO and UHC conversion data under reacting flow conditions. Subsequent modifications to the packed screen support by Matthey-Bishop, Inc. led to the catalyst support described in Appendix I, Table XIX which was tested under reacting conditions.

A tightly wound corrugated-metal-film catalyst support fabricated by the Johnson-Matthey Co. containing 82 openings/cm² was not tested under reacting flow conditions since the isothermal pressure drop of 47% was too high. The subsequent enlargement of the corrugated openings in this substrate led to the fabrication and testing of the metal substrate described in Table XVIII of Appendix I.

The 45 and 62 holes/cm² cordierite monoliths supplied by the W. R. Grace Co. described in Table XIV of Appendix I, exhibited moderately high pressure drops under reacting flow conditions. In an attempt to find a lower pressure drop material, some isothermal pressure drop tests were performed on a W. R. Grace cordierite substrate having larger holes. Compared to the W. R. Grace monoliths mentioned above, the new monoliths had 31 holes/cm², but still failed to meet the isothermal pressure drop requirement. No further work was done with the 31 hole/cm² monolith.

Some isothermal pressure drop tests were conducted on an alumina "sponge" catalyst support supplied by the Clyde Engineering Co. of Miami, Florida. The very fragile nature of this candidate material led to its complete destruction at the 25 m/s velocity of the pressure drop test. No further work was conducted with this support.

The detailed description of all the catalyst formulations tested is tabulated in Appendix II and summarized in Table VII. The procedure used to select the catalysts for this program included a thorough literature search and discussions with catalyst manufacturers. The literature search was compiled into an annotated bibliography and issued as an informal report (13). The report contains references to the general area of hydrocarbon oxidation, catalyst preparation techniques, inventions and processes involving homogeneous or heterogeneous catalysts.

TABLE VII. RELATIVE CATALYST ACTIVITIES FOR OVERALL $\phi = 0.28-0.30$ AT 376 kPa
AND 25.8 m/s REFERENCE VELOCITY (CATALYST LENGTH = 20.3 cm)

Catalysts	CH	JH	FH	UK	EH	KT	EH	KP	KN	KX	Pa	QE ^a
Catalytic Materials	Pt-Pd	Pt-Pd	Pt-Pd	Pt-Pd	Pt-Pd	Pt-Rh	Pt-Pd	Pd	Pt-Pd	Pt-Pd	Pt-Pd	None
Wt. Ratio	1/1	1/1	1/1	1/1	1/1	23/1	1/1	--	5/2	1/1	?	--
Mesh Coat	Al ₂ O ₃ +Stab	NiO+ SiO ₂	Al ₂ O ₃ +Stab	ZrO ₂ +CoO	Al ₂ O ₃ CeO	Al ₂ O ₃ CeO	Al ₂ O ₃ +Stab	None				
Wet Metal Loading, kg/m ³	1.7	1.7	1.7	1.7	1.7	1.31	1.7	0.39	2.79	5.49	?	None
Support Material	Cord.	Cord.	Cord.	SiC	Cord.	Cord.	Cord.	Cord.	Cord.	Cord.	Metal	Metal
Support Geometry	G	F	E	D	C	A	B	A	A	A	I	H
Support, m ² /m ³	2473	1537	1937	1094	1700	2109	996	2109	2109	2109	?	?
Support Openings/cm ²	42	16	35	10	34	45	10	45	45	45	?	?
Open Frontal Area, %	65	79	73	70	67	69	78	69	69	69	?	?
Isothermal χ_{IF}	8.4	3.3	4.2	3.3	4.9	9.3	3.3	9.3	9.3	9.3	47.3	?
Reacting χ_{IF}	13.8	4.5	5.4	6.0	13.6	12.5	4.5	19.4	19.4	19.4	--	54.6

Experimental Results	
Catalyst Inlet Temperature, K	1233
% CO Converted	88
% UHC Converted	98
NO _x Inlet, ppm	24
NO _x Outlet, ppm	38
	1166
	1189
	1166
	1266
	1144
	1139
	1299
	1211
	1222
	--
	--
	--
	--
	--

Support Geometry

- 0.127 cm irregular rectangle.
- 0.31 cm circular hole.
- 0.158 cm circular hole.
- 0.31 cm circular hole (slightly elliptical).
- 0.16 cm square hole.
- 0.16 x 0.32 cm rectangular hole.
- 0.16 cm triangular hole.
- Packed screen (18 mesh, 0.040 cm wire and 7.6 cm thick).
- Corrugated metal with 0.08 cm openings
- DuPont radial flow monolith.

- Corrugated SiC (Pure Carbon Co. - 0.31 cm opening).
- W. R. Grace, 2 x 2 spiral
- W. R. Grace, 0.165 cm irregular rectangle.
- Corrugated Metal (Johnson-Matthey-0.16 cm opening).

Notes

- DP too great to run under reacting conditions.
- 1/2 normal length (10.16 cm).
- Pd under Al₂O₃ wash coat.
- 20 hr. durability study completed.
- Rare earth oxides
- Base metal oxides of Cu, Cr and Mn.

TABLE VII. RELATIVE CATALYST ACTIVITIES FOR OVERALL $\phi = 0.28-0.30$ AT 376 kPa
AND 25.8 m/s REFERENCE VELOCITY (CATALYST LENGTH = 20.3 cm) (Cont'd.)

Catalysts	MRab	RQd	KR	RA	KU	MQb	FH&FQ	FZ	FVC	JG
Catalytic Materials	Pt-Pd	Pd	REO ^c	REO ^a	Pd	Pd	Pd-Pd	Pt-Pd	Pd	Pd
wt. Ratio	1/1	—	—	—	—	—	1/4.8	1/1	—	—
Wash Coat	Al ₂ O ₃ +Stab	Al ₂ O ₃ +CeO ₂	Al ₂ O ₃ +REO	La ₂ O ₃ SrO MnO ₃	Al ₂ O ₃ EMOf	Al ₂ O ₃ +CeO	Al ₂ O ₃ CeO Stab	Al ₂ O ₃ Stab	Al ₂ O ₃ Cr ₂ O ₃ MnO ₂	Al ₂ O ₃ +CeO CuO+Cr ₂ O ₃
Noble Metal Loading, kg/m ³	1.7	3.29	0	0	0.39	2.59	2.52	0.55	3.3	0.39
Support Material	Al ₂ O ₃	Cord.	Cord.	SrO	Cord.	Cord.	Cord.	Cord.	Cord.	Cord.
Support Geometry	?	A	A	K	A	L	A/E	E	E	F
Support, m ² /m ³	?	2109	2109	1428	2109	?	2022	1937	1937	1537
Support Openings/cm ²	?	45	45	-29	45	?	40	35	35	16
Open Frontal Area, %	?	69	69	-69	69	?	71	73	73	79
Leachrate, %/h	42.0	9.3	9.3	6.0	9.3	22.8	7.5	4.2	4.2	3.3
Reacting %/h	—	19.4	19.4	8.0	19.4	33.0	11.8	5.4	5.4	4.5
Experimental Results										
Catalyst Inlet Temperature, K	—	1200	1244	1175	1200	1177	1230	1244	1177	1255
% CO Converted	—	91	13	5	83	63	93	75	74	40
% USC Converted	—	96	50	65	92	62	92	74	62	60
NO _x Inlet, ppm	—	26	26	24	25	27	30	28	29	32
NO _x Outlet, ppm	—	38	32	32	33	34	33	28	30	33

TABLE VII. RELATIVE CATALYST ACTIVITIES FOR OVERALL $\phi = 0.28-0.30$ AT 376 kPa AND 25.8 m/s REFERENCE VELOCITY (CATALYST LENGTH = 20.3 cm) (Cont'd.)

Catalysts		FG	FY	QF ^d	PC&FL	FL	FF	FD&FE
Catalytic Materials	Pd	Pd	Pt	Pt-Pd	Pd	Pd-Ir		
Wt. Ratio	--	--	--	1/1	--	1/1		
Wash Coat	Al ₂ O ₃ +CeO CrO+Cr ₂ O ₃	Al ₂ O ₃ + Stab						
Noble Metal Loading, kg/m ³	0.39	3.3	5.27	2.7	5.5	1.7		
Support Material	Cord.	Cord.	Metal	Metal/Cord.	Cord.	Cord.		
Support Geometry	E	E	N	O,E	E	E		
Support, m ² /m ³	1937	1937	4100	1000	1937	1937		
Support Openings/cm ²	35	35		35	35	35		
Open Frontal Area, %	73	73	93	73	73	73		
Isothermal χ/E	4.2	4.2		3.5	--	4.5		
Reacting χ/E	5.4	5.4		5.5	--	5.7		
Experimental Results								
Catalyst Inlet Temperature, K	1200	1211	1200	1200	1200	1200	1200	1200
% CO Converted	64	78	94	67	--	50		
% UHC Converted	86	83	94	72	No Data Obtained Alone.	60		
NO _x Inlet, ppm	28	31	18	37	Des-	36		
NO _x Outlet, ppm	30	31	36	33	troyed.	38		

The criteria used to select various catalyst formulations gradually became more refined and specific as the initial set of results of CO and UHC conversions at various temperatures in the hybrid combustor were obtained. Initially, noble metal catalysts on stabilized alumina wash coats were selected for testing, since the literature study clearly showed this class of metals to be superior to all other metals for the gas phase oxidation of hydrocarbons at initial temperatures of 400 to 600 K. The unpublished results of studies performed at Exxon also showed that noble metals promoted ignition (light-off) of prevaporized-premixed JET-A and air mixtures at lower temperatures than required for base metal oxides and rare earth oxides viz., 520 K for noble metals as opposed to 750 and 930 K for base metal oxides and rare earth oxides, respectively (14). The maximum operating temperature of the noble metal catalysts is limited by the volatility of noble metals, wash coat sintering and noble metal crystallite growth at temperatures in excess of 1300 K (15). Catalyst deactivation can also be caused by poisoning due to sulfur, mercury, lead, etc. (16).

The catalyst described in Table VII and Appendix II were obtained from the various companies listed above. In some cases, the support was manufactured by one of these companies and the catalyst and wash coat were applied by one of the following companies:

- Oxy-Catalyst Inc., West Chester, Pa.
- W. R. Grace Co., Columbia, Md.
- Johnson-Matthey Co., Ltd., Reading, England
- Matthey-Bishop Co., Malvern, Pa.

4. METHODS OF PREPARING CATALYSTS FOR TESTING

Most of the candidate catalysts tested during this program consisted of cellular monolith segments that were 5.08 cm diameter and 5.08 cm long. Usually, four segments of the same catalyst were packed end-to-end in a 21.6 cm long thin wall (.033 cm) Hastelloy-X cylinder. To prevent bypass around the monoliths, a thin coat of cordierite cement was applied to the outer diameter of each monolith. After the cement was partially cured overnight at room temperature, the monoliths were pressed into the tight fitting Hastelloy-X cylinder. In this manner, the excess cement was neatly removed from the monolith and a gas tight seal was created. The monoliths were then prepared to accept the gas sample-thermocouple probes by drilling 0.317 cm diameter holes, 2.54 cm deep, normal to the gas flow axis at 2.54 cm intervals. These holes corresponded to the 0.317 cm diameter hole located in the Hastelloy-X cylinder. The holes were easily drilled in cordierite monoliths with conventional steel drills, but carbide drill bits were required to drill the holes in monoliths made of silicon carbide or alumina.

Some of the catalyst candidates were made of rolled metal screens or corrugated metal foils that were coated with high surface area Al_2O_3 which was impregnated with catalytic materials. When catalysts of this configuration were tested, the manufacturer of the catalyst was supplied with Hastelloy-X cylinders in which they mounted their catalysts. While assembling the metal screen substrate catalysts, the manufacturers provided a void at the location where the gas sample and thermocouple probes were to be inserted. Therefore, unlike the ceramic catalyst supported candidates, the metal screen substrate catalysts were a series of 2.54 cm long segments with a small void between adjacent segments. The corrugated metal foil catalysts were drilled in the same manner as the ceramic catalysts. The gas tight pressure seal around the metal supported catalysts was accomplished in the same manner as previously described for the ceramic substrate materials.

The Hastelloy-X cylinder which contained the catalyst was inserted into the catalytic combustion chamber. The gas sample-thermocouple probes were then inserted through the holes drilled into the catalysts which were concentric with the mating ports of the outer combustion chamber wall. The thermocouple leads and stainless steel gas sample lines were connected to the probes, and pressure checked via the soap bubble technique for leaks.

The catalyst combustion chamber was then bolted to the pre-combustion chamber and the water cooled counter-current heat exchanger. The entire hybrid combustor was checked for leaks and prepared for test firing with JP-4.

5. PRESSURE DROP CHARACTERISTICS OF SUPPORTS

One of the major considerations in developing a viable catalytic combustor is not to increase its volume over the volume of state-of-the-art aircraft combustors while maintaining the pressure drop through the combustor at operating conditions at less than 6%. We therefore measured the pressure drop through all catalysts tested with 400 K air at 0.31 MPa, and under various reacting conditions. Figure 10 is a summary of the pressure drop measurements obtained for a wide variety of catalysts with different geometrical configurations. The isothermal pressure drop data were obtained with catalysts that were 20.32 cm long (four, 5.08 cm long segments face-to-face). The reference velocity was varied from 10 to 26 m/s by maintaining constant pressure of 0.31 MPa and constant air temperature of 400 K, but varying the air flow rate. Two different methods were used to determine pressure drop. One method consisted of simultaneously measuring the pressure at the catalyst inlet and outlet face with a strain gauge differential pressure transducer. The other technique involved the individual measurement of the catalyst inlet and outlet pressures with a precision Bourdon-Tube gauge which was isolated from the catalyst chamber by an appropriate valving arrangement. Generally, the agreement between the two techniques was within 5%. The latter method was most often utilized because of its simplicity.

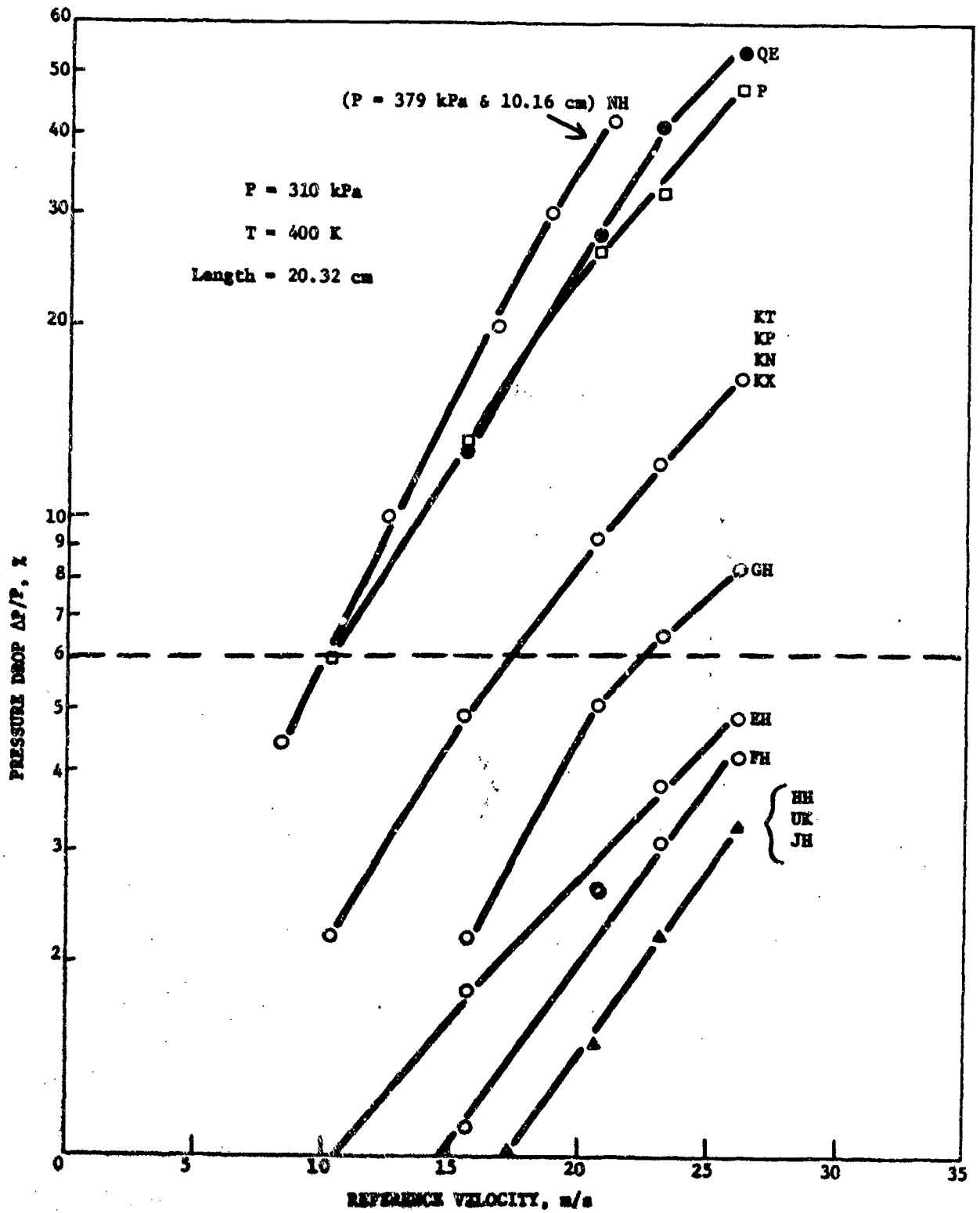


FIGURE 10: ISOTHERMAL PRESSURE DROP CHARACTERISTICS OF MONOLITHS

The geometry of any of the catalysts given in Figure 10 can be identified by referring to Table VII. The pressure drop data show that as the surface/volume ratio of the support geometry decreases, so does the isothermal pressure drop. Catalysts HH, UK and JH were observed to have the lowest pressure drops of any catalyst tested. Catalysts HH and UK had 0.31 cm diameter circular openings, while JH was made of 0.16 cm x 0.32 cm rectangular openings. Catalysts KT, KP, KN and KX exhibited similar pressure drops because they had the same support geometry. The relatively high pressure drop associated with these catalysts which were a product of the W. R. Grace Co., was due to the large cross-section of the wall material which separated adjacent channels. The W. R. Grace supports had a S/V ratio of $2109 \text{ m}^2/\text{m}^3$ compared to that of catalyst FH which was $1937 \text{ m}^2/\text{m}^3$. However, because of the difference in wall thickness between the two types of supports, catalyst FH had a lower pressure drop. The differences in wall thickness between substrates is due to the manufacturing techniques involved in their fabrication.

The highest pressure drops were measured in support geometries that were made of many discontinuous passages or channels in either metal or ceramic materials. Examples of supports made with discontinuous channels were catalysts NH and MQ which were made from DuPont Torvex^R and cordierite, respectively. The DuPont support provided many radial flow passages which were dead-ended to induce flow reversal and mixing. The cordierite support was made by W. R. Grace Co. and contained many small rectangular passages which imparted a swirling motion to the gas stream.

Other high pressure drop catalysts were those fabricated from tightly packed metal screens, or from corrugated and tightly wound metal foils such as catalysts P, PC and QE. Catalyst QF was also made from a metal foil but the size of the corrugations were enlarged compared to catalyst P. A catalyst of an entirely different design consisting of a foamed cellular skeleton of alumina which was made by a proprietary process from a polymeric foam material manufactured by the Scott Paper Co. of Chester, Pa. was tested but found too fragile for aircraft applications. The support contained 10 pores/cm² and was the product of the Clyde Engineering Co. of Miami, Fla. No additional information on the physical properties of this material was available.

In order to take advantage of the large S/V characteristics of some of the supports that had excessively high pressure drops when tested with 4 segments of the same geometry in series, some tests were conducted by combining 2 low pressure drop segments with 2 high pressure drop segments. Thus, combinations of catalysts FH and KQ, and PC and FL were tested. The results showed that the total pressure drop corresponded to the sum of the individual pressure drops from each segment.

The pressure drops measured under isothermal flow conditions (pre-combustor off) increased as expected when the pre-combustor was operated. The pressure rise was due to the increased volume of gas generated by the high temperatures in the pre-combustor which increased the actual gas velocity through the catalyst. As can be seen from a review of the pressure drop data in Table VII, the difference between isothermal and reacting flow

pressure drop in a particular catalyst geometry cannot be accounted for solely by the volumetric expansion of the air. Parameters such as Reynolds Number, friction factor, geometrical shape, and the viscosity of the gas as a function of temperature must be considered to completely understand the increase in pressure drop. In all the tests performed in this study with the pre-combustor operating, the flow through each channel in the parallel-walled catalyst monolithic support was in the turbulent flow regime. Typically, for a catalyst inlet temperature and pressure of 1200 K and 0.37 MPa, respectively, the Reynolds Number was in the range of 4500-5500.

6. EFFECT OF S/V ON CONVERSION

A series of tests with six different monolith geometries were performed at a pre-combustor ϕ of 1.5 which resulted in an overall ϕ of 0.3 at the inlet to the catalyst chamber (see Table VI). The reference velocity and pressure were maintained at 25.8 m/s and 0.38 MPa, respectively. The CO and UHC concentration at the catalyst bed inlet were in the range of 300 to 800 ppm. A 1.7 kg/m³ loading of (1/1) platinum/palladium was applied to the stabilized alumina wash coat which covered the entire support. Each test was performed with four, 5.08 cm long by 5.08 cm diameter segments arranged back-to-back. The results plotted in Figure 11 show that the CO and UHC conversions can be correlated with the S/V of the support. Complete descriptions for each of the six catalysts are provided in Appendices I and II and are summarized in Table VIII.

TABLE VIII

THE EFFECTS OF CATALYST LOADING AND
SUPPORT SURFACE AREA ON UHC AND CO CONVERSION

Catalyst	m ² /m ³	Wash Coat Loading (g/m ²)	Metal Loading (g/m ²)	Percent Conversion		Support Area (m ²)	(Metal Mass Load x Area)(g)
				CO	HC		
GH	2473	52.8	0.684	87	98	1.016	0.695
FH	1937	46.3	0.870	80	97	0.796	0.692
EH	1700	46.7	0.992	72	87	0.698	0.692
JH	1537	45.0	1.10	75	92	0.632	0.693
UK	1100	110	1.53	68	74	0.452	0.692
RH	996	100	1.79	52	47	0.409	0.732

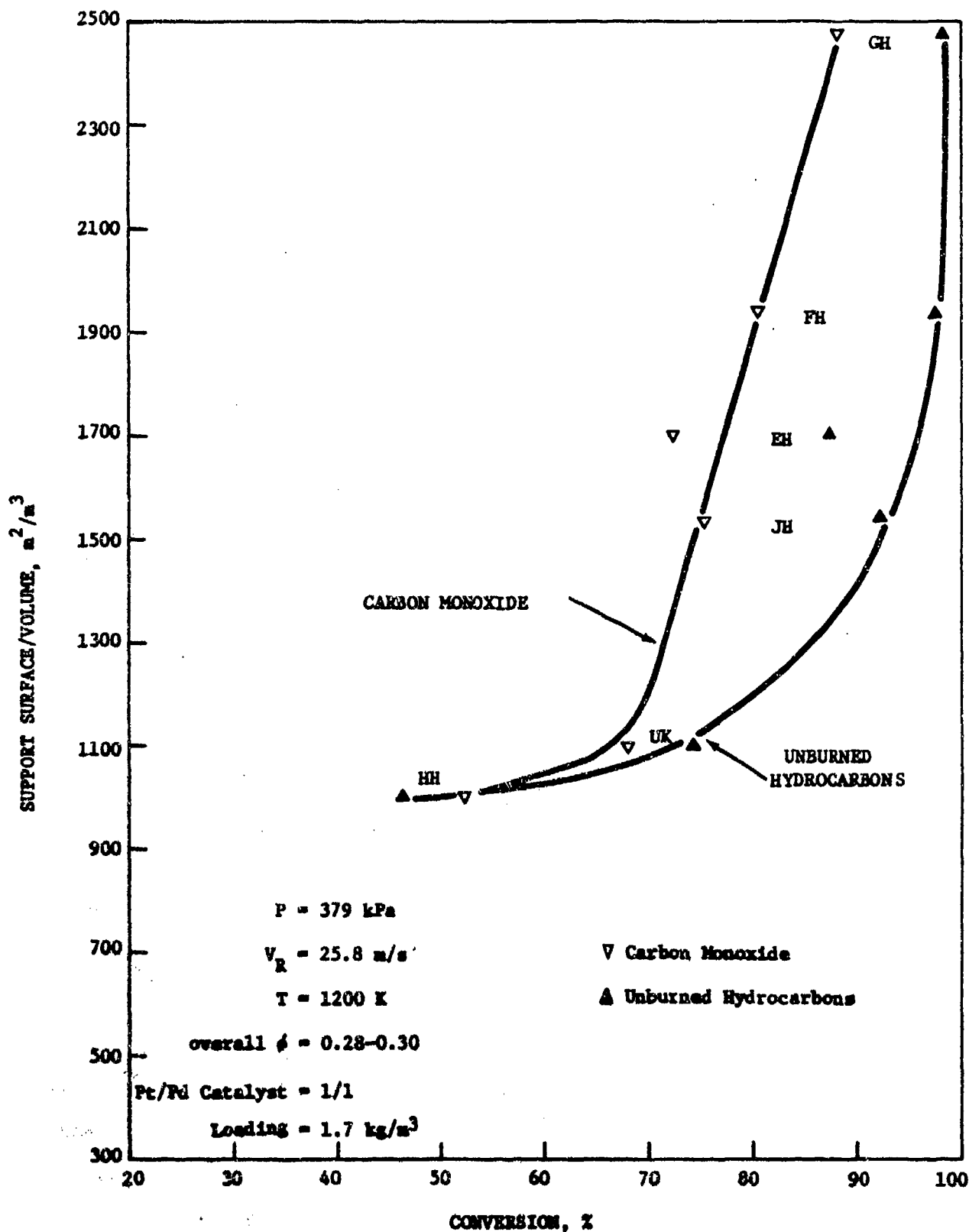


FIGURE 11: THE EFFECT OF SUPPORT SURFACE/VOLUME RATIO ON CONVERSION WITH A CONSTANT NOBLE METAL LOADING IN THE REACTOR

These data show that as the S/V ratio of the support decreased from 2473 m²/m³ to 996 m²/m³, the area of the support available for heterogeneous reactions decreased from 1.02 m² to 0.409 m² in the fixed reactor volume of 0.411 m³. In order to maintain a constant metal loading of about 0.7 g in the reactor, the amount of metal per unit area increased from 0.684 g/m² to 1.79 g/m² as area decreased. These results imply that surface area is an important consideration for UHC and CO conversion since the highest conversions occurred at the lowest metal loading per unit area. These data tend to confirm data presented in the literature that indicate that heterogeneous oxidation is diffusion controlled at 1200 K (11, 13). Thus, a desirable catalyst for CO and UHC conversion should have as large a surface area as possible without exceeding the 6% pressure drop criterion. It was also observed in these experiments that the oxidation of CO was slower than that of UHC.

In order to verify this strong effect of support surface area on UHC and CO conversions, a more detailed study was performed with catalyst FH and JH. The effect of temperature over the range of 800-1200 K on conversion was plotted in Figure 12. The slopes of the Arrhenius curves obtained for CO and UHC conversion indicated that the overall oxidation reactions were probably diffusion limited. The activation energies were 2.38 and 7.82 kJ/mol for the oxidation of CO and UHC, respectively. Interestingly, the activation energies for UHC oxidation with both catalysts were the same, and the activation energies for CO oxidation were also the same with both catalysts, but as stated previously, the oxidation of UHC was more temperature dependent than that of CO. These observations are consistent with the strong effects of surface area on UHC and CO conversions observed earlier. Other possible explanations of these results are provided by Cerkanowicz, et al., (17).

7. EFFECTS OF SUBSTRATE MATERIAL ON CO AND UHC CONVERSIONS

Physical properties of support materials such as heat capacity, thermal conductivity, and thermal expansion were considered important to the overall operation of the catalyst. A brief study was therefore made to determine the effect of these parameters on UHC and CO conversions. But, because there were only limited variations of the materials of construction currently available, the study could not be generalized. The materials that were available for testing included cordierite, silicon carbide (beta form) and nickel-chrome metal alloys. The composition of the catalysts which were fabricated using these materials are listed in Table VII, viz., UK and RA on silicon carbide, P, QU, QF and PC on metal alloys, and the remainder on cordierite.

The best comparison between cordierite and silicon carbide as supports can be made between catalysts UK and HH, both of which had similar geometrical shapes (0.31 cm round holes). Catalyst UK was made by the Norton Co. with silicon carbide, and catalyst HH was made by the General Refractories Co. with cordierite. Both catalysts were wash coated with SiO₂ stabilized alumina and impregnated with a 1.7 kg/m³ loading of (1/1) Pt/Pd. The wash coat and active metal were applied to the supports by Oxy-Catalyst, Inc. A comparison of the CO and UHC conversions in the temperature range of 1139-1166 K showed that the silicon carbide supported catalyst promoted higher conversions than the cordierite catalyst. The catalyst with the silicon carbide support achieved 16% better CO conversions and 28% better UHC conversions, under similar test conditions, than the catalyst with the cordierite support. Although insufficient data are available, preliminary indications are that silicon carbide is more active in promoting the oxidation reactions. It is doubtful that a direct catalytic effect can be attributed to

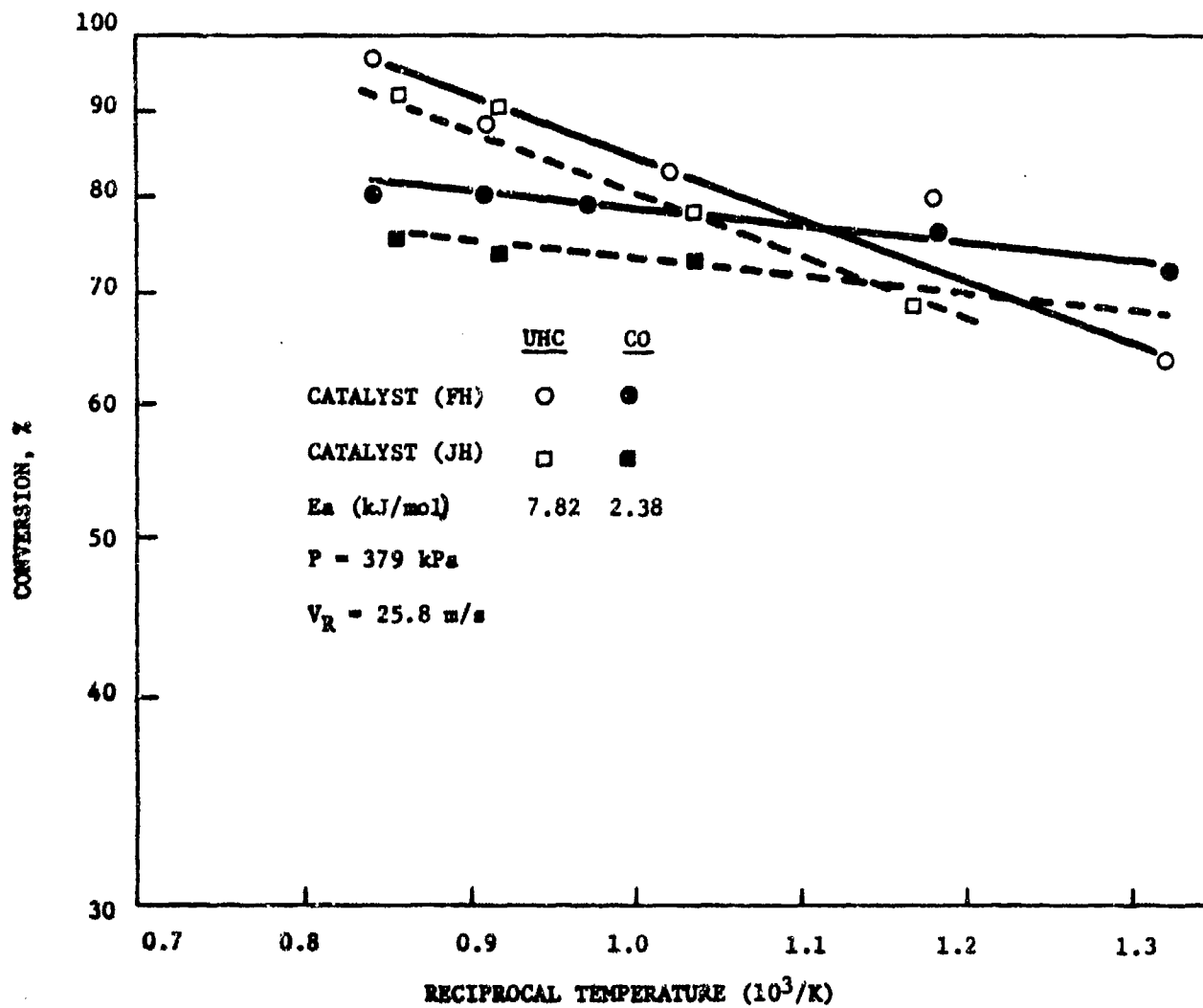


FIGURE 12: ARRHENIUS PLOT OF CO AND UHC OXIDATION ON Pt/Pd (1/1) CATALYSTS OF DIFFERENT GEOMETRIES

the silicon carbide, but as a result of the larger thermal conductivity of silicon carbide than that of cordierite, one may speculate that better heat transfer may have contributed to the higher activity of the silicon carbide catalyst. The thermal conductivity of beta-silicon carbide is $0.213 \text{ W/m}^\circ\text{C}$ at 1300 K, while cordierite had a thermal conductivity of $0.071 \text{ W/m}^\circ\text{C}$ at 1200 K. The specific heats of both materials were similar, viz., $0.8\text{-}1.3 \text{ kJ/kg C}^\circ(6)$.

During the testing of the silicon carbide catalysts, it was apparent that the response to thermal changes within the catalyst was very rapid. Thus, when the overall ϕ of the system was varied, a "step-change" in the gas temperature within the support was observed immediately. With cordierite, on the other hand, the gas temperature within the support changed much more gradually in response to the change in ϕ .

The effect of the silicon carbide support in catalyst RA (rare earth oxide catalyst) cannot be compared directly with other catalysts since catalyst RA contained no wash coat. When compared with catalyst KR, a cordierite supported rare earth oxide catalyst with an alumina wash coat, RA achieved slightly higher UHC conversion, but much lower CO conversion. In view of the few SiC supported catalysts tested and the scatter of the data, no definitive justification for specifying one substrate over another could be made.

A comparison of the effects of cordierite and metal foil supports on the conversion of CO and UHC cannot be made from the available data since the only successful metal supported catalyst had a S/V of $4100 \text{ m}^2/\text{m}^3$ which is nearly twice as great as the largest surface/volume of $2473 \text{ m}^2/\text{m}^3$ for the available cordierite supported catalyst. However, as was observed with the silicon carbide catalysts, the thermal response of metal supports was much superior to cordierite based catalysts.

Some comments on the subject of durability of catalyst supports at high temperatures are needed. Evidence of the potentially disastrous effect of high temperature on supports was obtained early in the experimental phase of the program. A severe problem concerned with melting of cordierite catalysts was encountered. The catalyst was observed to melt or deform when an ignition delay in the pre-combustor was experienced. Usually, a faulty ignition electrode was responsible for the ignition lag which could be on the order of a few seconds. During the period before ignition of the pre-combustor, the unburned JP-4 was deposited on the surfaces of the catalyst. Some fraction of the liquid fuel was adsorbed by the support material or wash coat or both. Subsequent ignition of the pre-combustor gave rise to near stoichiometric flame temperatures on the surface of the catalyst which caused the support to melt or become sufficiently plastic to be badly deformed. In order to determine if this severe thermal condition was being catalytically promoted, a cordierite support without wash coat or catalyst materials was tested. The support melted even though the measured gas temperatures within the support never exceeded 1200 K, which is substantially less than the melting point of cordierite. It was therefore concluded that it was not necessary for the observed phenomena to be catalytically promoted.

It was thought that the problem associated with faulty ignition could be mitigated if the catalyst support was made of a high melting point and high thermal conductivity material. However, catalyst QF, which contained a high temperature metal alloy foil support melted when an ignition delay of the pre-combustor occurred. Again, as had been observed in tests with cordierite supported catalysts, the measured gas temperature never exceeded 1200 K within the catalyst bed or at the entrance of the bed. The melting point of the metal alloy, although not determined, was estimated to be about 1800 K.

During the tests with silicon carbide catalyst, no melting or deformation of the support was observed. If an ignition lag in the pre-combustor did occur, there was no way of detecting it within the catalyst with the employed techniques, since the useful operating temperature of silicon carbide in an oxidizing atmosphere is presumed to be in excess of 1900 K.

8. EFFECTS OF WASH COAT MATERIALS ON CO AND UHC CONVERSIONS

Activity of supported catalysts is significantly enhanced by the application of a high surface area material to the surfaces of the support. The BET (Brunauer, Emmett and Teller (18)) surface areas of gamma-alumina wash coats applied to some of the candidate catalysts before exposure to gas temperatures above 1200 K were measured by Oxy-Catalyst Inc., to be on the order of 140-160 m²/g (19). After exposure to high temperatures, the surface areas of unstabilized wash coat materials were reduced to 1.0 m²/g. However, depending upon the concentration and preparation techniques employed, and type of stabilizers in the wash coat, the surface area of the alumina could be maintained at values approaching 10 m²/g. The various wash coats applied to the catalysts tested in this program are listed in Table IX.

TABLE IX

WASH COAT COMPOSITIONS

- Al₂O₃ + SiO₂
- NiO + SiO₂
- ZrO₂ + CoO
- Al₂O₃ + CaO₂
- Al₂O₃ + CuO + Cr₂O₃ + MnO₂

Although BET surface areas were not measured after the catalysts were exposed to high temperature oxidizing streams, some rough indications of the effectiveness of the wash coat on CO and UHC conversions were discerned from the results. A comparison of the UHC and CO conversions at 1200 K for catalysts KP and KU, which were 0.127 irregular rectangle opening cordierite monoliths from the W. R. Grace Co., showed that for the same Pd loadings, the ZrO₂ + CoO wash coated catalyst had less activity than the Al₂O₃ + CuO + Cr₂O₃ + MnO₂ wash coated catalyst. It should be noted that the catalyst KP had twice as much wash coat material as catalyst KU. Thus, an alternate explanation might be that excessive wash coat material is detrimental to the activity of the catalysts.

The effect of wash coat loading for the catalysts having the same noble metal loading, but different S/V, can also be seen when comparing catalysts GH and UK. Both catalysts contain approximately 13 g of noble metal per kg of wash coat, but catalyst UK contained twice the wash coat loading (on an area basis) and achieved approximately 75% the conversion of catalyst GH for UHC and CO. A similar observation can be made for catalysts FH and HH. Both catalysts contained about 17 g of noble metal per kg of wash coat, but catalyst HH had about twice the wash coat loading, i.e., 100 g/m² as compared to 46 g/m² for catalyst FH. In this case, catalyst HH converted only about half the CO and UHC that FH achieved. It should be noted that in the comparison of GH and UK, and FH and HH, there was also a S/V change of about 2 for each pair. Thus the possible wash coat effect cannot be fully disassociated from a S/V effect.

A comparison of the effect of dissimilar wash coat materials on CO and UHC conversions can be made with catalysts KT and KU. Both catalysts had similar support geometries but different noble metal loadings and wash coats. Catalyst KT had a noble metal loading which was 1.31 kg/m³, consisting of a 23/1 (by wt.) mixture of Pt/Rh on a NiO + SiO₂ wash coat. Catalyst KU had a 0.39 kg/m³ loading of palladium on an Al₂O₃ + CuO + Cr₂O₃ + MnO₂ wash coat. Although catalyst KU had 1/3 the noble metal loading of catalyst KT, the CO and UHC conversions measured at 1200 K for catalyst KU were 19 and 22% greater, respectively, than the conversions observed for catalyst KT. Since the activities of platinum and palladium for hydrocarbon oxidation in the temperature range of 1000-1200 K would not be expected to be vastly different, it appeared that the difference between the CO and UHC conversions in catalysts KT and KU were due to variations in wash coat formulations.

Sufficient test data were not available to allow for significant comparisons to be made on the effect of CeO and SiO₂ in Al₂O₃ on UHC and CO conversions. Also, because of the nature of this program, which was primarily to evaluate a large number of available catalysts, no detailed results were sought on the effects of wash coat formulations on catalytic activity. The results presented above are very speculative in view of the large number of variables that can affect catalyst activity.

9. THE EFFECTS OF CATALYST FORMULATION ON CO, UHC AND NO_x CONVERSIONS

The preceding sections discussed how the effectiveness of oxidation catalysts depends on various chemical and physical parameters associated with the support material, its geometrical configuration, and the wash coat formulation. None of these parameters, by themselves, are as important in the oxidation of a hydrocarbon as the type of active catalytic metal which is impregnated into the wash coat. To understand the activity of catalytic metals in hydrocarbon oxidation reactions, each of the candidate metals or combinations of metals were tested over the same range of gas temperatures, equivalence ratios, and pressures. Having previously obtained indications of the effects of the catalyst support (material, wash coat, etc.) on UHC and CO conversions, the specific effect of the catalytic materials and their loadings on the conversion of potential pollutants was sought. Table VII summarizes the experimental test results obtained for all the candidate catalysts under the test conditions listed in Table III under condition 1.

The activity of noble metal catalysts on CO and UHC conversion is compared in Table X. Based on the data in Table X, it can be concluded that within experimental scatter there is little apparent advantage in using either Pt or Pd as the active metal. The two other noble metals tested were Rh and Ir, and they show lower activity than Pt and Pd. Comparing catalysts KT which contains 0.63 g/m^2 Pt/Rh = 23, catalysts KU containing 0.19 g/m^2 Pd and KN containing 1.33 g/m^2 Pt/Pd = 2.5, one can see that KU contains an intermediate noble metal loading but is the least effective oxidation catalyst of the three. Similarly, when comparing catalysts FH and FD + FE which contained about 0.9 g/m^2 noble metals each, it can be seen that the Pt/Ir = 1 catalyst (FD + FE) was less active than the Pt/Pd = 1 catalyst (FH). It must be emphasized that these results are presented to indicate apparent trends and should not be used to eliminate any one of the noble metals from consideration as a catalytic component. None of the results presented above were duplicated, nor were corrections introduced for other factors such as wash coat composition to clearly focus on the metal activity. In general, one can say that activity improved with increased noble metal loading and increased S/V. It is also apparent from Table X that catalysts that are very active for CO oxidation are also very active for UHC oxidation. The CO conversion data from all experiments was compared against the UHC conversion using a linear least squares regression technique and was found to correlate well. The fraction of explained variance (R^2) was 70%, i.e., 70% of the variation is accounted for by the line. Figure 13 presents a plot of conversion of CO vs. conversion of UHC. It can be seen in Figure 13 that UHC conversions are generally slightly higher than CO conversions but correlate along the diagonal. Thus, as inferred before, UHC conversion seems to occur at a higher rate than CO at the same operating conditions.

TABLE X
EFFECT OF NOBLE METAL COMPOSITION ON OXIDATION ACTIVITY

<u>Catalyst</u>	<u>S/V</u> <u>m⁻¹</u>	<u>Conversion</u>		<u>Wash</u> <u>Coat</u> <u>g/m²</u>	<u>Metal</u> <u>Loading</u> <u>g/m²</u>	<u>Metal Ratio</u>
		<u>CO</u> <u>%</u>	<u>UHC</u> <u>%</u>			
KT	2109	69	70	52.3	0.63	Pt/Rh = 23
KN	2109	82	86	39.2	1.33	Pt/Pd = 2.5
KX	2109	82	67	60.0	2.60	Pt/Pd = 1
KU	2109	82	92	37.5	0.19	Pt/Pd = 0
KQ	2109	91	96	44.1	1.55	Pt/Pd = 0
FH	1937	80	97	46.3	0.87	Pt/Pd = 1
FZ	1937	75	74	49.2	0.28	Pt/Pd = 1
FY	1937	78	83	49.2	1.70	Pt/Pd = 0
FV	1937	74	62	49.2	1.69	Pt/Pd = 0
FG	1937	64	86	40.5	0.20	Pt/Pd = 0
FD + FE	1937	50	60	47.8	0.88	Ir/Pd = 1
JR	1537	75	92	45.0	1.10	Pt/Pd = 1
JG	1537	40	60	49.6	0.25	Pt/Pd = 0

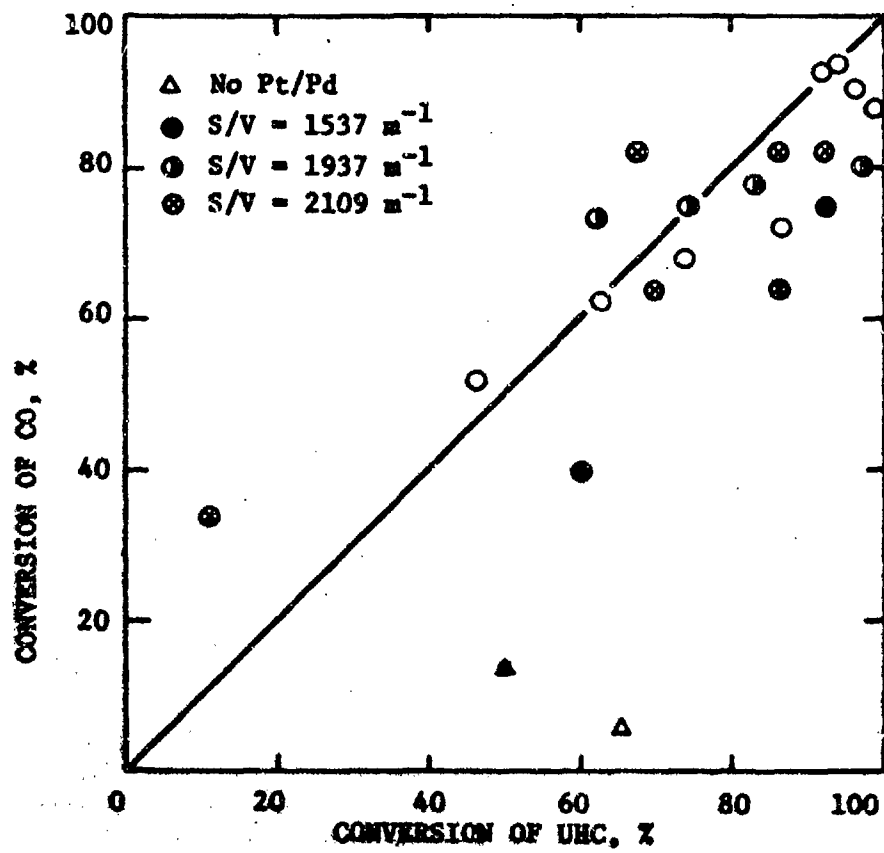


FIGURE 13: COMPARISON OF CO CONVERSION WITH UHC CONVERSION

10. THE TEMPERATURE DEPENDENCY OF CATALYST ACTIVITY FOR UHC AND CO CONVERSION AND NO_x PRODUCTION

To determine the temperature dependency of catalytic oxidation of UHC, CO and NO_x precursors as a function of catalysts, a majority of the catalysts described in Table VII and Appendix II were tested over a range of inlet temperatures from 800 to 1200 K. The pre-combustor air inlet was maintained at 25 m/s and the combustion chamber pressure was held constant at 0.37 MPa. The gas temperature at the catalyst bed inlet was varied by maintaining constant air flows but varying the JP-4 flow rate. As was discussed in Section III, the overall equivalence ratio of the gas mixture entering the catalyst was determined by the equivalence ratio of the pre-combustor primary combustion zone, which was varied from 1.5 to 0.6. The corresponding range of overall ϕ was 0.3 to 0.12. These experimental test conditions simulated the aircraft gas turbine "idle" power setting. The operating parameters which described the various power settings of aircraft gas turbine engines were given in Table II.

The temperature dependency of catalyst activity toward UHC, CO and NO_x conversions are given in Figures 14 through 32. The plots were prepared to show the percent change in UHC, CO and NO_x concentrations experienced by the pre-combustor gases traversing a 20.3 cm long catalyst bed. Gas sample probe measurements at the inlet and outlet of the catalyst bed were obtained as a function of catalyst bed inlet temperature. The ordinate is the percentage change in concentration rather than the absolute concentration, because the concentration of CO, UHC and NO_x entering the catalyst varied slightly due to fluctuations in the fuel flow rate, which were on the order of 5% of the indicated rotameter flow. The air flow rates were corrected for temperature changes but uncertainties in the rotameter readings were about 5% of the total air flow rate.

A review of the temperature dependency plots for each catalyst shows that an increase in the NO_x concentration, without exception, occurred probably as a result of the catalytic oxidation of nitrogenous molecules which were formed in the pre-combustion zone. It is believed that nitrogen bearing molecules other than NO or NO₂, such as NH₃ or HCN, were formed in small concentrations in the pre-combustion zone. The catalytic oxidation of NH₃ and HCN, especially over noble metal catalysts, may have been nearly complete, with the result that the measured NO_x concentrations at the catalyst exit were greater than the values measured at the catalyst inlet. Tests conducted with inert catalyst supports or a catalyst chamber void of all material showed that homogeneous oxidation reactions did not cause the NO_x concentration to increase. In general, it was observed that if a particular catalyst achieved high CO and UHC conversions, then the increase in NO_x across the catalyst was also very large, on the order of 45-50%. In referring to Figures 16 and 17 which describe the activity of noble metal catalysts FI and KQ, it can be seen that the NO_x concentration curves are not very temperature dependent. The fact that the maximum increase in NO_x

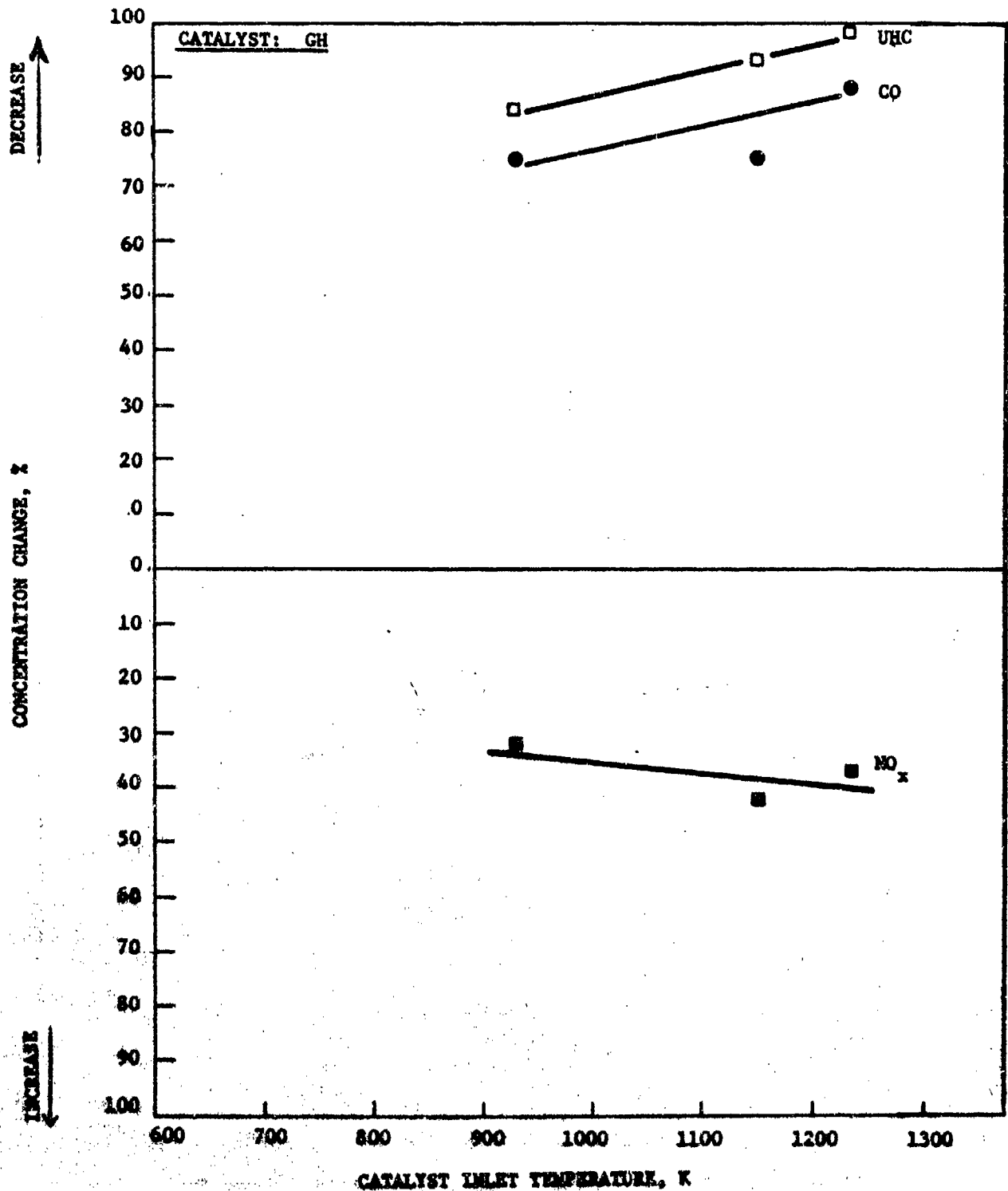


FIGURE 14: EFFECTS OF CATALYST INLET TEMPERATURE ON CO, UHC AND NO_x CONVERSION

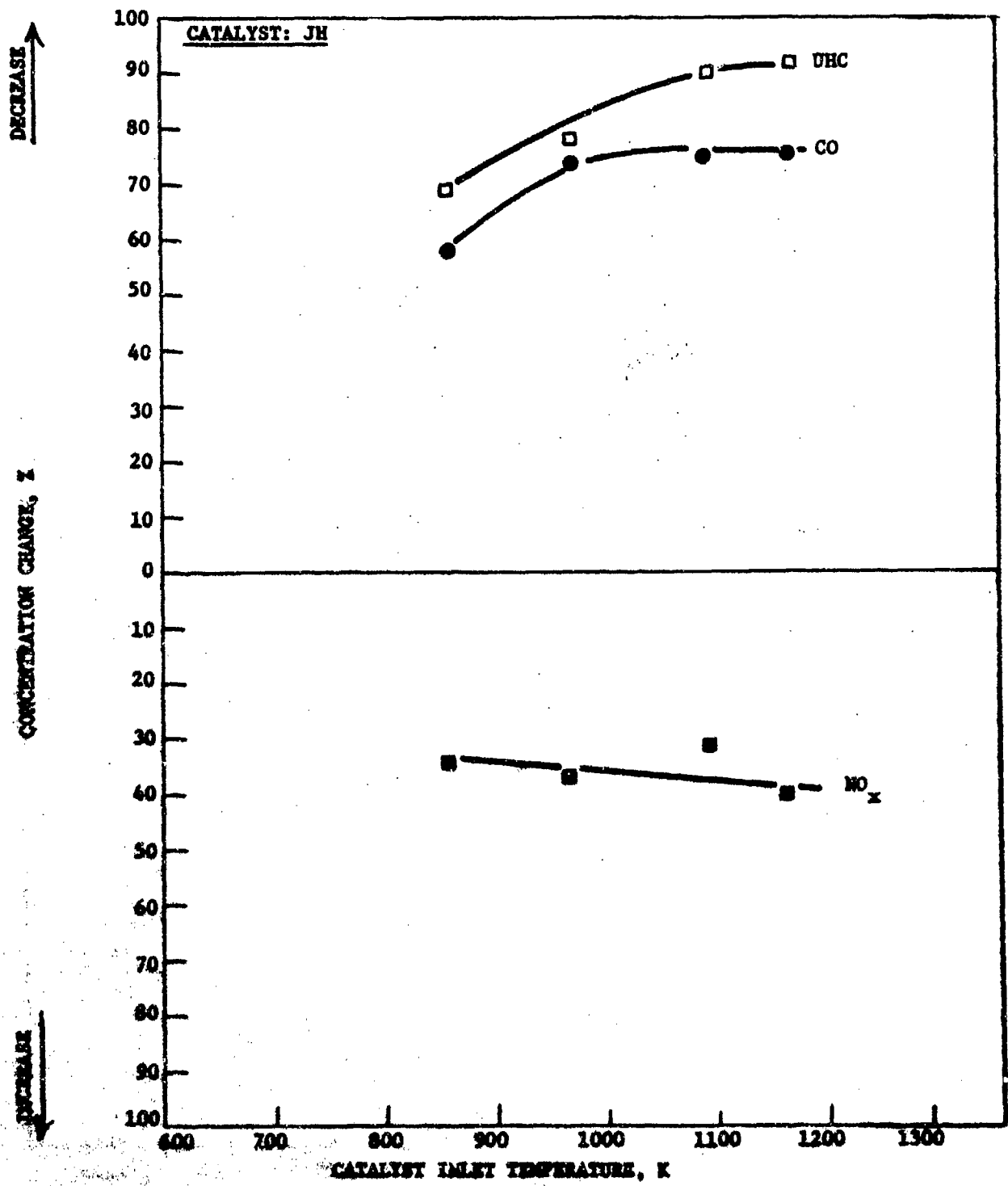


FIGURE 15: EFFECTS OF CATALYST INLET TEMPERATURE ON CO, UHC AND NO_x CONVERSION

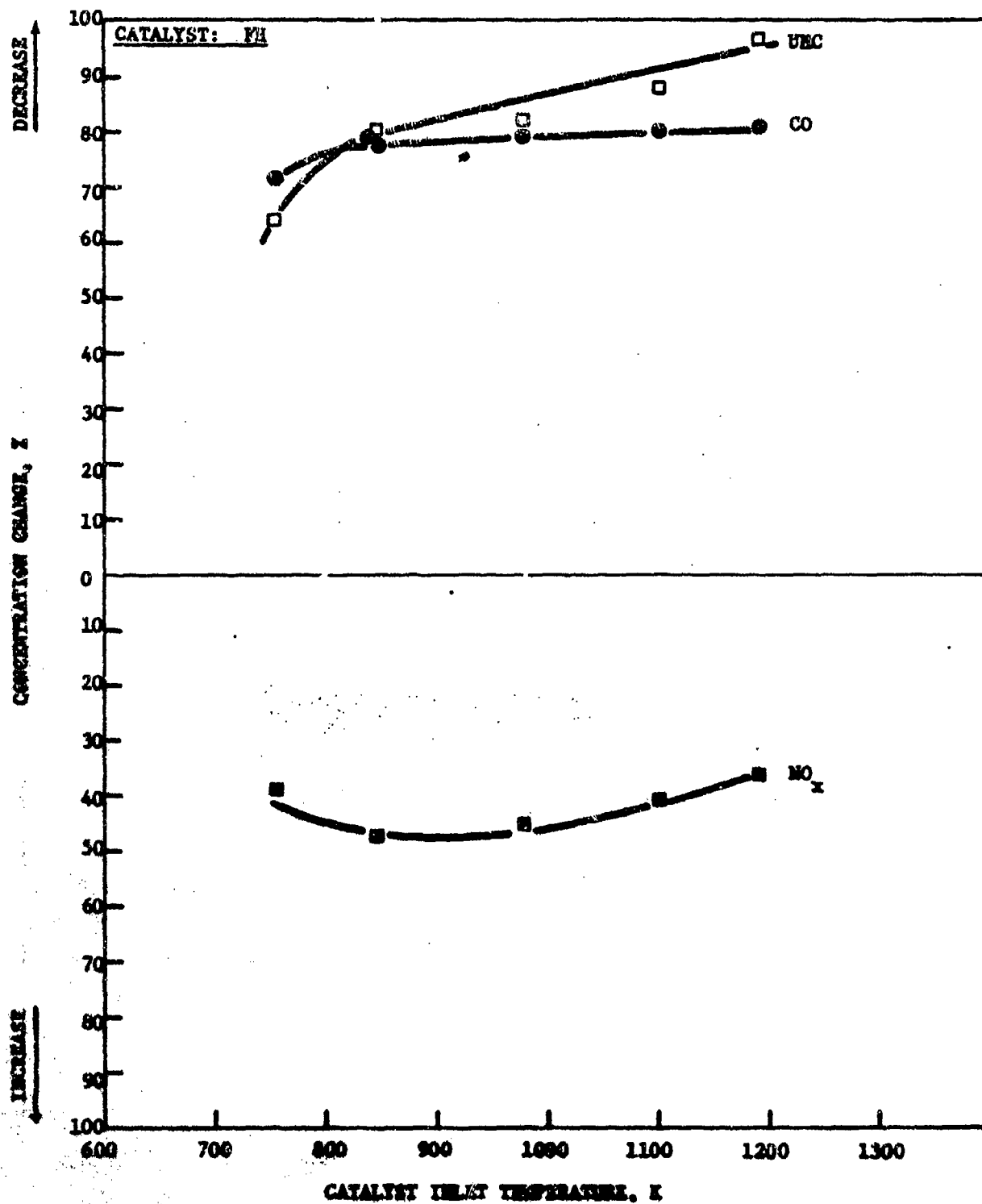


FIGURE 16: EFFECTS OF CATALYST INLET TEMPERATURE ON CO, UMC AND NO_x CONVERSION

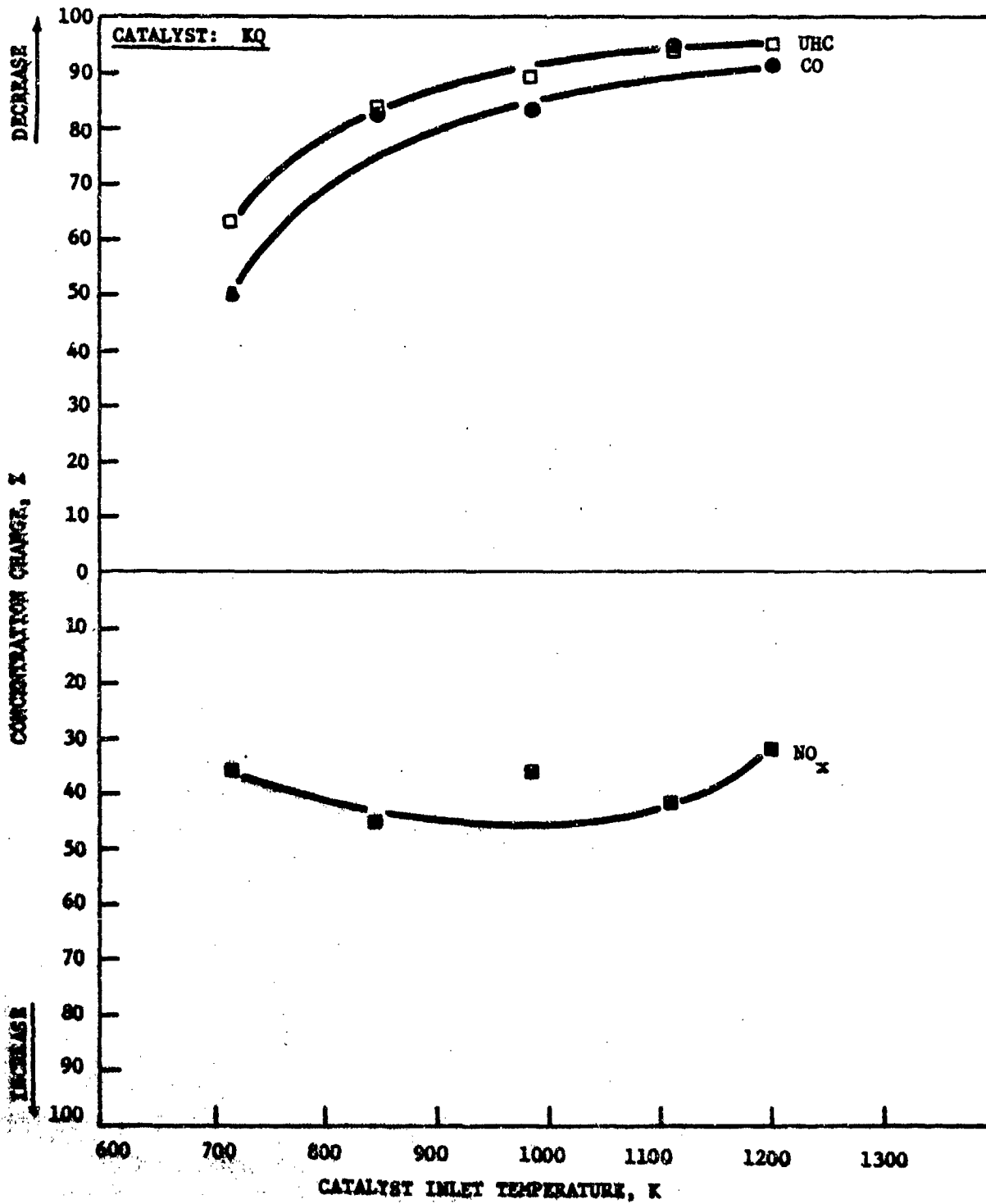


FIGURE 17: EFFECTS OF CATALYST INLET TEMPERATURE ON CO, UHC AND NO_x CONVERSION

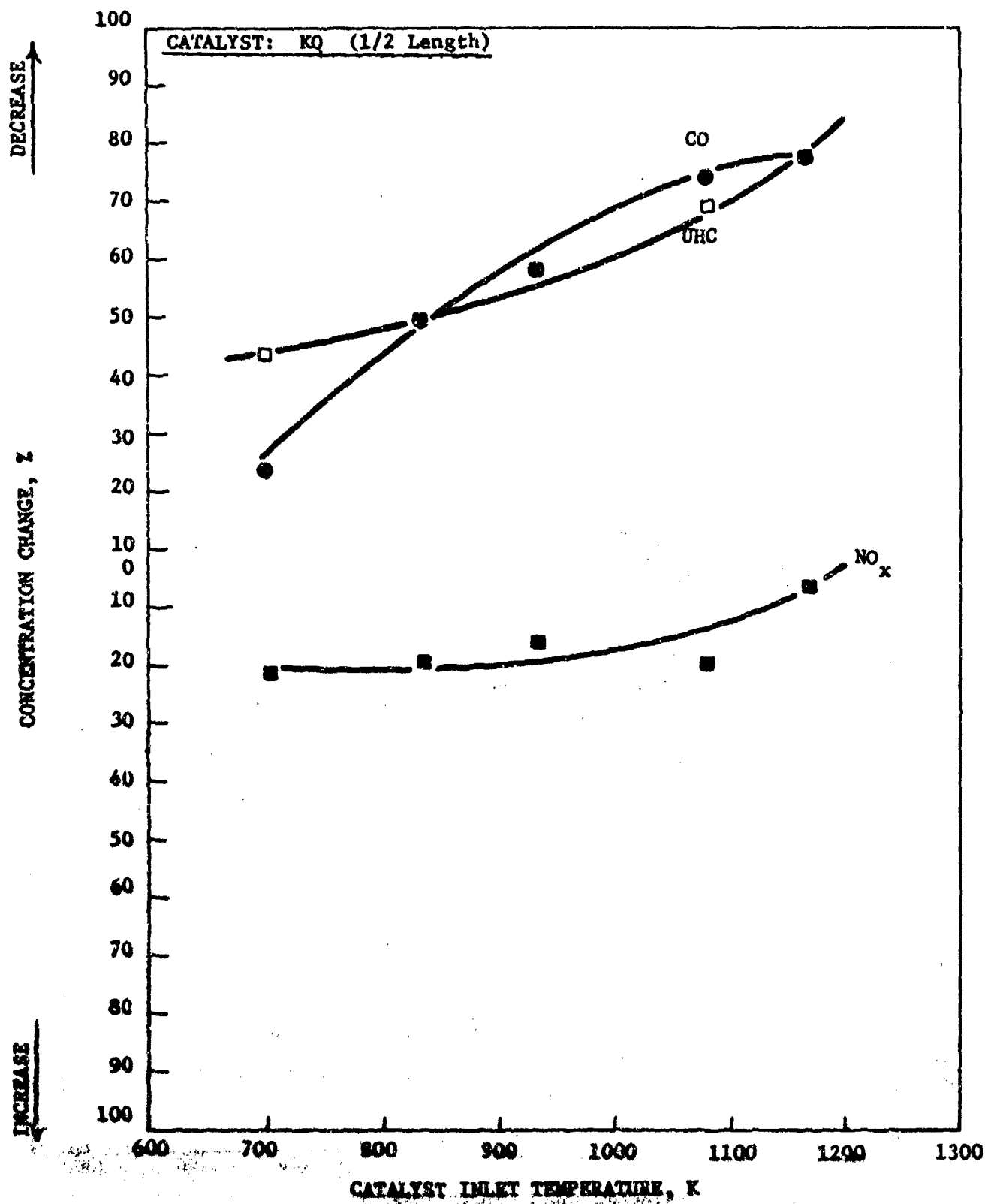


FIGURE 18: EFFECTS OF CATALYST INLET TEMPERATURE ON CO, UHC AND NO_x CONVERSION

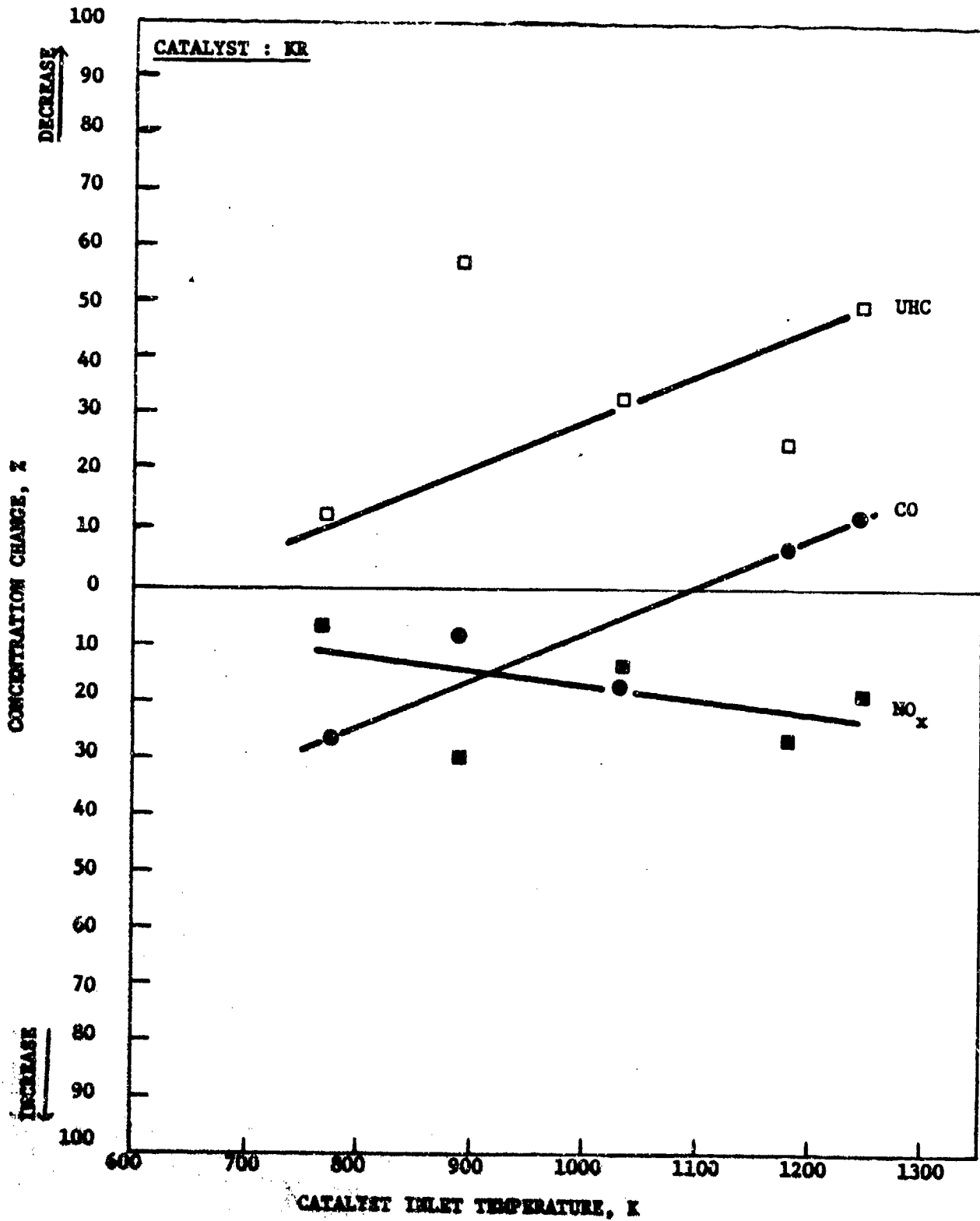


FIGURE 19: EFFECTS OF CATALYST INLET TEMPERATURE ON CO, UHC AND NO_x CONVERSION

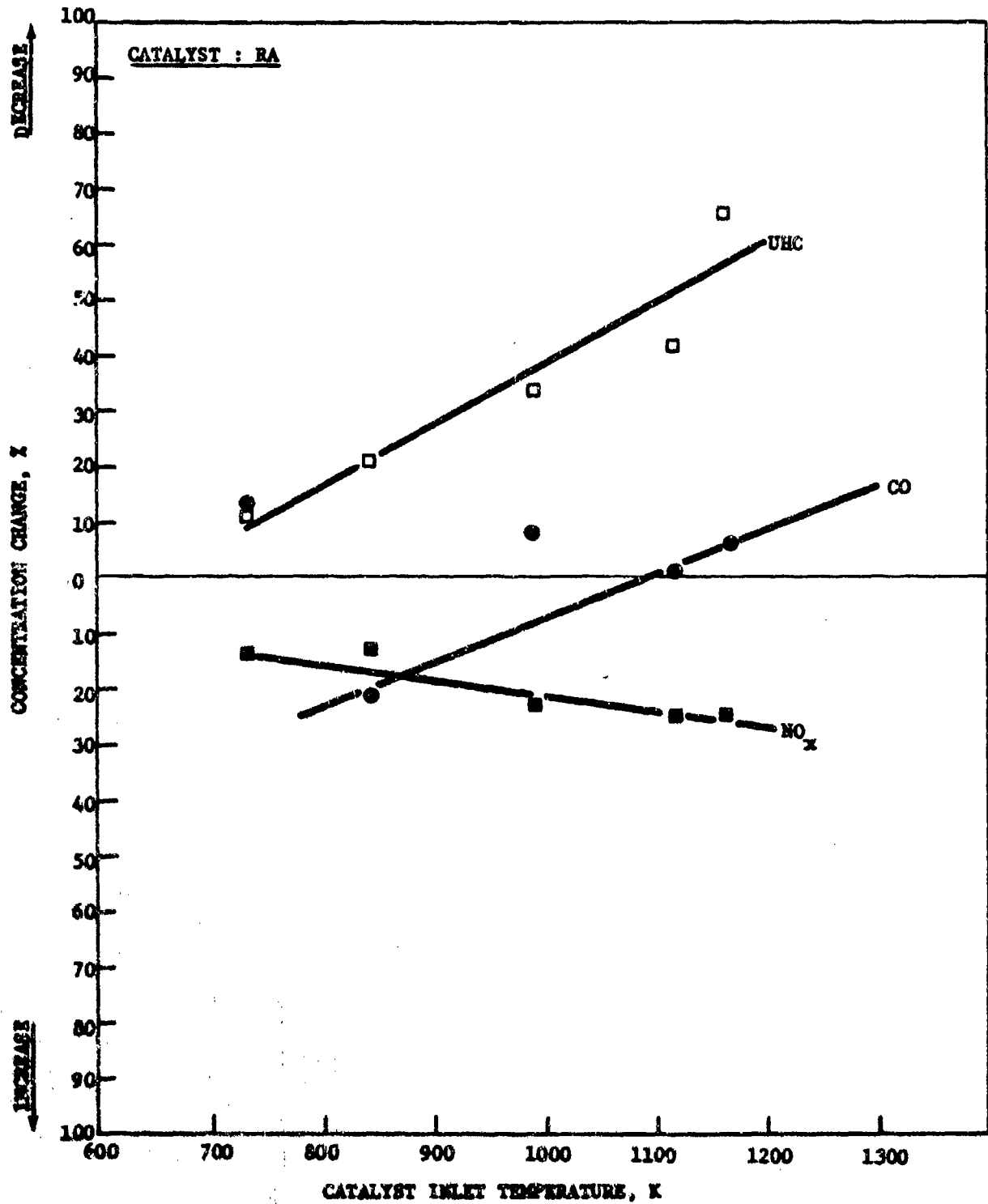


FIGURE 20: EFFECTS OF CATALYST INLET TEMPERATURE ON CO, UHC AND NO_x CONVERSION

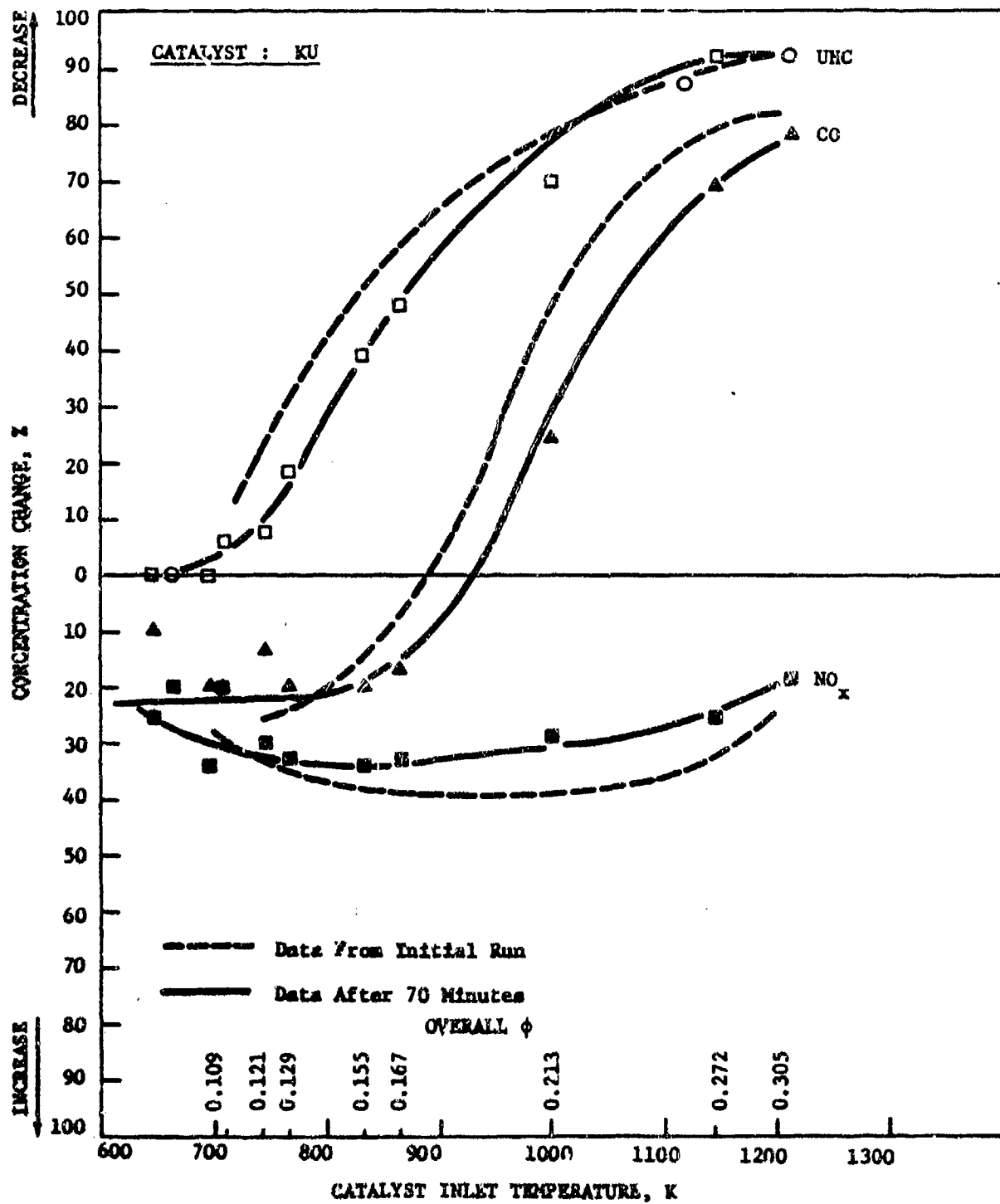


FIGURE 21: EFFECTS OF CATALYST BED INLET TEMPERATURE ON CO, UHC AND NO_x CONVERSION

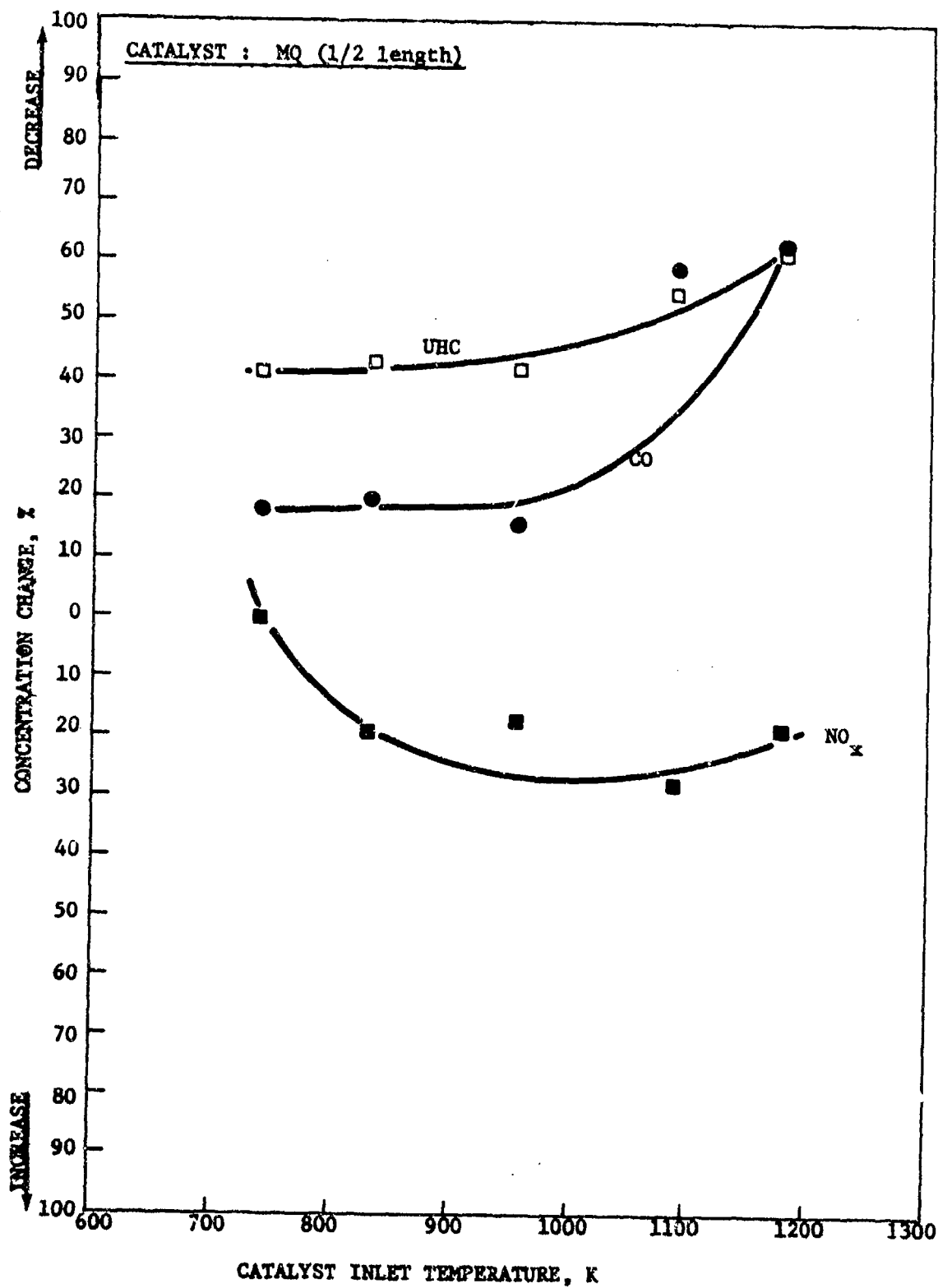


FIGURE 22: EFFECTS OF CATALYST INLET TEMPERATURE ON CO, UHC AND NO_x CONVERSION

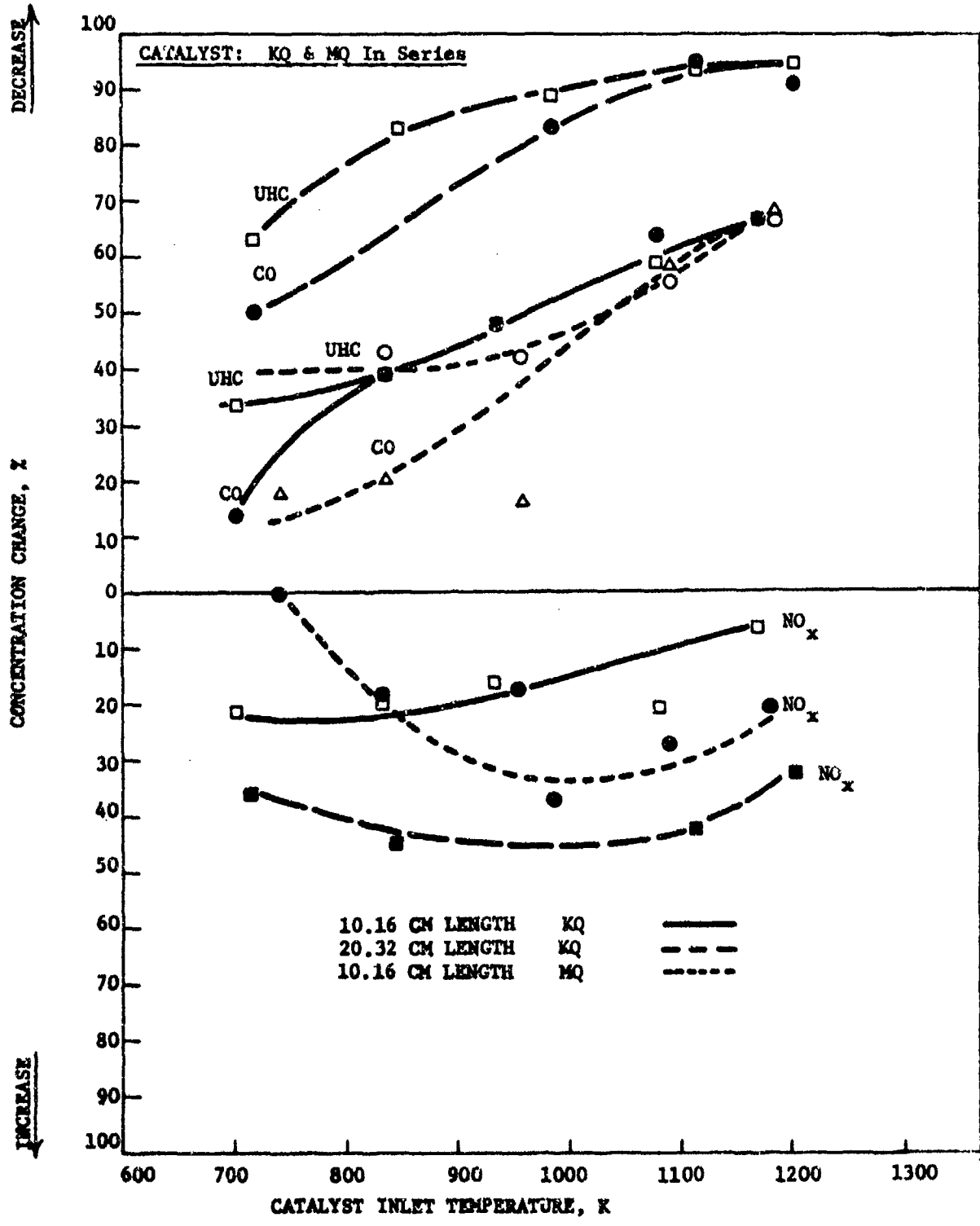


FIGURE 23: EFFECTS OF CATALYST INLET TEMPERATURE ON CO, UHC AND NO_x CONVERSION

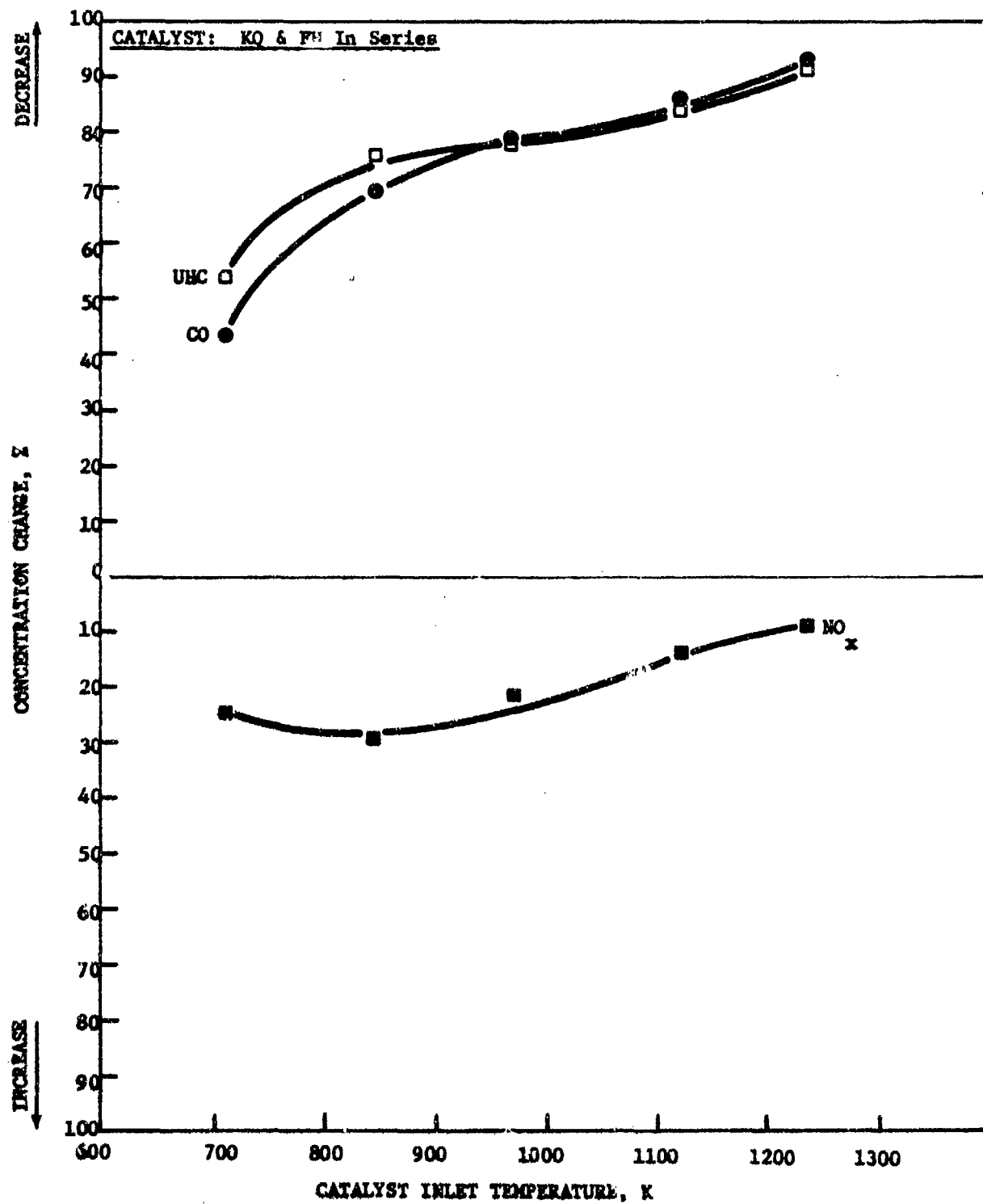


FIGURE 24: EFFECTS OF CATALYST INLET TEMPERATURE ON CO, UHC AND NO_x CONVERSION

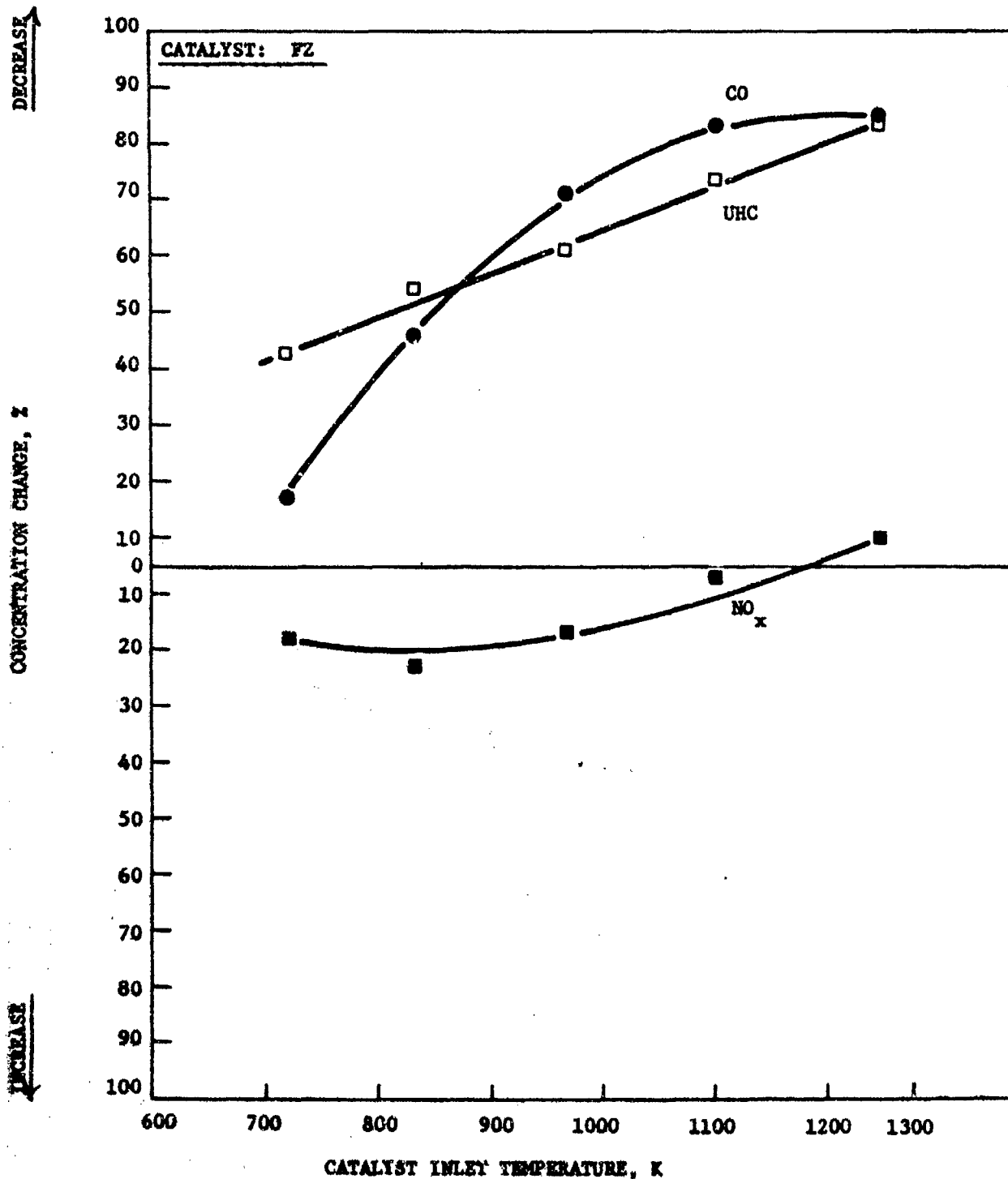


FIGURE 25: EFFECTS OF CATALYST INLET TEMPERATURE ON CO, UHC AND NO_x CONVERSION

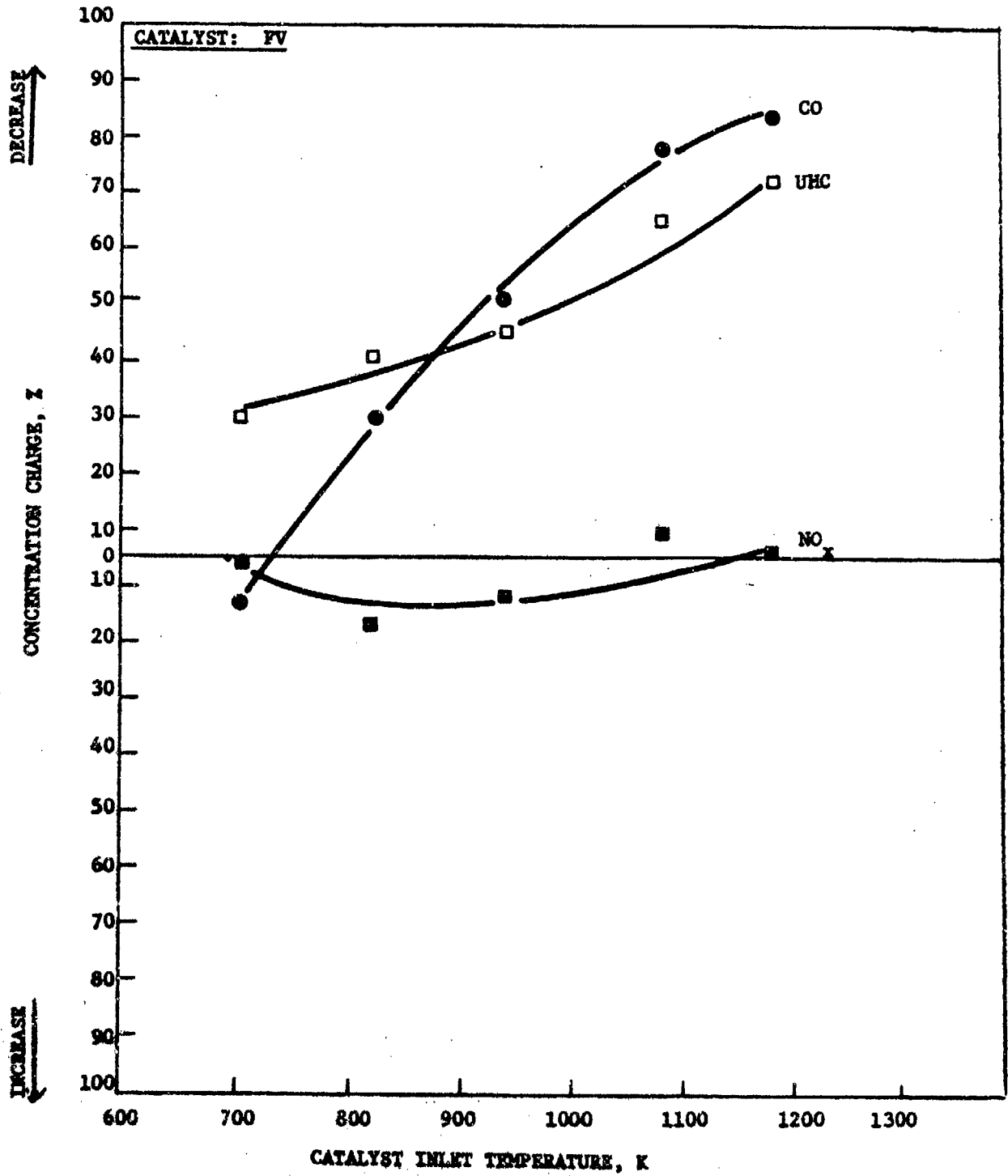


FIGURE 26: EFFECTS OF CATALYST INLET TEMPERATURES ON CO, UHC AND NO_x CONVERSION

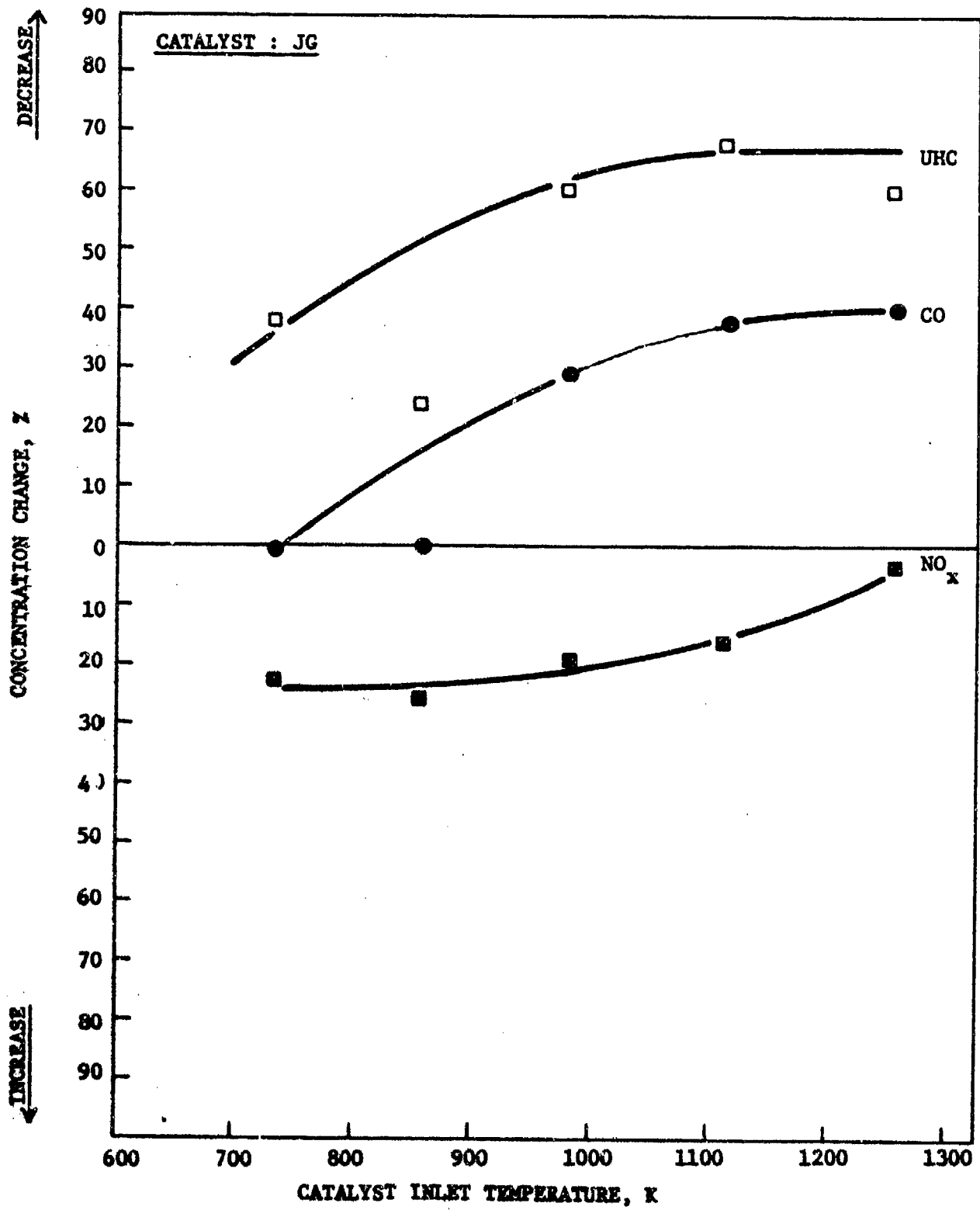


FIGURE 27: EFFECTS OF CATALYST INLET TEMPERATURE ON CO, UHC AND NO_x CONVERSION

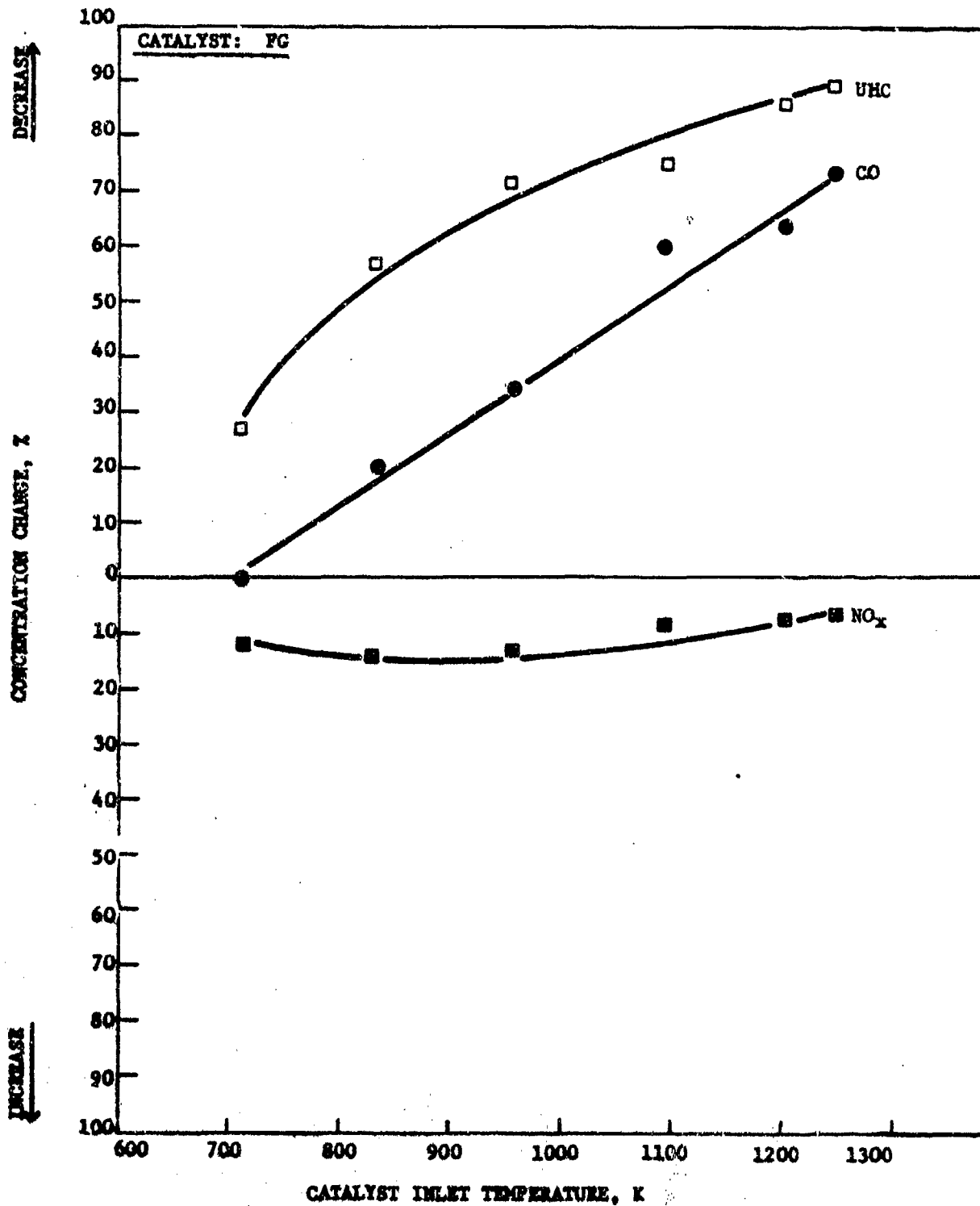


FIGURE 28: EFFECTS OF CATALYST INLET TEMPERATURE ON CO, UHC AND NO_x CONVERSION

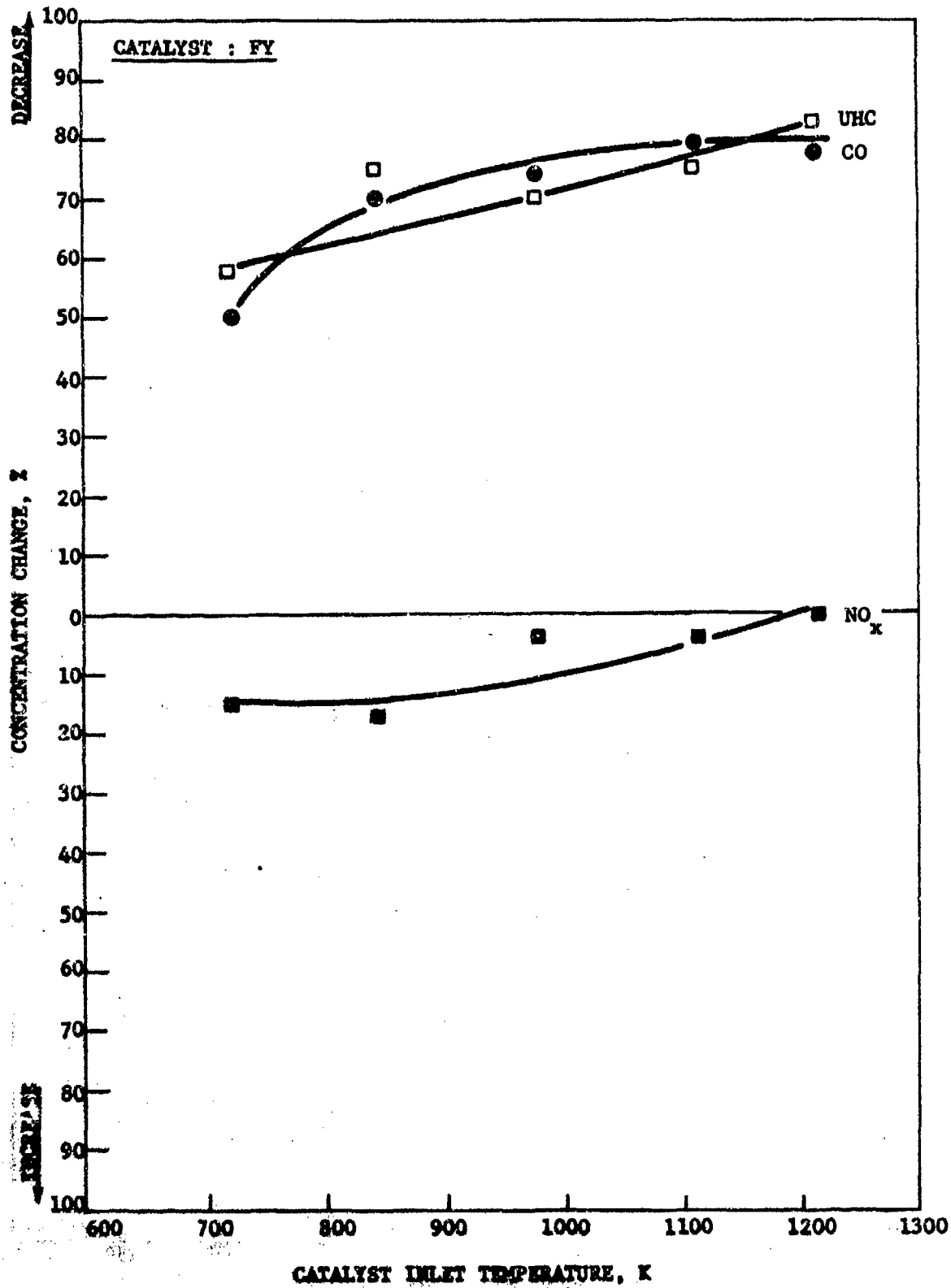


FIGURE 29: EFFECTS OF CATALYST INLET TEMPERATURE ON CO, UHC AND NO_x CONVERSION

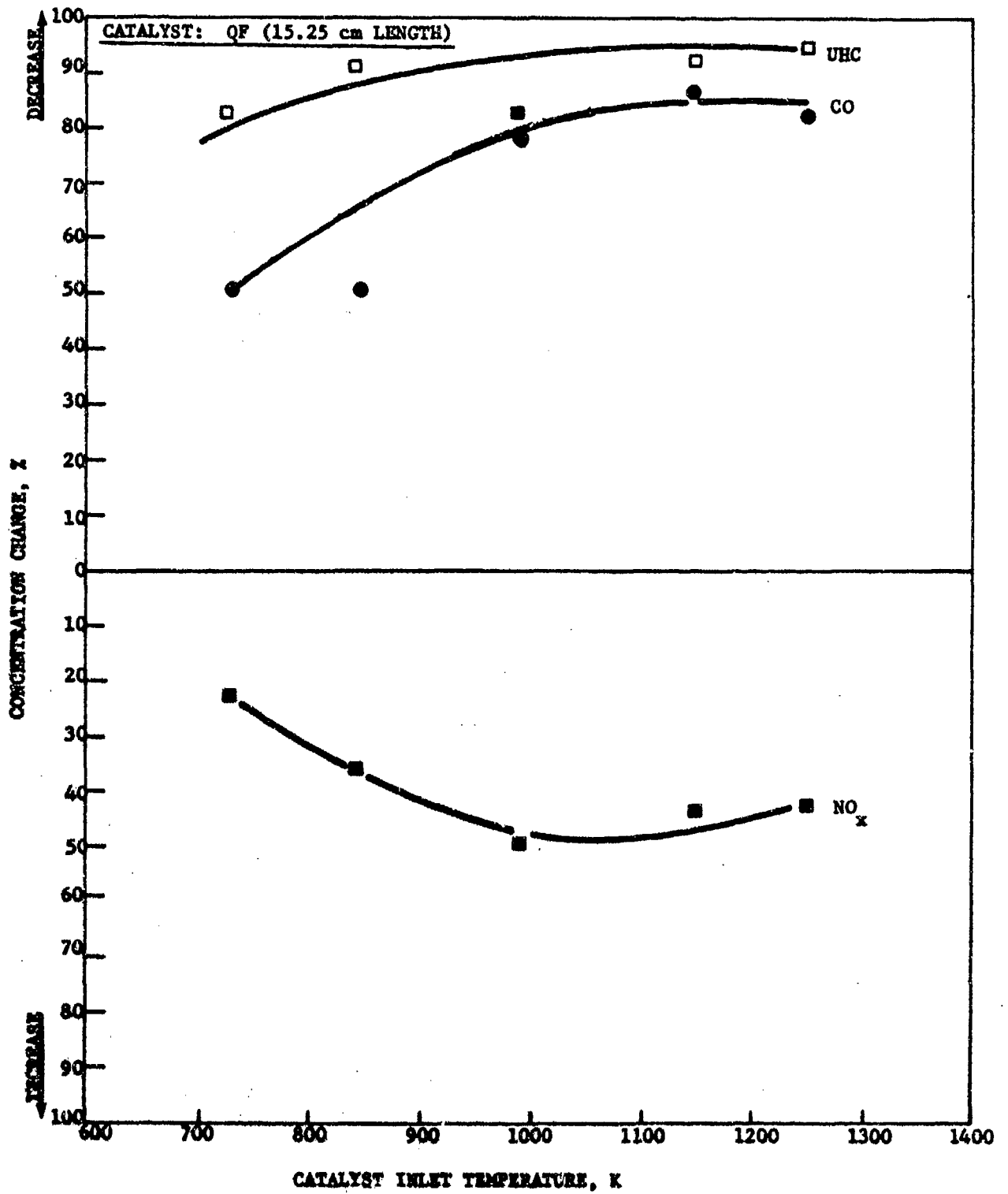


FIGURE 30: EFFECTS OF CATALYST INLET TEMPERATURE ON CO, UHC AND NO_x CONVERSION

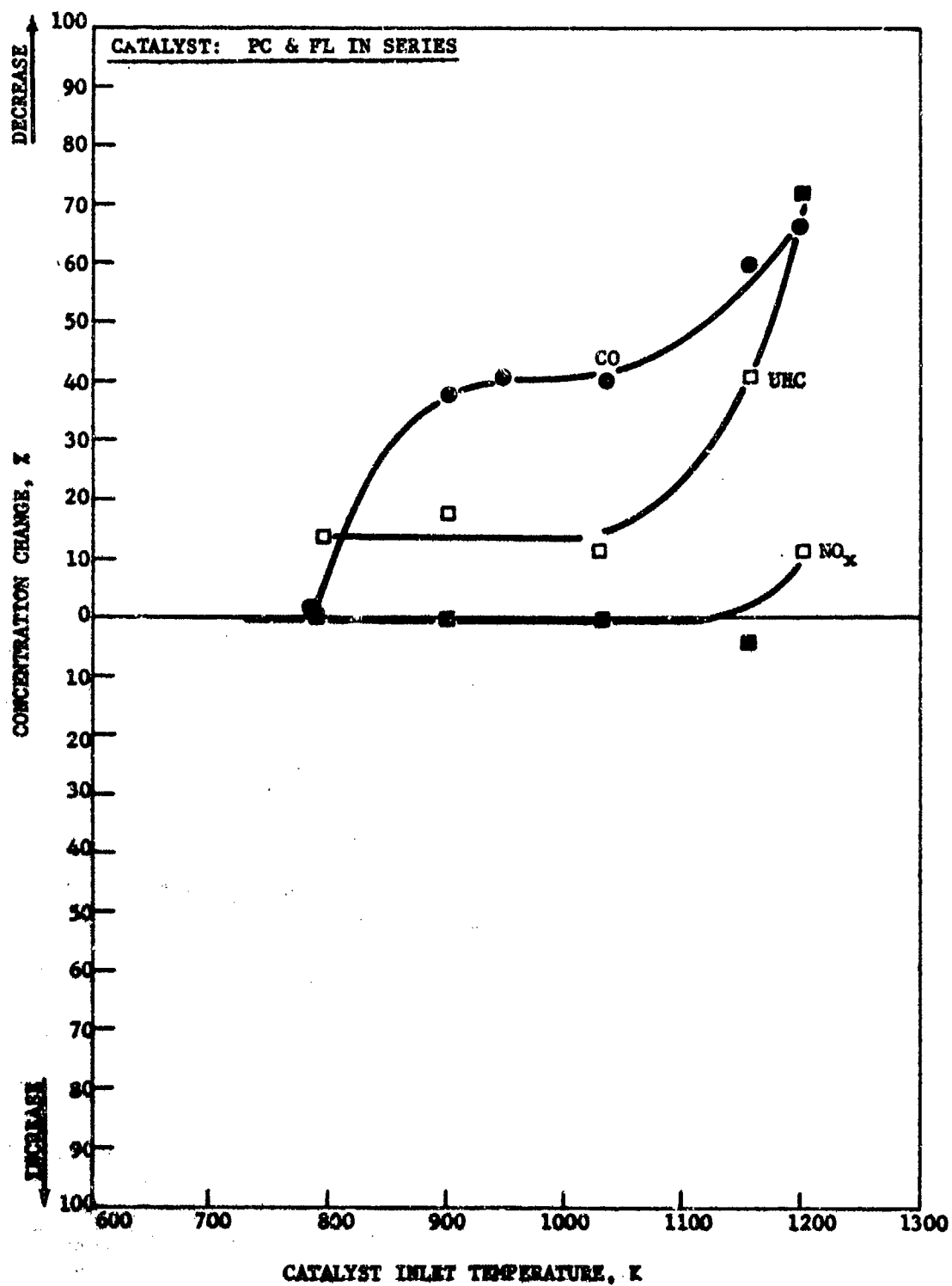


FIGURE 31: EFFECTS OF CATALYST INLET TEMPERATURE ON CO, UHC AND NO_x CONVERSION

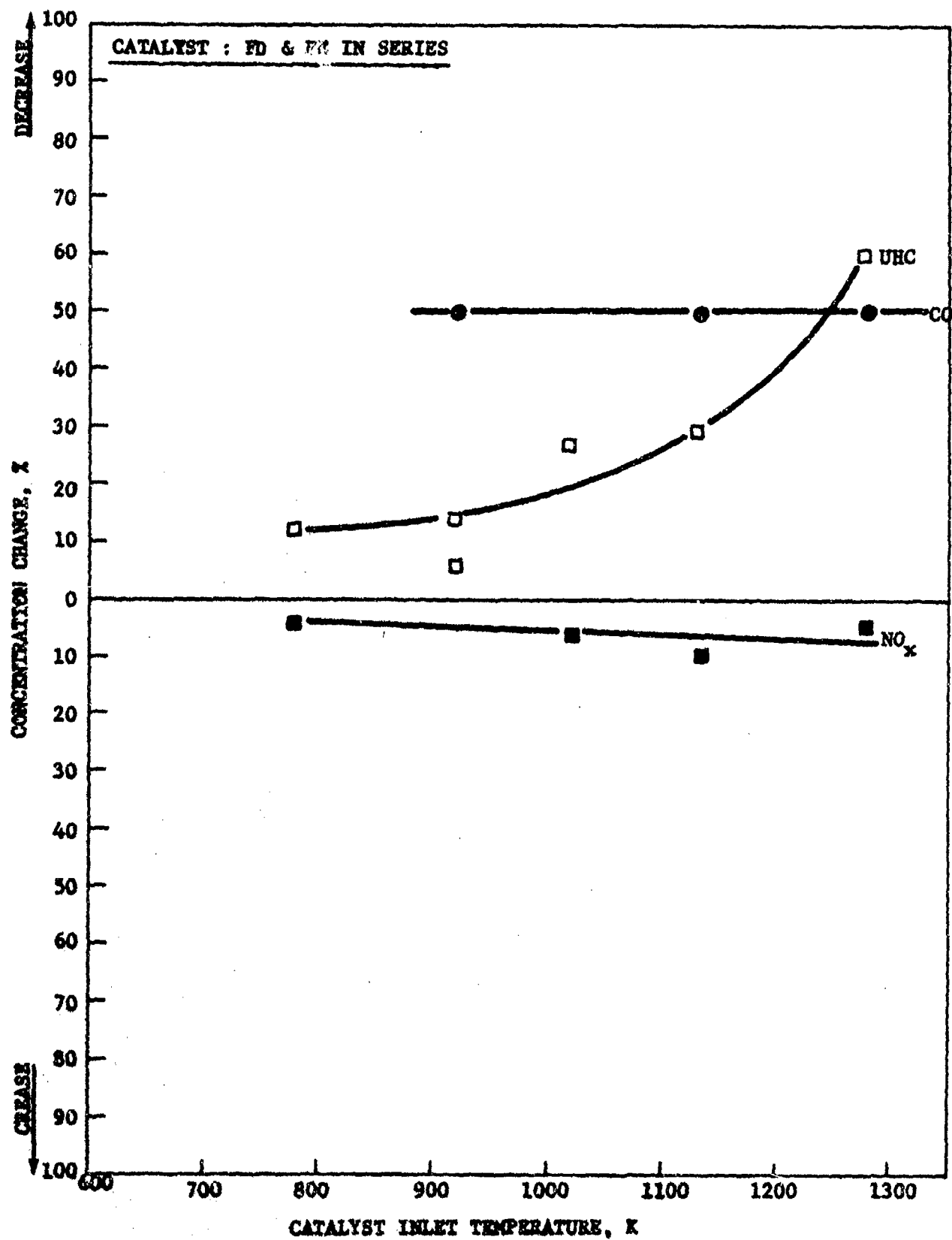


FIGURE 32: EFFECTS OF CATALYST INLET TEMPERATURE ON CO, UHC AND NO_x CONVERSION

concentration occurred in the temperature range of 900-1000 K may be related to the equivalence ratio of the pre-combustor. Referring to Table VI which summarized the relationship between pre-combustor ϕ , overall ϕ and catalyst inlet temperature, it can be seen that the maximum increase in NO_x concentration in catalyst FH and KQ coincided with near-stoichiometric pre-combustor operation. Similar effects were observed for nearly all noble metal catalysts. This was, however, not the case with rare earth oxide catalysts KR and RA shown in Figures 19 and 20, respectively. By comparing the REO catalysts with noble metal catalysts, it was observed that the increase in NO_x concentration seemed to be more temperature dependent with REO catalysts. The curves showing the effect of temperature on concentration change of emissions can be used to predict the activity of a combination of catalyst segments. Such combinations are desirable to overcome pressure drop limitations. Thus, two 5.08 cm long segments of catalyst KQ which had acceptable UHC and CO conversion characteristics (see Figure 17), but an undesirable pressure drop, were combined with two 5.08 cm long segments of a low pressure drop catalyst FH (see Figure 16). This combination is referred to as catalyst FH & KQ in Table VII and its emissions are included in Figure 24. Catalyst FH was previously observed to convert 80 and 97% of the CO and UHC, respectively, at 1200 K and the pressure drop under reacting conditions was 5.4%. Under the same test conditions, catalyst KQ had a pressure drop of 19% with 91 and 56% CO and UHC conversions, respectively. The combination of catalysts FH and KQ resulted in a reacting flow pressure drop of 11.8%, and CO and UHC conversions of 93 and 92%, respectively. These results demonstrated that the catalyst can be tailored by judiciously choosing the proper support geometries to achieve desirable pressure drop characteristics and low emissions.

The search for catalysts that would remain active after exposure to temperatures in excess of the 1300 K for long periods of time was directed at other than noble metal catalysts, since noble metals migrate, form crystallites, and vaporize, thus promoting catalyst deactivation. The catalytic activity of rare-earth oxides was found to be insufficient (see Figures 19 and 20). Catalyst KR and RA contained mixtures of rare earth oxides (REO) on cordierite and silicon carbide supports, respectively. The cordierite supported REO was wash coated with stabilized Al_2O_3 , while catalyst RA consisted of a corrugated silicon carbide support which was coated with a mixture of lanthanum, strontium and manganese oxides in the absence of any wash coat material. The data in Table VII showed that the presence of the high surface area Al_2O_3 wash coat on KR did not significantly affect the UHC and CO conversions compared to catalyst RA which had no wash coat and a much smaller geometrical surface area support than catalyst KR. The REO loadings were 68.25 g/m^2 on RA compared to 13 g/m^2 for catalyst KR. Since such massive catalyst loadings did not produce acceptable CO and UHC conversions on high surface area supports, no further testing was conducted in this program. One of the interesting characteristics of REO catalysts was that they seemed to be fairly good hydrocarbon oxidation catalysts, especially at temperatures in excess of 1200 K, but poor catalysts for CO conversion.

The REO catalysts were ineffective in promoting the CO oxidation reactions below 1100 K. This effect was evidenced by the fact that the CO conversion curves for both catalysts passed through the ordinate zero in Figures 19 and 20 at 1100 K. At 800 K, both REO catalysts generated nearly 30% more CO than had entered the catalyst bed. At this low temperature, where the overall ϕ was about 0.15, the hydrocarbon conversions were only about 10%. Thus, hydrocarbons were apparently incompletely oxidized to CO.

The thermal deactivation of a noble metal promoted base metal oxide catalyst was observed to occur during the testing of catalyst KU. In Figure 21, the temperature dependency of catalyst activity toward CO and UHC conversion and NO_x production is plotted for two different run durations. The dashed curves were obtained over a 70 minute period beginning with a fresh catalyst. The solid curves were obtained after an accumulated test time of 140 minutes. Apparently, catalyst deactivation was occurring even over such a short period of time. Whether this mechanism was due to sintering of the wash coat, migration of the noble metals or some reaction between the noble metals and the base metal oxides was not determined. Subsequent to the completion of the tests, it was learned from a private communication with Dr. W. Retallick of Oxy-Catalyst, Inc., that he had observed similar catalyst deactivation processes when copper was one of the base metals used in the presence of platinum or palladium (19). Dr. Retallick postulated that copper and noble metals react in some manner which is detrimental to activity maintenance at high temperatures. Since noble metal promoted base metal oxide catalysts were among the most active tested during the program, a study of the effects of eliminating the copper from the catalyst formulation was initiated. Catalyst FV was prepared from square opening cordierite impregnated with 3.3 kg/m^3 palladium and $\text{Cr}_2\text{O}_3 + \text{MnO}_3$ with an Al_2O_3 wash coat applied over the active materials. The results of the test with FV are plotted in Figure 26 and show that compared to the results obtained with catalyst KU plotted in Figure 20, the activity of catalyst KU containing CuO was superior to the copper-free catalyst. Since the wash coat was applied over the active materials, the test did not provide the desired comparison with a copper bearing catalyst. It was surprising that any CO or UHC conversions were observed at all for catalyst FV. Time did not permit the testing of a properly prepared catalyst free of copper.

A combination of catalysts containing 1.7 kg/m^3 loadings of palladium or iridium on SiO_2 stabilized alumina were tested on square hole cordierite supports. Two segments of each type of catalyst (FD & FE) were arranged in an alternating fashion within the catalyst chamber. The test results, shown in Figure 32 and Table VII, indicated that the combination of Pd and Ir was not a good hydrocarbon oxidation catalyst, but a better catalyst for CO oxidation. The data plotted in Figure 32 were not typical of noble metal catalysts previously tested in that the level of CO conversion remained essentially constant at 50% over the temperature range from 900 to 1275 K. The large increase in NO_x concentration formerly measured in noble metal catalysts was not observed with the combination catalyst FD & FE. From these preliminary test results it appeared that the incorporation of iridium into a platinum-palladium catalyst may promote the CO oxidation reactions and maintain high UHC conversion.

One of the catalysts that exhibited high CO and UHC conversion in the temperature range from 1000 to 1250 K, and met the 6% pressure drop requirement, was catalyst QF. The catalyst was manufactured by the Johnson-Matthey Co., Ltd. of England. This novel catalyst consisted of a corrugated and rolled metal alloy film wash coated with highly stable Al_2O_3 and impregnated with 5.27 kg/m^3 of platinum. On a mass per unit area basis, the platinum distribution was 1.04 g/m^2 . The interesting aspect of this catalyst was that its S/V ratio, viz., $4100 \text{ m}^2/\text{m}^3$, was much larger than the best non-metal support geometry which was $2473 \text{ m}^2/\text{m}^3$ for a triangular geometry monolith (GH). The large S/V ratio of the metal support resulted from the extremely thin wall between adjacent corrugations which was 0.05 mm. The alumina wash coat was applied in a manner which precluded spalling or cracking. The temperature dependency of catalyst QF toward UHC and CO conversion and NO_x production is shown in Figure 30. Because catalyst QF was a very active CO and UHC oxidation catalyst, it was also observed to be an efficient promoter of the oxidation of NO_x precursors, as evidenced by the 50% increase in NO_x measured across the catalyst.

One important distinction to be kept in mind when comparing the temperature dependency of QF with the other catalyst candidates is that the length of QF was 15.25 cm compared to the majority of other catalysts where the length was 20.3 cm.

The high CO and UHC conversions obtained with catalyst QF were due mainly to the large geometrical surface area of the catalyst support, made possible by the thin walls of the cells. The actual geometrical surface area of the 15.25 cm long by 5.08 cm diameter catalyst was 1.56 m^2 compared to 0.761 m^2 available in an equivalent length of catalyst GH.

11. THE EFFECT OF BED LENGTH AND TEMPERATURE ON CONVERSIONS

Some interesting data concerning the effect of catalyst bed length on CO and UHC conversions and NO_x productions were obtained for catalyst KQ over a temperature range between 700 and 1200 K. The air preheat temperature was 400 K. The combustion chamber pressure was 0.37 MPa and the reference velocity was 25 m/s. Catalyst bed inlet temperatures were changed by varying the JP-4 flow rate while maintaining a constant air flow. The effect of catalyst bed length on conversions was found by running a series of tests with two, 5.08 cm long catalyst segments inserted in the catalyst chamber and another set of tests with four catalyst segments in the catalyst chamber. During each series of tests, the temperature of the pre-combustor gases was varied over the same range. CO, UHC and NO_x concentrations were measured with the multi-probe sampling devices described in Section III.

The results of the tests were plotted in Figures 33 and 34 which show the percent change in CO, UHC or NO_x concentration as a function of total catalyst length for various catalyst temperatures. All of the curves had their origin at zero concentration change since, without a catalyst present in the chamber, little or no change of UHC, CO or NO_x was observed. The curves showing CO conversions as a function of temperature indicated that a catalyst bed length of 20 cm ($L/D = 4$) was required for 90% conversion at 1200 K. At low temperatures, the curves indicate that much longer beds

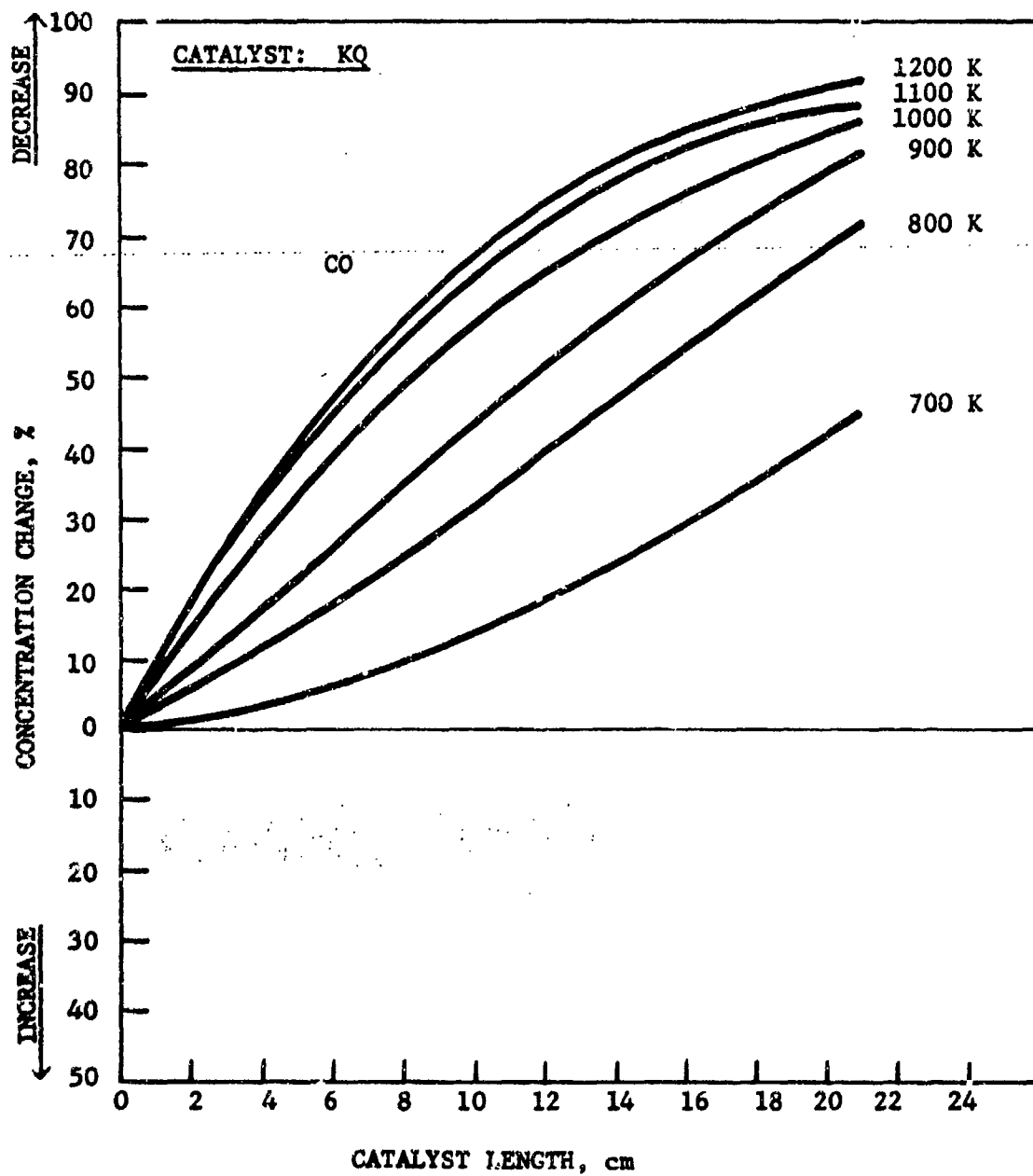


FIGURE 33: EFFECT OF CATALYST LENGTH AND INLET TEMPERATURE ON CO CONVERSION

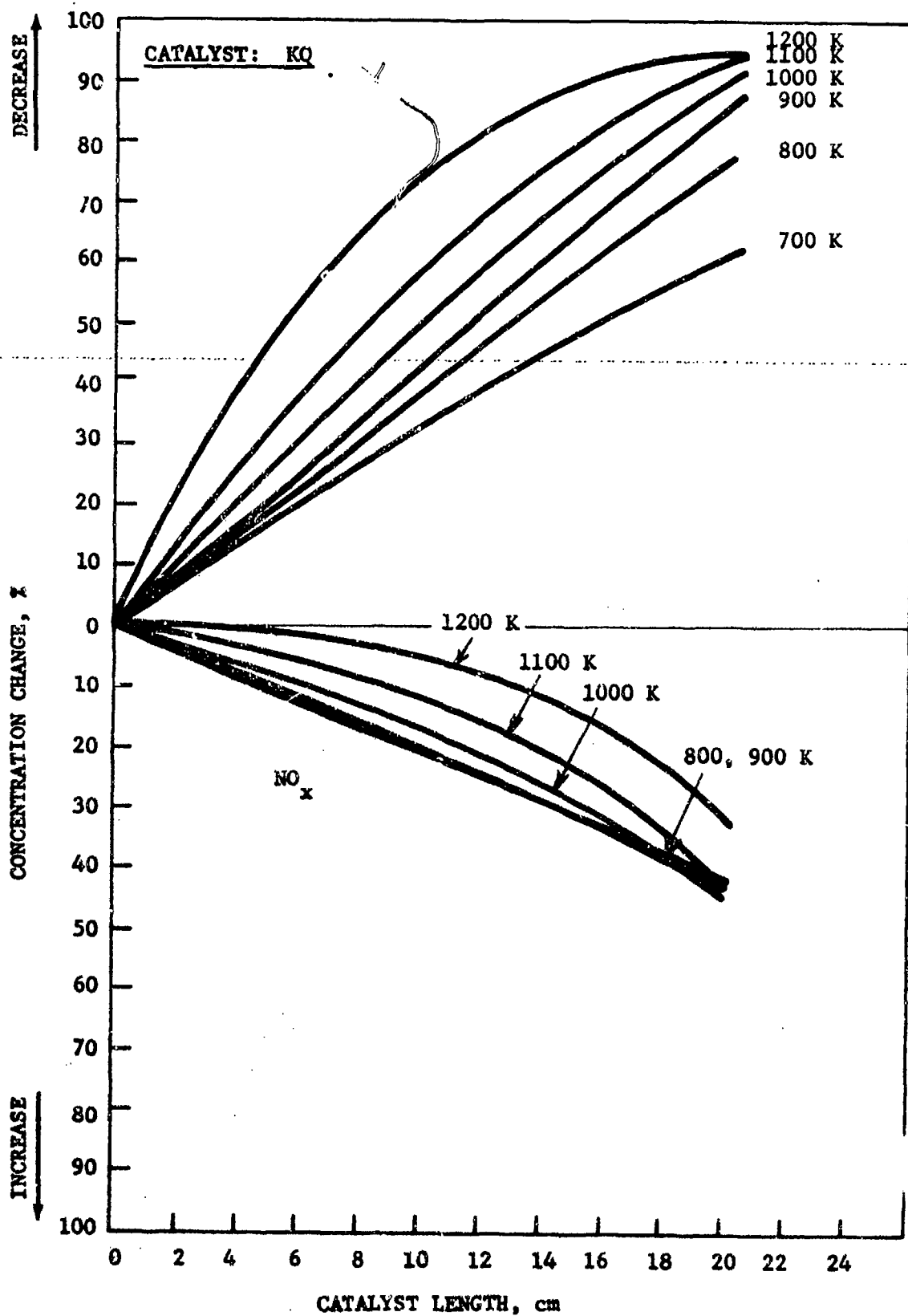


FIGURE 34: EFFECT OF CATALYST LENGTH AND TEMPERATURE ON UHC AND NO_x CONVERSION

containing similar noble metal loading are required for high CO conversions. Similar effects are plotted in Figure 34 and show UHC and NO_x concentration changes as a function of temperature and bed length. The set of curves plotted for NO_x conversions as a function of temperature shows the effect of the pre-combustor equivalence ratio. As can be seen, the maximum increase in NO_x concentration is observed to occur in the temperature range of 900-1000 K, with the lowest increase in NO_x concentration occurring at 1200 K and at temperatures less than 700 K. The pre-combustor ϕ was near 1.0 when the catalyst bed inlet temperature was 930 K.

12. THE RESULTS OF A 20 HOUR DURABILITY TEST OF CATALYSTS QF AND KQ

After reviewing the results of the catalyst screening tests which were summarized in Table VII, two of the most effective CO and UHC oxidation catalysts were selected for a 20 hour durability test at 1200 K. The temperature at which the tests were conducted was chosen to accelerate catalyst deactivation and thus approximate realistic operation. The catalysts chosen for this test were KQ and QF. The results of the test are plotted in Figures 35 and 36. Total accumulated test time at 1200 K catalyst inlet temperature were plotted against the percent change of CO, UHC and NO_x concentrations which were observed across the catalysts. It should be noted that the durability test was conducted by running the combustor for approximately 5 hours a day for 4 days. Thus, the durability runs were a severe test of catalyst sensitivity to intermittent operation, i.e., thermal cycling. Figure 35 shows that catalyst QF converted 94% of the hydrocarbons and 81% of the CO at the beginning of the test. The catalyst also increased the NO_x concentration by 42%. After 16.5 hours of accumulated test time at 1200 K, the UHC and CO conversions were 88 and 94%, respectively, while no increase in the catalyst inlet NO_x concentration occurred at this time. It is apparent from the shape of the NO_x data points that some change occurred to the catalyst which may have selectively inhibited the conversion of nitrogenous molecules to NO_x . The sudden drop in CO and UHC conversions after 16.5 hours was due to the inadvertent destruction of the catalyst. This occurred as a result of an ignition delay experienced in starting the pre-combustor which allowed JP-4 to be deposited on the catalyst surface. Subsequent ignition of the pre-combustor led to the generation of near stoichiometric gas temperatures on the catalyst surface. Extensive deformation and melting of the metal support resulted. Upon closer inspection of the catalyst support it was found that in the area immediately surrounding the melted zone, the alumina wash coat remained intact and no separation of the wash coat from the metal support was evident. Testing of catalyst QF was discontinued after a total of 18.75 hours at 1200 K.

In order to attempt to explain the gradual decrease in the percent change in NO_x concentration observed in catalyst QF, the NO , NO_2 and NO_x data which were measured during every test, were plotted in Figure 37. Figure 37 shows that at the beginning of the 20 hour test the NO_2 concentration began to increase to about 50% of the initial concentration measured at the

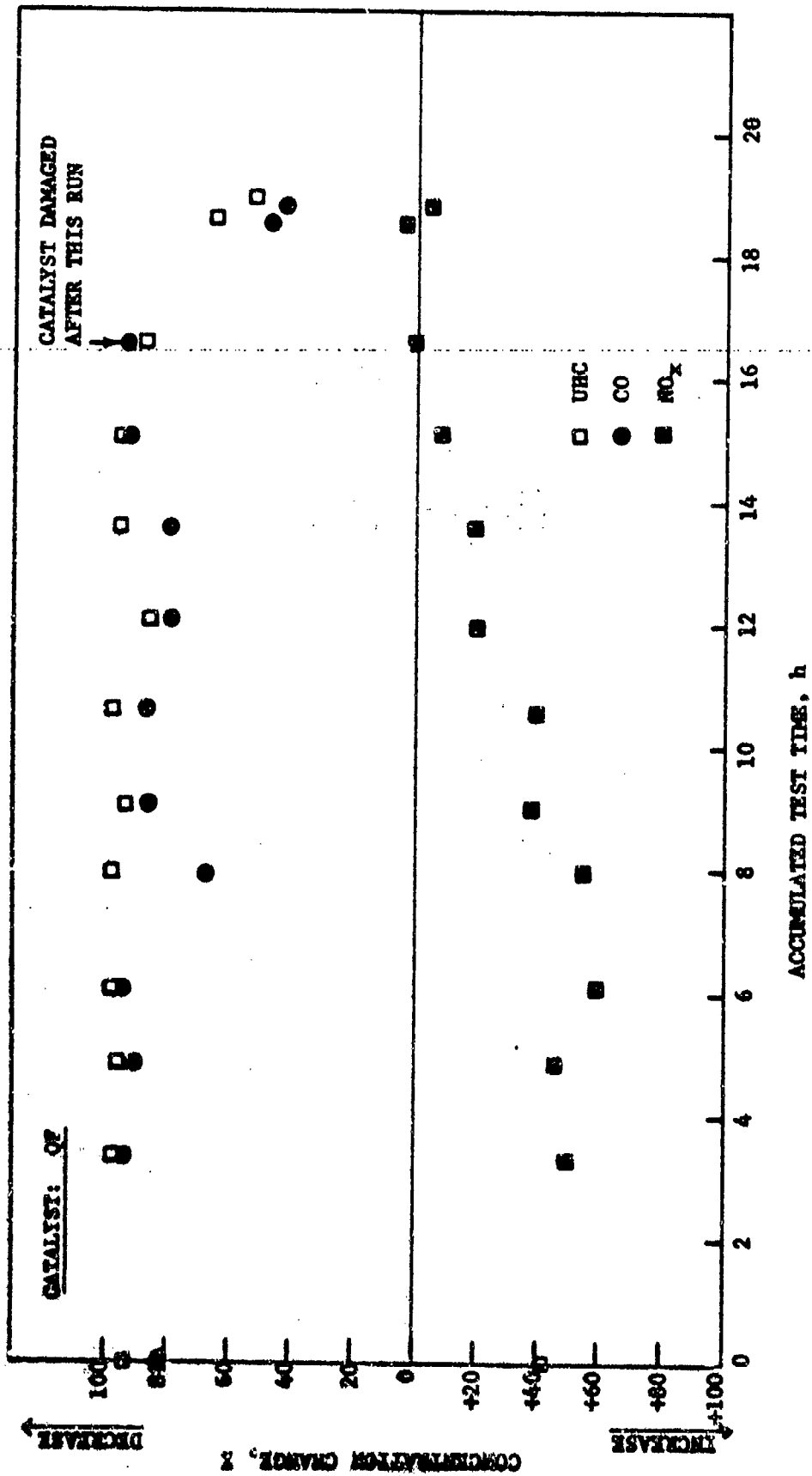


FIGURE 35: TWENTY HOUR TEST OF CATALYST QF AT 1200 K

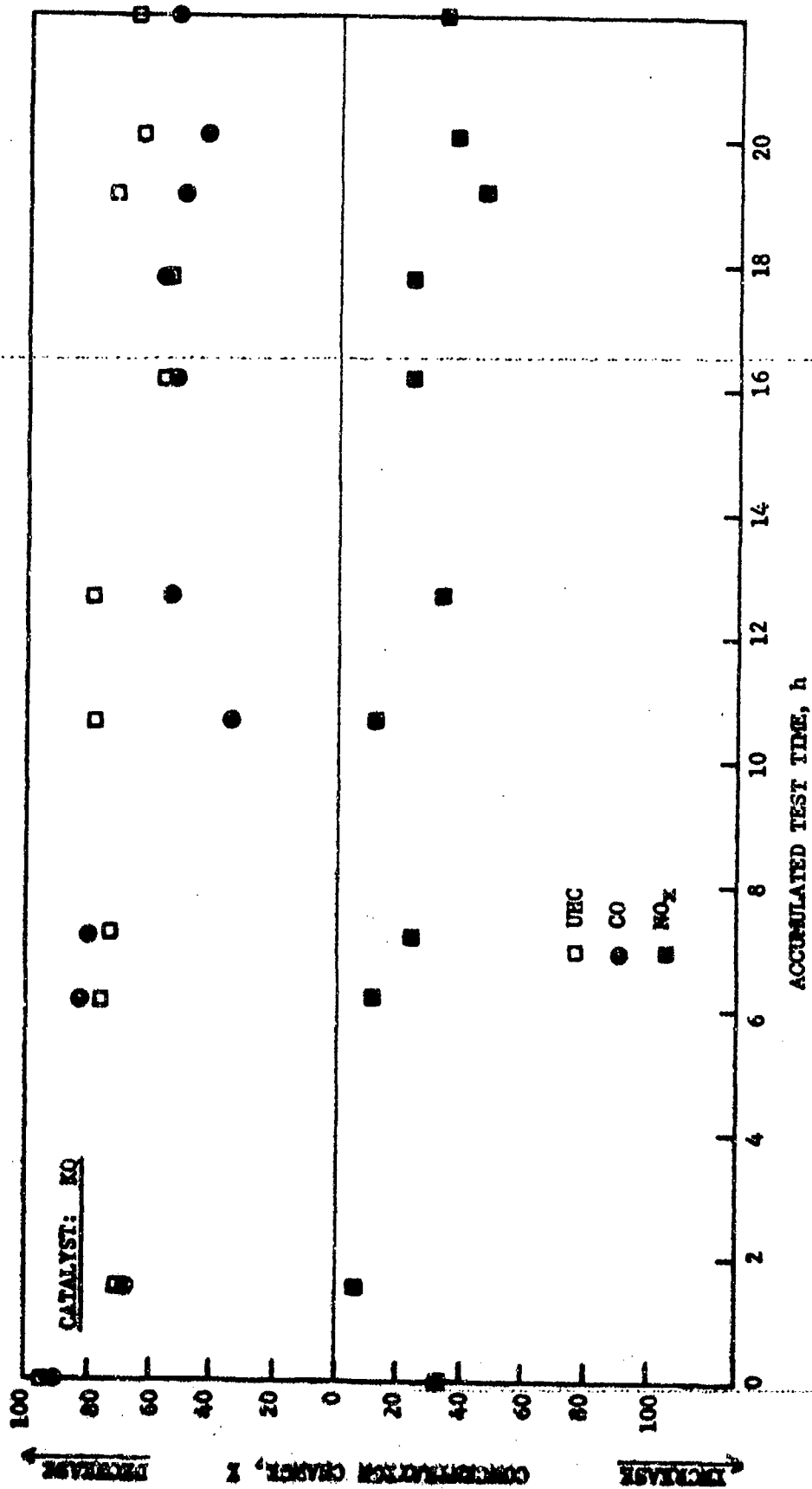


FIGURE 36: TWENTY HOUR TEST OF CATALYST EQ AT 1200 K

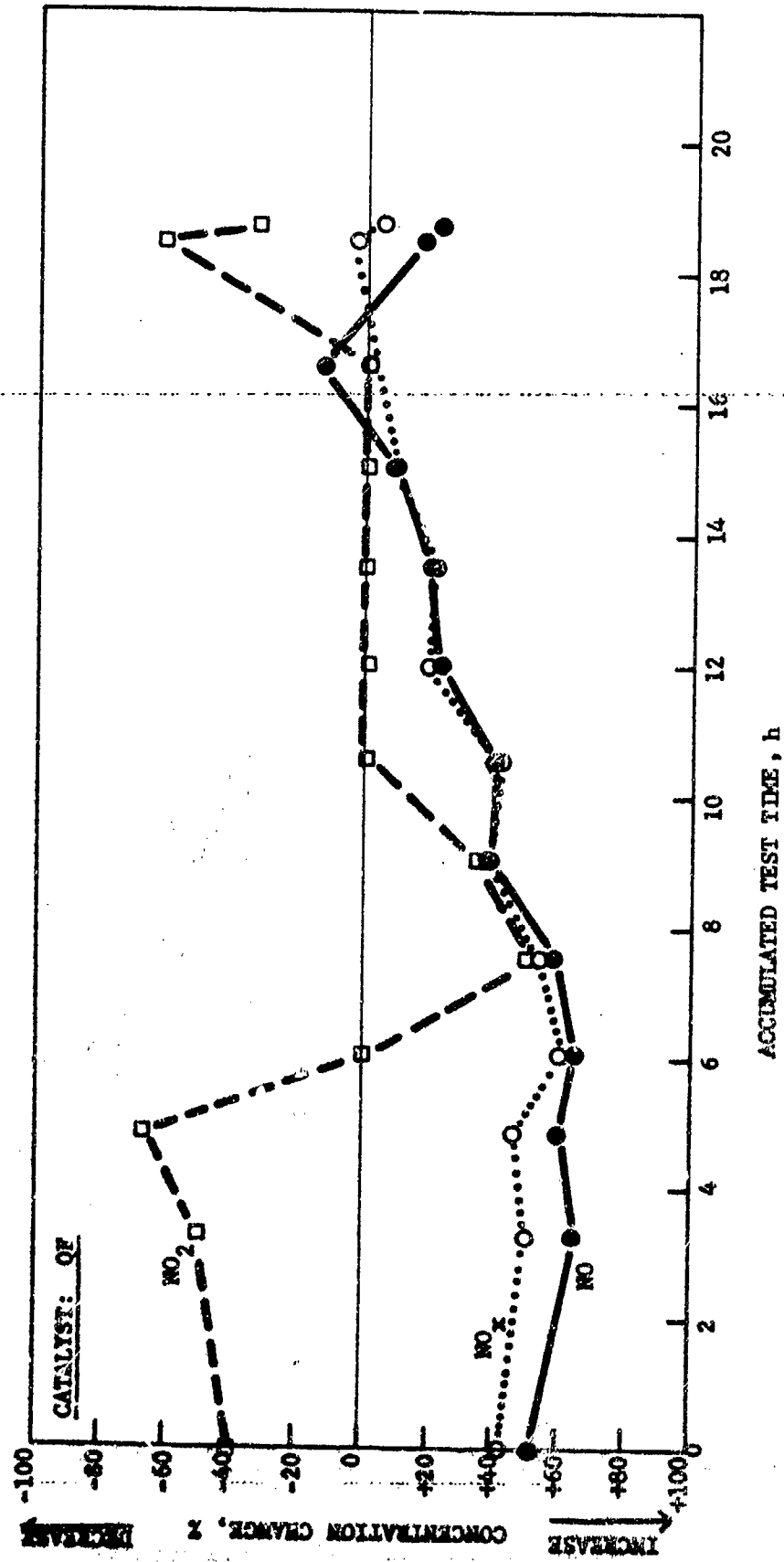


FIGURE 37: EFFECTS OF CATALYST AGING AT 1200 K ON NO_x CONCENTRATION CHANGE

catalyst inlet. NO and NO_x concentration changes remained fairly constant at 55%. In the subsequent period, after 7.5 hours, the change in NO, NO₂ and NO_x concentrations relative to the catalyst bed inlet concentrations began to approach zero. When no change in the NO, NO₂ or NO_x concentrations was observed to occur across the catalyst, typical total NO_x concentrations at the catalyst inlet were 20-25 ppm. The sudden change in the slopes of the curves at 16.5 hours was due to the destruction of the catalyst.

The 20 hour CO, UHC and NO_x test data for catalyst KQ were plotted in Figure 36 which showed that after 22 hours of accumulated time at 1200 K, the hydrocarbon conversions decreased from 94 to 67% while the CO conversions decreased from 90 to 53%. Over the same period, the NO_x concentration increase remained fairly constant between 10 and 40%.

From a comparison of the 20-hour test data of catalysts QF and KQ it was clear that the activity of catalyst KQ began to decrease rapidly after 12.5 hours, but the catalyst activity stabilized at a new, lower level and remained fairly constant through the remainder of the test. Catalyst QF, however, did not show any indications of deactivation for UHC and CO conversions at the end of 16.5 hours, but changes in the NO_x conversion characteristics were evident throughout the entire period.

13. METHODS FOR DETERMINING COMBUSTION EFFICIENCY AND THE EMISSION INDEX OF EXHAUST PRODUCTS

All of the experimental studies were conducted with a hybrid catalytic combustor, which consisted of a conventional pre-combustion stage followed by a catalytic combustion stage. The combustion efficiencies and emission indices in both sections of the combustor were calculated from the measurements of unburned hydrocarbons, CO and NO_x. The measured gas temperatures in both stages of combustion confirmed the calculated combustion efficiencies.

This section of the report is divided into three parts which describe the methods used for the calculation of combustion efficiency, emission indices, and checking the material balances.

a. Emission Index of CO, UHC and NO_x

The emission index, EI, of a combustion product is defined as the grams of the measured constituent relative to one kg of fuel. This definition eliminates the effects of dilution of the products by air (20).

The general equation used to define EI is

$$EI_i = X_i \frac{(MW)_i}{(MW)_{\text{exhaust}}} \cdot \left[1 + \frac{A}{F} \right] \cdot 10^3 \text{ g/kg fuel} \quad (1)$$

where the subscript, i, is either CO, CH₄ or NO₂. In the calculations for NO_x, the mole fraction of NO + NO₂ was used with the molecular weight (MW)_i of NO₂ used in the equation. The measured mole fraction of the constituent is denoted by X_i. The overall air-fuel ratio (by weight) was obtained from the measured flow rates. The molecular weight of the exhaust gases, (MW)_{exhaust}, was 29 since all the test data were obtained under very lean mixture conditions.

In the emission index calculations for unburned hydrocarbons, the molecular weight of the hydrocarbon was taken as 16 since methane was used to calibrate the hydrocarbon flame ionization detector instrument.

b. Combustion Efficiency

Combustion efficiency is defined as: (21)

$$\eta_b = \left[1 - \left[.232 (EI)_{CO} + (EI)_{C_xH_y} \right] 10^{-3} \right] 100 \quad (2)$$

where: η_b = combustion efficiency

EI_i = emission index in g/kg fuel for exhaust constituent i.

The combustion efficiencies and emission indices for CO, UHC and NO_x (as NO₂) for each catalyst tested are summarized in Appendix III.

c. Material Balance Calculations

The volume percent carbon in the combustion gas samples as a function of equivalence ratio, ϕ , were calculated assuming that the unburned hydrocarbons were expressed as methane. Derivations of these equations can be found in a AFAPL-TR-72-80 (15).

$$\% \text{ Carbon} = \frac{400 \phi}{n \phi + 4.76 (4 + n)} \quad (3)$$

where: n = hydrogen/carbon for JP-4 = 1.9

The volume percent oxygen was calculated from the following equation:

$$\% \text{ Oxygen} = \frac{100 (1 - \phi) (4 + n)}{n \phi + 4.76 (4 + n)} \quad (4)$$

The material balance equations used to compute the carbon balance and oxygen balance are:

$$\% \text{ Carbon} = \frac{(1.9 \phi + 28.04)}{4 \phi} \times \text{measured mole fraction of carbon containing compounds} \quad (5)$$

$$\% \text{ Oxygen} = 32.1 \phi + (0.321 \phi + 4.76) \times \text{measured mole fraction of oxygen compounds} \quad (6)$$

SECTION V

DISCUSSION

In the preceding sections, it was shown that when the pre-combustor was operated fuel-rich at an equivalence ratio (ϕ) of 1.5, and an overall ϕ of 0.3, then about 20-30 ppm NO_x were produced. Essentially no thermal NO_x is expected to be generated according to the Zeldovich Mechanism (22) as indicated from calculations of combustion at fuel-rich and fuel-lean conditions, and illustrated in Figure 38. NO_x produced from the rich combustion of nitrogen-free fuels is not predictable from the Zeldovich Mechanism (22). Fennimore (23) postulated that a significant fraction of the NO_x produced under stoichiometric to rich conditions is a result of the oxidation of carbon nitrogen compounds produced under air deficient combustion, and he called this source "Prompt NO_x ". The significant contribution of "Prompt NO_x " to total NO_x in gas turbines under stoichiometric and fuel-rich operating conditions has been calculated by Shaw (20). Equilibrium calculations showed that under fuel rich conditions ($\phi = 1.5$) the formation of NH_3 and HCN should be very small (5). However, because of the observed increase in NO_x concentration across the catalytic stage of the HCC, it was presumed that the production of kinetically controlled nitrogeneous molecules, such as HCN and NH_3 , were being catalytically converted to oxides of nitrogen.

The level of exhaust emissions at the hybrid combustor exit was, in most cases, below the EPA specifications for subsonic turbofan or turbojet aircraft engines manufactured on or after January 1, 1981 (1). Table XI compares the EPA limitations on emissions (1) with the average effluents from the HCC durability tests of catalysts QF and KQ. The emissions from the HCC were corrected to the EPAP units ($102 \text{ mg/N}\cdot\text{h}\cdot\text{cycle} = \text{lb}_m/\text{lb}_f\cdot\text{h}\cdot\text{cycle}$) using the approximate procedure suggested by Gott and Bastress (24). In order to estimate the HCC emissions over the LTO cycle, it was assumed that the emission indices at full power (pressure ratio = 25 per Table II) would be the same as those at idle (pressure ratio = 3 per Table II). This assumption may be rationalized by considering that the difference in emissions between idle and full power operation is due to dilution of the HCC ($\phi = 0.3$) effluent. These oversimplified calculations are only intended to provide an initial estimate of the EPAP values. Clearly, data at both idle and full power operation would be needed to refine the estimates presented in Table XI. Only UHC emissions specifications were difficult to meet using the HCC concept. Nevertheless, Catalyst QF could meet the 1979 new aircraft affluent standard.

An alternate calculation using the data presented by Roberts, et al., (25) for a conventional JT 8D-17 engine normalized to idle operation was carried out. The HCC emissions data was scaled in proportion to the JT 8D-17 data. The results of this calculation are summarized in Table XI. It was found in this calculation that only NO_x emissions did not meet the 1981 standards. The two estimated EPAP parameters for each of the pollutants tend to bracket a realistic value. The Gott and Bastress values emphasize the

idle emissions, thus indicating higher values for CO and UHC emissions than would be expected over the LTO cycle. The Roberts, et al. data, on the other hand, emphasized power operation thereby overestimating the NO_x emissions. Thus, assuming that realistic EPAP values lie between the limits presented, one could see that the HCC method of operating an aircraft combustor shows promise of meeting the 1981 new aircraft pollution limitations.

TABLE XI
COMPARISON OF HCC EFFLUENTS WITH EPA
1981 NEW AIRCRAFT LIMITATIONS

	EPA Limit mg/N·h·cycle	HCC Catalyst QF mg/N·h·cycle		HCC Catalyst KQ mg/N·h·cycle	
		Gott ^a	Roberts ^b	Gott ^a	Roberts ^b
UHC	41 ^c	50	15	263	79
CO	439	111	35	430	137
NO _x	306	212	407	273	526

^a Using the modified EPA parameter suggested by Gott and Bastress (24) and emissions data averaged over the durability runs at 1200 K.

^b Using an EPA parameter scaled from JT 8D-17 data (25) and emissions data averaged over the durability runs at 1200 K.

^c The UHC limit for 1979 new aircraft is 82 mg/N·h·cycle (1) and the 1979 limits for the other pollutants are the same as the 1981 limits.

From the emissions data obtained in the 20 h durability tests of the two noble metal catalysts at 1200 K, it may be inferred that the sensitivity of catalyst QF to the reactions responsible for the conversion of NH₃ and HCN to NO_x was affected by catalyst conditioning at 1200 K. It should also be noted that pollutants were minimized at an overall equivalence ratio of 0.3, or correspondingly at a catalyst inlet temperature of 1200 K. This equivalence ratio generally corresponds to full power operation (take-off), but it was assumed that combustor by-pass air would dilute the catalyst effluent in an actual engine design to the appropriate equivalence ratio of 0.14 for idle conditions.

The conversion of nitrogenous molecules other than NO_x compounds in the Thermo Electron Corp. chemiluminescent analyzer used during the program, has been shown by Sawyer (26) to be very inefficient, especially if a stainless steel converter is utilized, as was the case in this study. The catalysts tested in the program were more efficient than the stainless steel converter in the instrument. Sawyer's results indicated that 90% of the NH₃ was converted to NO_x over a platinum catalyst at 1270 K when the mole concentration of O₂ was in excess of 1%. Under similar conditions, 42% of the HCN was converted to NO_x.

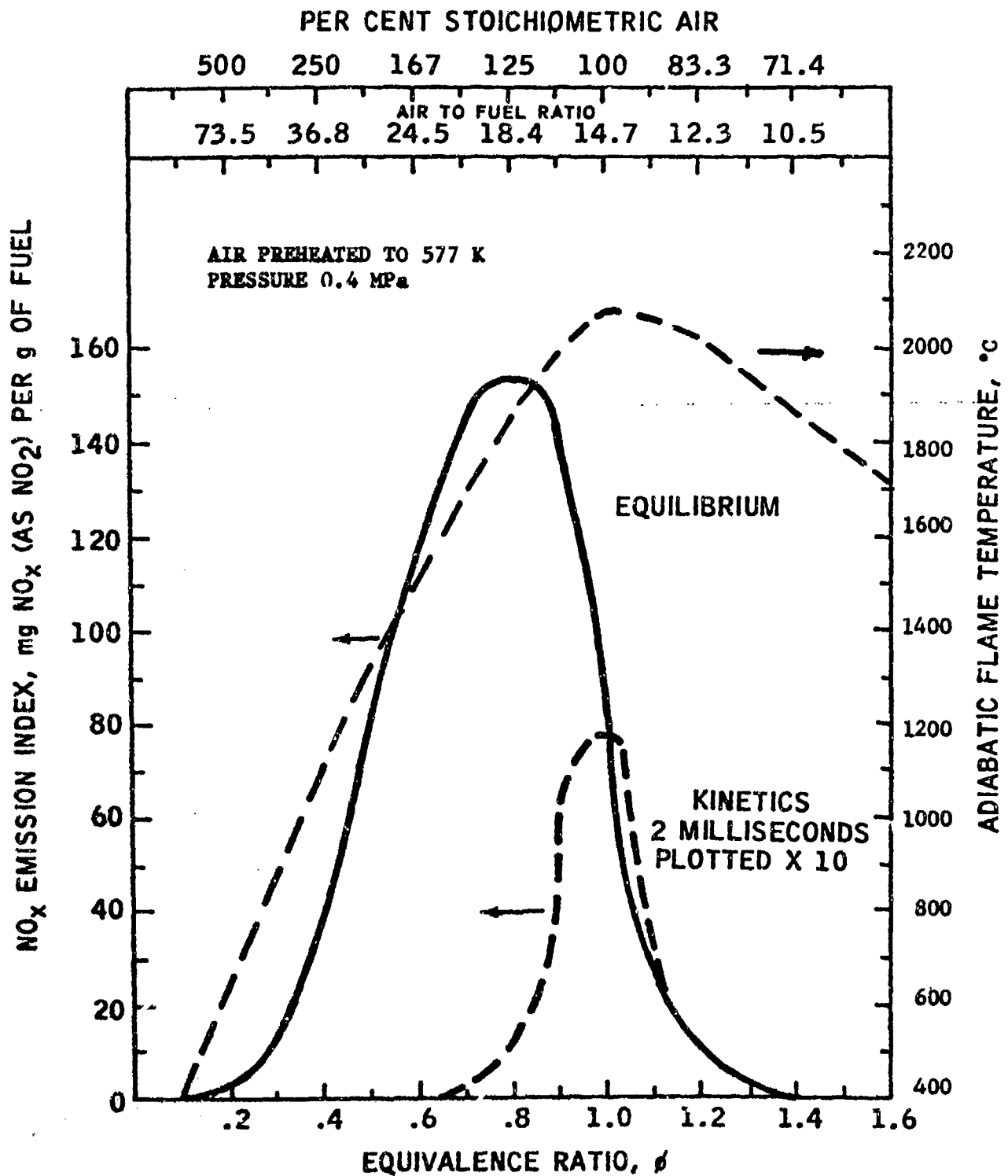


FIGURE 38: NO_x EQUILIBRIUM IN JP-4 COMBUSTION

The nitrogen content of JP-4 is in the range of 5-20 ppm (27) and the sulfur concentration of the test fuel was analyzed to be 535 ppm. No attempt was made to measure SO₂ and SO₃ emissions, because at high combustion temperatures equilibrium does not favor the production of SO₃.

The catalytic conversion of nitrogenous molecules to oxides of nitrogen observed in this study indicates that the utilization of high nitrogen content fuels such as coal or shale derived distillates, in combustors equipped with a catalytic stage, may encounter problems with high NO_x emissions. Also, preliminary work in various laboratories have indicated that staged combustion may be effective in controlling NO_x from fuel bound nitrogen (28). Along this line, Martin (29) showed that higher temperature or longer residence time, or both, tend to reduce the concentration of NO_x precursors at $\phi \approx 1.4$. Thus, high pressure ratio gas turbine engines, operated in the HCC mode, could maintain low NO_x emissions at full power as well as idle. This data provides some justification for the assumptions used in calculating the EPAP values in Table XI. Thus, hybrid catalytic combustion as a special form of staged combustion, may have an inherent advantage for controlling both thermal and fuel derived NO_x.

An attempt to measure the NH₃ and HCN concentrations at the inlet and outlet of the catalyst stage of the hybrid combustor was unsuccessful. The utilization of standard specific electrode analytical techniques did not indicate the presence of any NH₃ or HCN. It was thought that because both these compounds can be readily adsorbed on the walls of the gas sample lines, they never reached the aqueous solutions through which they were to be bubbled. If reliable HCN and NH₃ concentration measurements in the range of 1-20 ppm are to be made, improved techniques for sampling and analysis must be developed (7).

Most of the data on emissions was presented on a relative basis to avoid the problems associated with fluctuations in emissions data. It is helpful to understand the range of these fluctuations. Table XII presents a comparison of the pre-combustor data presented in Table III with the average data obtained from the durability runs with Catalysts QF and KQ. It should be noted that over the two-20 hour periods, the average pre-combustor effluents (input to the catalysts) were almost identical. In comparing these average inputs to the catalyst with the inputs measured when the pre-combustor was developed, one can see that the average measured emissions concentrations for UHC and NO_x actually fell between condition 1 and condition 2. The CO emissions, on the other hand, were considerably lower during the catalyst testing period than would have been predicted from the original emissions map.

TABLE XII
EMISSIONS FROM HYBRID COMBUSTOR

Pre-Combustor Condition	1		2		1		1	
Catalyst	None		None		KQ		QF	
Catalyst Inlet Temp., K	1067		1076		1200		1200	
Emission Indices, g/kg	<u>In</u>	<u>Out</u>	<u>In</u>	<u>Out</u>	<u>In</u>	<u>Out</u>	<u>In</u>	<u>Out</u>
CO	36.35	-	17.56	-	7.19	3.68	6.75	0.949
UHC	14.13	-	1.99	-	7.32	2.25	7.34	0.427
NO _x	1.39	-	2.38	-	1.69	2.34	1.69	1.813

One of the most significant problems encountered during the course of the program was the destruction of some catalysts when an ignition delay of the pre-combustor occurred as a result of electrical ignitor failures. The unburned fuel which was adsorbed on the catalyst surface during the brief ignition lag time, eventually was combusted under near stoichiometric conditions. The fact that catalyst destruction occurred when cordierite or metal catalyst supports were utilized indicated that the problem cannot be satisfactorily handled by merely altering the thermal conductivity of the support material. This problem was never experienced with silicon carbide supported catalysts. Although the number of catalysts destroyed via the ignition delay of the pre-catalyst was small, the disastrous results that occurred require that a solution to this problem be found if reliable hybrid catalytic combustors are to be developed. Conventional gas turbine combustors occasionally experience ignition delay problems at start-up, either due to cold climactic conditions or fouled ignitors, but because the turbine engine components are good heat-sinks and made of non-porous materials, no deleterious effects result.

One of the potential solutions to this problem in hybrid catalytic combustors consists of fabricating the inlet face of the catalyst bed from a support material that is capable of withstanding the high flame temperatures

that result from the ignition delay of the pre-combustor. Silicon carbide or silicon nitride catalyst supports are available in high surface/volume geometries that have good wash coat adhesion properties. Since these support materials are expensive compared to cordierite or metal, only a short segment at the entrance to the catalyst bed would be made of refractory material. The remainder of the catalyst bed support could be fabricated from the less expensive materials. Another possible solution would entail automatically purging the catalyst after each failure to ignite the fuel in the pre-combustor.

The decrease in catalytic activity for CO and UHC conversions via wash coat sintering, noble metal crystallization and deleterious reactions between noble metals and some base metal oxides have been observed during the course of this program. The need for more thermally stable wash coat materials and noble metal formulations that do not crystallize is apparent. Also, the variations of support geometry available for high CO and UHC conversions, low pressure-drop, and high velocity applications was limited to three configurations: 0.16 cm squares, 0.16 cm x 0.32 cm rectangles, and the Johnson-Matthey, Ltd. thin-wall corrugated metal support.

Group VIII metals consisting of Pt-Pd combinations or Pd on stabilized Al_2O_3 wash coats were more effective CO and UHC oxidation catalysts than either mixtures of rare-earth oxides or base metal oxides. An iridium-palladium catalyst was not as effective in converting CO and UHC as Pd or Pt by themselves. Cobalt oxide did not improve the activity of ZrO_2 wash coated cordierite impregnated with palladium. The noble metal (Pt or Pd) promoted-base metal oxide catalysts had good initial activities for CO and UHC conversions, but because of high temperature reactions between CuO and Pd, catalyst deactivation occurred after only 70 minutes of operation at 1200 K. Addition of NiO to a SiO_2 wash coat impregnated with 1.31 kg/m³ of a 23/1 wt ratio of Pt/Rh did not produce acceptable CO or UHC conversions compared to noble metals on Al_2O_3 .

The most satisfactory catalyst evaluated consisted of a corrugated and rolled metal monolith that was wash coated with very stable Al_2O_3 and impregnated with Pt. Of the two catalysts tested for a 20-hour period at 1200 K, the metal supported catalyst showed no signs of deactivation for CO or UHC conversions, but may have become conditioned to prevent the conversion of nitrogen containing compounds such as NH_3 or HCN to NO_x . This result requires careful verification since it indicated that the catalyst could be made selective, to either react the nitrogen compounds produced in the primary zone to molecular nitrogen, or allow them to pass unreacted. Much more work is required in this area in order to hypothesize a mechanism that can account for the observed catalyst behavior.

Although the results presented here support the technical feasibility of catalytic combustion for aircraft turbine engines, there remain many practical problems which must be considered. The most significant problems involve the physical durability of the catalyst and the transient response in flight. Clearly, a catalyst that could fracture or spall in flight, could damage the turbine and endanger the flight crew. Other considerations associated with engine response and operability in flight must be carefully analyzed.

SECTION VI

DESIGN OF 7.6 CM DIAMETER COMBUSTORS

The design criteria and fabrication details of two 7.6 cm hybrid catalytic combustors to be delivered to Wright Patterson AFB are described in this section. Also, the required documentation for the system safety analysis is provided here.

1. DESIGN AND FABRICATION OF COMBUSTORS FOR LARGE SCALE TESTING

One of the program's tasks was to design and fabricate two, 7.6 cm diameter hybrid catalytic combustors to be tested in the combustion facility of the Aero Propulsion Laboratory at Wright Patterson Air Force Base. The only difference between the two combustors is that different catalysts are utilized in each one. Based upon the results of the catalyst screening tests and the 20 hour durability tests, catalysts KQ and QF which are described in Table VII were selected. Since the pressure drop associated with the support geometry utilized in catalyst KQ was excessive, the support geometry will be changed to the General Refractories Company's 0.16 cm square hole configuration which was shown to have acceptable pressure drop properties. The support formerly used in catalyst KQ was the W. R. Grace Company's Poramic[®] cordierite that had a 0.127 cm irregular rectangle geometry. Because of the nature of the design of the Poramic support, excessive pressure drops were observed at reference velocities in excess of 20 m/s. The General Refractories Company's cordierite support will be wash coated with stabilized alumina and impregnated with 3.3 kg/m³ of palladium by W. R. Grace Company.

The second combustor will be equipped with the corrugated metal supported catalyst designated in Table VII as QF. The only change that will be made to this catalyst consists of the addition of an equal weight of palladium to platinum, so that the total noble metal loading will be 5.3 kg/m³. The catalyst is supplied by the Johnson-Matthey Company, Ltd. of Reading, England.

Both types of catalysts will be supplied in 3.8 cm long segments which will be mounted into Hastelloy-X cylinders with a 3.5 cm space between adjacent segments. The number of segments inserted into each Hastelloy-X cylinder will vary depending upon the support geometry of the catalyst, but the total support thickness of each assembly will not exceed 20 cm. The Hastelloy-X cylinder containing the catalysts will be installed into the catalyst chamber shown in Figure 39. A photograph of the components of the 7.6 cm HCC is shown in Figure 40. The design of the entire assembly is such that the hybrid catalytic combustor can be tested within the Aero Propulsion Laboratory's tubular test facility.



FIGURE 40: PHOTOGRAPH OF HCC COMPONENTS

The pre-combustor was designed for a total air flow rate of 300 g/s. Other important design criteria were: 0.3 MPa combustor pressure, 400 K air preheat, and reference velocity of 25 m/s at the catalyst chamber entrance. The geometry of the 5.08 cm diameter pre-combustor utilized during the catalyst screening phase of the program has been preserved in the 7.6 cm diameter combustor design. Since the air flow rates in the 5.08 cm combustor were 140 g/s, the areas of the orifices and annuli in the 5.08 cm combustor were doubled in the 7.6 cm combustor design. Thus, similar air velocities will be maintained at the critical points in the large combustor. The flow characteristics of the 7.6 cm combustor, except for higher air flow rates, are similar to the 5.08 cm combustors, and are summarized in Section III.

The materials of construction were Type 316 stainless steel and Hastelloy-X which was utilized exclusively in the pre-combustor can and the catalyst cylinder.

The pre-combustor was designed to be capable of operating over an equivalence ratio in the range of 0.1-0.3. Overall combustion efficiencies are expected to be in excess of 99.5% over much of the equivalence ratio range, while emissions are expected to be within the range to meet the 1981 EPA specifications for new aircraft engines.

2. PRELIMINARY HAZARDS LIST

The awareness of possible dangerous situations that may arise during the operation of the hybrid catalytic combustor is important to the personnel who will be conducting the combustion tests at AFAPL. In accordance with the contractual requirements and MIL-STD-882, the following list of possible hazardous situations was prepared after reviewing the 20 areas of concern in paragraph 5.8.2 of MIL-STD-882.

1. System environmental constraints
2. Pressure vessels and plumbing
3. Safe operation and maintenance of the system
4. Fire ignition and propagation sources
5. Resistance to shock damage

The fifteen remaining topics contained in the MIL-STD-882 do not pertain to the type of hardware represented by the 7.6 cm diameter combustor delivered to AFAPL. A brief qualitative discussion of the five topics of direct concern to the safe operation and maintenance of the combustor is given below.

a. System Environmental Constraints

The combustor consists of two major components: the pre-combustor and the catalytic combustor. The materials of construction are type 304 and 316 welded stainless steel. Schedule 40 pipe is used for the outer pressure

bearing walls of the pre-combustor and the catalytic combustor. Mating flanges were 1.1 MPa (150#) pattern. The service temperature for the forged, type 304 stainless steel flanges is 810 K at 379 kPa, and the continuous working pressure of the 7.6 cm pipe at 810 K is greater than 5.0 MPa. In order to preserve the pressure rating of the system at high temperatures (air preheat), the gaskets should be of the Flexitallic-type where asbestos and stainless steel are the materials of construction.

b. Pressure Vessels and Plumbing

Although there are no pressure vessels supplied with the system, a point of concern is the possible leakage of fuel from the fuel supply tube which is located at the combustor inlet. The short, 1.57 rad (90°) bend, type 304 stainless tube has a hot working pressure far in excess of the 2.0 MPa recommended fuel injection pressure. However, if the swagelok tube nuts become damaged from mishandling, a fuel leak could occur which would result in high unburned hydrocarbon concentrations in the combustor due to poor mixing. The fuel line connections should be carefully checked after each run to assure that no fuel leaks have occurred.

c. Safe Operation and Maintenance of the System

The only components within the combustor that may require occasional replacement are the pressure atomizing fuel spray nozzle and the ignition electrode. Either of these components may become fouled with carbonaceous deposits after long test periods, and should be inspected frequently to prevent premature failure. If the aluminum oxide insulator of the ignitor becomes fouled with carbon, it should be removed from the combustor and soaked in chromic acid for a period of about 6-8 hours.

The pressure atomizing fuel spray nozzle contains a particulate filter which should be inspected after every 10 hours of operation. The screen or sintered metal filter element is easily cleaned by soaking it in a hydrocarbon solvent. If the filter element becomes badly plugged, it is wise to replace the element to prevent a high fuel line pressure drop.

d. Fire Ignition and Propagation Sources

During normal combustor operations there are no problems anticipated with "flashback" within the combustor. However, as previously stated, if a fuel leak should develop in the fuel supply line, a high concentration of unburned hydrocarbons in the combustion products stream could result.

e. Resistance to Shock Damage

Since the catalyst support material is made of cordierite, which is a rather fragile ceramic material compared to the other materials of construction used in the combustor, it must be handled with great care. The cordierite supported catalyst is mounted inside a Hastelloy-X tube which will prevent any physical damage to the catalyst during normal handling.

In summary, there are no other hazardous conditions which are expected to occur during the operation of the combustor, but in order to prevent the overheating of the combustor components and catalyst, sufficient temperature data should be made available from various points within the combustor to assure that component failure will not occur.

SECTION VII

CONCLUSIONS AND RECOMMENDATIONS

The feasibility of the Hybrid Catalytic Combustor operating in the aircraft gas turbine engine "idle-mode" has been demonstrated. The results show that the utilization of this concept makes it possible to obtain heat release rates on the order of $1 \text{ kJ/Pa}\cdot\text{s}\cdot\text{m}^3$, and CO and NO_x emissions below the EPA standards for subsonic turbofan and turbojet aircraft engines manufactured on or after January 1, 1981 (1). UHC emissions from the HCC exceeded the standard slightly using the method of calculation developed by Gott and Bastress (24), while NO_x emissions exceeded the standard using an alternate method of calculations based on data presented by Roberts, et al., (25). The problems usually associated with catalytic combustors such as cold-starts and pre-vaporization and pre-mixing of the fuel were overcome by the utilization of the hybrid concept since, during the pre-combustion mode, the device was operated essentially as a conventional gas turbine annular combustor.

The combustion efficiencies measured during hybrid operation were always greater than 98% over the entire range of fuel-air mixtures studied, and more specifically, greater than 99.5% in the range of mixtures that simulated engine idle or high power conditions.

The experimental results indicated that the technique of staged combustion can be used in a gas turbine combustor to prevent the formation of thermally generated NO_x . The catalytic section of the combustor apparently converted the small amounts of HCN and NH_3 produced during rich combustion in the pre-combustor to acceptable concentrations of NO_x . Pre-conditioning of an active catalyst may have influenced the reactions which are believed responsible for the conversion of nitrogenous species to NO_x .

The durability of the catalyst was observed to be sensitive to the degree of pre-combustion of JP-4, as evidenced by the thermal deformation of the catalyst support when unburned fuel resulting from an ignition delay of the pre-burner was adsorbed on the catalyst surface and subsequently oxidized under near-stoichiometric conditions. This problem may be eliminated by the use of a fully reliable pre-combustor electrical ignitor, or by the insertion of a silicon carbide or silicon nitride catalyst support at the entrance to the catalyst bed as a scavenger and guard for the actual catalyst. A review of the test data indicated that more thermally stable catalyst wash coat materials and catalytic metal preparation will be required if the loss of catalytic activity for CO and UHC conversions is to be lessened for operating temperatures in excess of 1200 K.

The combustion of high nitrogen content fuels, i.e., distillates from coal or shale (27), should be evaluated in the hybrid catalytic combustor since the available data indicate that low NO_x emissions may be possible by suitable catalyst pre-conditioning and staged combustion.

In the future, any monolithic catalyst support development efforts should also include materials such as silicon carbide, silicon nitride, metal foils or other refractory-type materials that have been shown to be capable of high temperature operation with good wash coat adhesion.

As a result of this research, it appears that an efficient, low emissions hybrid catalytic combustor can be developed to operate over the entire range of gas turbine power settings from idle, to full power. It should be noted that the HCC approach is not limited to idle operation, but can indeed operate effectively at full power as demonstrated by operating the combustor at $\phi = 0.3$. No attempt was made to determine how an engine using a HCC system would operate over the LTO cycle. The feasibility of using HCC for idle operation, followed by an all catalytic high power mode, is currently being considered by the Air Force (30). It must be emphasized that actual engine tests must be conducted to fully assess the feasibility of the HCC concept.

APPENDIX I

DESCRIPTION OF SUPPORT GEOMETRY AND MATERIALS

This appendix is a summary of required design information concerning the physical characteristics of monolithic catalyst supports. Each support geometry is identified with a capital letter and corresponds to the support configuration found in Table VII of the text. All of the information was obtained from the manufacturer of the support material.

Table XIII

Manufacturer: General Refractories Co., Philadelphia, Pennsylvania

Support Material: Cordierite, Versagrid, (2 MgO · 2 Al₂O₃ · 5 SiO₂)

(Identification in Table VII)	<u>C</u>	<u>B</u>	<u>E</u>	<u>G</u>	<u>F</u>
<u>Support Geometry</u>	<u>Round</u>	<u>Round</u>	<u>Square</u>	<u>Triangular</u>	<u>Rectangle</u>
Cell size (mm)	1.6	3.2	1.6	1.6	1.6 x 3.2
Wall thickness (mm)	0.28	0.30	0.28	0.28	0.28
Frontal Open Area (%)	67	78	73	65	79
Holes/cm ²	33.5	9.8	34.9	42.3	16.4
Surface/Volume (m ² /m ³)	1701	985	1937	2473	1537
Maximum use temp. (°X)	1750	1750	1750	1750	1750
<u>Compressive Strength (kg/cm²)</u>					
● Parallel to cell direction	281	116	232	197	186
● Perpendicular to cell direction	17.6	14.1	52.7	17.6	26.4

Table XIV

Manufacturer: W. R. Grace & Co., Research Division, Columbia, Maryland

Support Material: Poramic[®] 49, 50% Cordierite with 20% Mullite, 5% α -Al₂O₃ and 25% non-crystalline.

<u>Support Geometry</u>	<u>A</u>		<u>L</u>
	<u>Poramic 290 (square)</u>	<u>Poramic 400 (square)</u>	<u>Poramic (Rectangle) Double - Diagonal</u>
Cell size (mm)	1.52	1.27	4.76
Wall thickness (mm)	0.30	0.25	0.35
Frontal Open Area (%)	69	64	75
Holes/cm ²	45	62	18
Surface/Volume (m ² /m ³)	2109	2370	--
Maximum use temp. (K)	1750	1750	1750
<u>Compressive Strength (kg/cm²)</u>			
• Parallel to cell direction	196	84	--
• Perpendicular to cell direction	28	13	--

Table XV

Manufacturer: Norton Industrial Ceramics Division, Worcester, Massachusetts

Support Material: 99+% Silicon Carbide (Spectramic[®])

<u>Support Geometry</u>	<u>D</u>
	<u>Round</u>
Cell size (mm)	3.2
Wall thickness (mm)	<0.3
Frontal Open Area (%)	70
Holes/cm ²	11
Surface/Volume (m ² /m ³)	1100
Maximum use temp. (K)	1920
<u>Compressive Strength (kg/cm²)</u>	
• Parallel to cell direction	49
• Perpendicular to cell direction	--

Table XVI

Manufacturer: Nippon Sealol Co., Ltd. (Pure Carbon Co.
St. Mary's, Pennsylvania)

Support Material: Silicon Carbide (Polycrystalline Self-Bonded)

(Identification in Table VII)

K

Support Geometry

Rolled Corrugated Sheet

Cell size (mm)	3.0
Wall thickness (mm)	0.35
Frontal Open Area (%)	54
Holes/cm ²	9
Surface/Volume (m ² /m ³)	1428
Maximum use temp. (K)	1900

Compressive Strength (kg/cm²)

- Parallel to cell direction —
- Perpendicular to cell direction —

Table XVII

Manufacturer: DuPont, Wilmington, Delaware

Support Material: TORVEX (Al₂O₃)

(Identification in Table VII)

J

Support Geometry

Cross - Flow

Cell size (mm)	4.75
Wall thickness (mm)	0.76
Frontal Open Area (%)	65
Holes/cm ²	--
Surface/Volume (m ² /m ³)	836
Maximum use temp. (K)	1770

Compressive Strength (kg/cm²)

- Parallel to cell direction --
- Perpendicular to cell direction --

APPENDIX II

CATALYST DESCRIPTION

This appendix contains a description of each candidate catalyst tested during the program. A description of the catalyst support and active catalyst materials is given. The identification code found at the head of each description refers to the catalyst found in Table VII of the text.

CATALYST DESCRIPTION

IDENTIFICATION CODE (GH)

<u>SUPPORT</u>	<u>CATALYTIC COMPONENTS</u>	
General Manufacturer: Refractories Co.	Manufacturer: Oxy-Catalyst, Inc.	
Material: Cordierite	Wash Coat Composition: $Al_2O_3 + SiO_2$	
Geometry: 0.16 cm. triangle	Wash Coat Weight (g/m^2): 52.83	
Surface/Volume (m^2/m^3): 2473	Active Materials:	
Percent Open Area: 65	<u>(kg/m^3)</u>	<u>(g/m^2)</u>
	Pt <u>0.85</u>	<u>.342</u>
	Pd <u>0.85</u>	<u>.342</u>
	<u> </u>	<u> </u>
	<u> </u>	<u> </u>

COMBUSTION SYSTEM ASSEMBLY

Length of catalytic segment (cm) : 5.08
Number of segments : 4
GAP between segments (cm) : 0
Total catalyst volume (cm^3) : 411

REMARKS: Two of the 4 segments had unstabilized wash coats and the other two segment's wash coats were stabilized with SiO_2 .

CATALYST DESCRIPTION

IDENTIFICATION CODE (JH)

<u>SUPPORT</u>	<u>CATALYTIC COMPONENTS</u>															
General Manufacturer: Refractories Co.	Manufacturer: Oxy-Catalyst Inc.															
Material: Cordierite	Wash Coat Composition: $Al_2O_3 + SiO_2$															
Geometry: .16x.32 cm. rectangle	Wash Coat Weight (g/m^2): 44.96															
Surface/Volume (m^2/m^3): 1537	Active Materials:															
Percent Open Area: 79																
	<table><thead><tr><th></th><th>(kg/m^3)</th><th>(g/m^2)</th></tr></thead><tbody><tr><td>Pt</td><td><u>0.85</u></td><td><u>0.549</u></td></tr><tr><td>Pd</td><td><u>0.85</u></td><td><u>0.549</u></td></tr><tr><td></td><td><u> </u></td><td><u> </u></td></tr><tr><td></td><td><u> </u></td><td><u> </u></td></tr></tbody></table>		(kg/m^3)	(g/m^2)	Pt	<u>0.85</u>	<u>0.549</u>	Pd	<u>0.85</u>	<u>0.549</u>		<u> </u>	<u> </u>		<u> </u>	<u> </u>
	(kg/m^3)	(g/m^2)														
Pt	<u>0.85</u>	<u>0.549</u>														
Pd	<u>0.85</u>	<u>0.549</u>														
	<u> </u>	<u> </u>														
	<u> </u>	<u> </u>														

COMBUSTION SYSTEM ASSEMBLY

Length of catalytic segment (cm) : 5.08
Number of segments : 4
GAP between segments (cm) : 0
Total catalyst volume (cm^3) : 411

REMARKS:

Two of the four segments had unstabilized wash coats and the other two segment's wash coats were stabilized with SiO_2 .

CATALYST DESCRIPTION

IDENTIFICATION CODE (FH)

<u>SUPPORT</u>	<u>CATALYTIC COMPONENTS</u>		
General Manufacturer: Refractories Co.	Manufacturer: Oxy-Catalyst Inc.		
Material: Cordierite	Wash Coat Composition: $Al_2O_3 + SiO_2$		
Geometry: 0.16 cm. square	Wash Coat Weight (g/m^2): 46.28		
Surface/Volume (m^2/m^3): 1937	Active Materials:		
Percent Open Area: 73		<u>(kg/m^3)</u>	<u>(g/m^2)</u>
	Pt	<u>0.85</u>	<u>0.435</u>
	Pd	<u>0.85</u>	<u>0.435</u>
		<u> </u>	<u> </u>
		<u> </u>	<u> </u>

COMBUSTION SYSTEM ASSEMBLY

Length of catalytic segment (cm) : 5.08
Number of segments : 4
GAP between segments (cm) : 0
Total catalyst volume (cm^3) : 411

REMARKS:

Two of the four segments had unstabilized wash coats and the other two segment's wash coats were stabilized with SiO_2 .

CATALYST DESCRIPTION

IDENTIFICATION CODE (EH)

<u>SUPPORT</u>	<u>CATALYTIC COMPONENTS</u>															
General Manufacturer: Refractories Co.	Manufacturer: Oxy-Catalyst Inc.															
Material: Condierite	Wash Coat Composition: $Al_2O_3 + SiO_2$															
Geometry: 0.158 cm. circle	Wash Coat Weight (g/m^2): 46.7															
Surface/Volume (m^2/m^3): 1700	Active Materials:															
Percent Open Area: 67																
	<table><thead><tr><th></th><th><u>(kg/m^3)</u></th><th><u>(g/m^2)</u></th></tr></thead><tbody><tr><td>Pt</td><td><u>0.85</u></td><td><u>0.496</u></td></tr><tr><td>Pd</td><td><u>0.85</u></td><td><u>0.496</u></td></tr><tr><td></td><td><u> </u></td><td><u> </u></td></tr><tr><td></td><td><u> </u></td><td><u> </u></td></tr></tbody></table>		<u>(kg/m^3)</u>	<u>(g/m^2)</u>	Pt	<u>0.85</u>	<u>0.496</u>	Pd	<u>0.85</u>	<u>0.496</u>		<u> </u>	<u> </u>		<u> </u>	<u> </u>
	<u>(kg/m^3)</u>	<u>(g/m^2)</u>														
Pt	<u>0.85</u>	<u>0.496</u>														
Pd	<u>0.85</u>	<u>0.496</u>														
	<u> </u>	<u> </u>														
	<u> </u>	<u> </u>														

COMBUSTION SYSTEM ASSEMBLY

Length of catalytic segment (cm) : 5.08
Number of segments : 4
GAP between segments (cm)₃ : 0
Total catalyst volume (cm³) : 411

REMARKS: Two of the 4 segments had unstabilized wash coats and the other two segment's wash coats were stabilized with SiO_2 .

CATALYST DESCRIPTION

IDENTIFICATION CODE ()

SUPPORT

Manufacturer: W. R. Grace
Material: Cordierite
Geometry: 0.127 cm. square
Surface/Volume (m^2/m^3): 2109
Percent Open Area: 69

CATALYTIC COMPONENTS

Manufacturer: W. R. Grace
Wash Coat Composition: 53 wt% NiO + SiO₂
Wash Coat Weight (g/m^2): 52.26
Active Materials:

	<u>(kg/m^3)</u>	<u>(g/m^2)</u>
Pd	<u>1.25</u>	<u>0.60</u>
Rh	<u>0.055</u>	<u>0.027</u>
	<u> </u>	<u> </u>
	<u> </u>	<u> </u>

COMBUSTION SYSTEM ASSEMBLY

Length of catalytic segment (in) : 5.08
Number of segments : 4
GAP between segments (cm) : 0
Total catalyst volume (cm³) : 411

REMARKS:

W. R. Grace Davox - 607

CATALYST DESCRIPTION

IDENTIFICATION CODE (HH)

<u>SUPPORT</u>	<u>CATALYTIC COMPONENTS</u>
General Manufacturer: Refractories Co.	Manufacturer: Oxy-Catalyst, Inc.
Material: Cordierite	Wash Coat Composition: $Al_2O_3 + SiO_2$
Geometry: 0.31 cm. circle	Wash Coat Weight (g/m^2): 100.4
Surface/Volume (m^2/m^3): 996	Active Materials:
Percent Open Area: 78	
	<u>(kg/m^3)</u> <u>(g/m^2)</u>
	Pt <u>0.85</u> <u>0.848</u>
	Pd <u>0.85</u> <u>0.848</u>

COMBUSTION SYSTEM ASSEMBLY

Length of catalytic segment (cm) : 5.08
Number of segments : 4
GAP between segments (cm) : 0
Total catalyst volume (cm^3) : 411

REMARKS: Two of the 4 segments had unstabilized wash coats and the other two segment's wash coats were stabilized with SiO_2 .

CATALYST DESCRIPTION

IDENTIFICATION CODE (KP)

<u>SUPPORT</u>	<u>CATALYTIC COMPONENTS</u>		
Manufacturer: W. R. Grace	Manufacturer: W. R. Grace		
Material: Cordierite	Wash Coat Composition: ZrO ₂		
Geometry: .127 cm. square	Wash Coat Weight (g/m ²): 75.1		
Surface/Volume (m ² /m ³): 2109	Active Materials:		
Percent Open Area: 69		(kg/m ³)	(g/m ²)
	Zr	<u>0.389</u>	<u>0.184</u>
	CoO	<u>57.27</u>	<u>27.17</u>
		_____	_____
		_____	_____

COMBUSTION SYSTEM ASSEMBLY

Length of catalytic segment (cm) : 5.08
Number of segments : 4
GAP between segments (cm) : 0
Total catalyst volume (cm³) : 412

REMARKS:

W. Grace Davox - 516

CATALYST DESCRIPTION

IDENTIFICATION CODE (KX)

<u>SUPPORT</u>	<u>CATALYTIC COMPONENTS</u>		
Manufacturer: W. R. Grace	Manufacturer: W. R. Grace		
Material: Cordierite	Wash Coat Composition: 25 wt% CeO + Al ₂ O ₃		
Geometry: .127 cm. square	Wash Coat Weight (g/m ²): 60.03		
Surface/Volume (m ² /m ³): 2109	Active Materials:		
Percent Open Area: 69	(kg/m ³)	(g/m ²)	
	Pt	2.75	1.30
	Pd	2.75	1.30

COMBUSTION SYSTEM ASSEMBLY

Length of catalytic segment (cm) : 5.08
Number of segments : 4
GAP between segments (cm)₃ : 0
Total catalyst volume (cm³) : 411

REMARKS:

W. R. Grace Davax - 512B

CATALYST DESCRIPTION

IDENTIFICATION CODE (KQ)

<u>SUPPORT</u>	<u>CATALYTIC COMPONENTS</u>	
Manufacturer: W. R. Grace	Manufacturer: W. R. Grace	
Material: Cordierite	Wash Coat Composition: 25 wt% CeO + Al ₂ O ₃	
Geometry: .127 cm. square	Wash Coat Weight (g/m ²): 44.1	
Surface/Volume (m ² /m ³): 2109	Active Materials:	
Percent Open Area: 69		
	(kg/m ³)	(g/m ²)
	Pd	3.27
		1.55

COMBUSTION SYSTEM ASSEMBLY

Length of catalytic segment (cm) : 5.08
Number of segments : 4
GAP between segments (cm) : 0
Total catalyst volume (cm³) : 411

REMARKS:

W. R. Grace Davax - 517

CATALYST DESCRIPTION

IDENTIFICATION CODE (KR)

<u>SUPPORT</u>	<u>CATALYTIC COMPONENTS</u>	
Manufacturer: W. R. Grace	Manufacturer: W. R. Grace	
Material: Cordierite	Wash Coat Composition: 25 wt% REO(a) + Al ₂ O ₃	
Geometry: .127 cm. square	Wash Coat Weight (g/m ²): 44.15	
Surface/Volume (m ² /m ³): 2109	Active Materials:	
Percent Open Area: 69	(kg/m ³)	(g/m ²)
	REO(a) <u>27</u>	<u>13.02</u>
	<u> </u>	<u> </u>
	<u> </u>	<u> </u>
	<u> </u>	<u> </u>

COMBUSTION SYSTEM ASSEMBLY

Length of catalytic segment (cm) : 5.08
Number of segments : 4
GAP between segments (cm) : 0
Total catalyst volume (cm³) : 411

REMARKS:

W. R. Grace Davex - 521

(a) Commercial mixture of rare earth oxides

CATALYST DESCRIPTION

IDENTIFICATION CODE (RA)

<u>SUPPORT</u>	<u>CATALYTIC COMPONENTS</u>	
Manufacturer: Pure Carbon Co.	Manufacturer: General Refractories Co.	
Material: SiC	Wash Coat Composition: None	
Geometry: .31 cm. corrugation	Wash Coat Weight (g/m^2): None	
Surface/Volume (m^2/m^3): 1428	Active Materials:	
Percent Open Area: 68	<u>(kg/m^3)</u>	<u>(g/m^2)</u>
	R ₂ O ^(a) Mixture ~ <u>97.3</u>	~ <u>68.25</u>
	_____	_____
	_____	_____
	_____	_____

COMBUSTION SYSTEM ASSEMBLY

Length of catalytic segment (cm) : 10.16
Number of segments : 2
GAP between segments (cm) : 0
Total catalyst volume (cm^3) : 411

REMARKS:

(a) Rare Earth Oxide mixture fused to SiC monolith with no wash coat or any other high surface area material.

CATALYST DESCRIPTION

IDENTIFICATION CODE (KU)

<u>SUPPORT</u>	<u>CATALYTIC COMPONENTS</u>		
Manufacturer: W. R. Grace	Manufacturer: W. R. Grace		
Material: Cordierite	Wash Coat Composition: 12.34 wt% BMO(a) + Al ₂ O ₃		
Geometry: 1.27 cm. square	Wash Coat Weight (g/m ²): 37.47		
Surface/Volume (m ² /m ³): 2109	Active Materials:		
Percent Open Area: 69	(kg/m ³)	(g/m ²)	
	Pd	0.389	0.185
	CuO + Cr ₂ O ₃ + MnO ₂	28.22	13.39
		_____	_____
		_____	_____

COMBUSTION SYSTEM ASSEMBLY

Length of catalytic segment (cm) : 5.08
Number of segments : 4
GAP between segments (cm) : 0
Total catalyst volume (cm³) : 411

REMARKS:

W. R. Grace Davex - 523

(a) Base Metal Oxides of Cu, Cr and Mn.

CATALYST DESCRIPTION

IDENTIFICATION CODE (MQ)

<u>SUPPORT</u>	<u>CATALYTIC COMPONENTS</u>		
Manufacturer: W. R. Grace	Manufacturer: W. R. Grace		
Material: Cordierite	Wash Coat Composition: 25 wt% CeO + Al ₂ O ₃		
Geometry: 0.635 cm x 0.144 cm rectangle	Wash Coat Weight (g/m ²): Not Known		
Surface/Volume (m ² /m ³): Not Known	Active Materials:		
Percent Open Area: 75		<u>(kg/m³)</u>	<u>(g/m²)</u>
	Pd	<u>2.60</u>	<u>Not Known</u>
		_____	_____
		_____	_____
		_____	_____

COMBUSTION SYSTEM ASSEMBLY

Length of catalytic segment (cm) : 5.08
Number of segments : 2
GAP between segments (cm) : 0
Total catalyst volume (cm³) : 205

REMARKS: Two segments of this catalyst were tested. The catalysts were located at the entrance end of the catalyst chamber with a 10.16 cm. gap between the catalyst and the end of the chamber.

CATALYST DESCRIPTION

IDENTIFICATION CODE (FZ)

<u>SUPPORT</u>	<u>CATALYTIC COMPONENTS</u>		
General	Manufacturer: Oxy-Catalyst, Inc.		
Manufacturer: Refractories Co.	Wash Coat Composition: $Al_2O_3 + SiO_2$		
Material: Cordierite	Wash Coat Weight (g/m^2): 49.2		
Geometry: 0.16 cm square	Active Materials:		
Surface/Volume (m^2/m^3): 1937		<u>(kg/m^3)</u>	<u>(g/m^2)</u>
Percent Open Area: 73	Pt	<u>0.275</u>	<u>0.142</u>
	Pd	<u>0.275</u>	<u>0.142</u>
		_____	_____
		_____	_____

COMBUSTION SYSTEM ASSEMBLY

Length of catalytic segment (cm) : 5.08
Number of segments : 4
GAP between segments (cm) : 0
Total catalyst volume (cm^3) : 411

REMARKS:

CATALYST DESCRIPTION

IDENTIFICATION CODE (FV)

<u>SUPPORT</u>		<u>CATALYTIC COMPONENTS</u>		
Manufacturer:	General Refractories Co.	Manufacturer: Oxy-Catalyst, Inc.		
Material:	Cordierite	Wash Coat Composition: Al ₂ O ₃ + SiO ₂		
Geometry:	0.16 cm square	Wash Coat Weight (g/m ²): 49.2		
Surface/Volume (m ² /m ³):	1937	Active Materials:		
Percent Open Area:	73			
		(kg/m ³)	(g/m ²)	
		Pd	3.3	1.69
		Cr ₂ O ₃ + MnO ₂	68.1	35.2
			_____	_____
			_____	_____

COMBUSTION SYSTEM ASSEMBLY

Length of catalytic segment (cm) : 5.08
Number of segments : 4
GAP between segments (cm) : 0
Total catalyst volume (cm³) : 411

REMARKS:

During the preparation of this catalyst, the Pd was applied under the Cr₂O₃ + MnO₂ coating.

CATALYST DESCRIPTION

IDENTIFICATION CODE (JG)

<u>SUPPORT</u>	<u>CATALYTIC COMPONENTS</u>															
General Manufacturer: Refractories Co.	Manufacturer: W. R. Grace															
Material: Cordierite	Wash Coat Composition: 25 wt% CeO + Al ₂ O ₃															
Geometry: .16 x .32 cm rectangle	Wash Coat Weight (g/m ²): 49.59															
Surface/Volume (m ² /m ³): 1537	Active Materials:															
Percent Open Area: 79																
	<table><thead><tr><th></th><th>(kg/m³)</th><th>(g/m²)</th></tr></thead><tbody><tr><td>Pd</td><td><u>0.389</u></td><td><u>0.253</u></td></tr><tr><td>CuO + Cr₂O₃</td><td><u>9.586</u></td><td><u>6.24</u></td></tr><tr><td></td><td><u> </u></td><td><u> </u></td></tr><tr><td></td><td><u> </u></td><td><u> </u></td></tr></tbody></table>		(kg/m ³)	(g/m ²)	Pd	<u>0.389</u>	<u>0.253</u>	CuO + Cr ₂ O ₃	<u>9.586</u>	<u>6.24</u>		<u> </u>	<u> </u>		<u> </u>	<u> </u>
	(kg/m ³)	(g/m ²)														
Pd	<u>0.389</u>	<u>0.253</u>														
CuO + Cr ₂ O ₃	<u>9.586</u>	<u>6.24</u>														
	<u> </u>	<u> </u>														
	<u> </u>	<u> </u>														

COMBUSTION SYSTEM ASSEMBLY

Length of catalytic segment (cm) : 5.08
Number of segments : 4
GAP between segments (cm) : 0
Total catalyst volume (cm³) : 411

REMARKS:

W. R. Grace Davison Code 915 (Diesel Exhaust catalyst)

CATALYST DESCRIPTION

IDENTIFICATION CODE (FG)

<u>SUPPORT</u>		<u>CATALYTIC COMPONENTS</u>		
Manufacturer:	General Refractories Co.	Manufacturer: W. R. Grace		
Material:	Cordierite	Wash Coat Composition: 25 wt% CeO + Al ₂ O ₃		
Geometry:	0.16 cm. square	Wash Coat Weight (g/m ²): 40.5		
Surface/Volume (m ² /m ³):	1937	Active Materials:		
Percent Open Area:	73	(kg/m ³)	(g/m ²)	
		Pd	0.389	0.20
		CuO + Cr ₂ O ₃	10.36	5.36
			_____	_____
			_____	_____

COMBUSTION SYSTEM ASSEMBLY

Length of catalytic segment (cm) : 5.08
Number of segments : 4
GAP between segments (cm) : 0
Total catalyst volume (cm³) : 411

REMARKS:

W. R. Grace Davison Code 915 (Diesel Exhaust Catalyst)

CATALYST DESCRIPTION

IDENTIFICATION CODE (F2)

<u>SUPPORT</u>		<u>CATALYTIC COMPONENTS</u>		
Manufacturer:	General Refractories Co.	Manufacturer:	Oxy-Catalyst, Inc.	
Material:	Cordierite	Wash Coat Composition:	Al ₂ O ₃ + SiO ₂	
Geometry:	0.16 cm square	Wash Coat Weight (g/m ²):	49.2	
Surface/Volume (m ² /m ³):	1937	Active Materials:		
Percent Open Area:	73		(μg/cm ³)	(g/m ²)
		Pd	<u>3.3</u>	<u>1.7</u>
			_____	_____
			_____	_____
			_____	_____

COMBUSTION SYSTEM ASSEMBLY

Length of catalytic segment (cm) : 5.08
Number of segments : 4
GAP between segments (cm) : 0
Total catalyst volume (cm³) : 411

REMARKS:

CATALYST DESCRIPTION

IDENTIFICATION CODE (QF)

<u>SUPPORT</u>	<u>CATALYTIC COMPONENTS</u>		
Manufacturer: Johnson Matthey	Manufacturer: Johnson Matthey		
Material: Metal (Ni alloy)	Wash Coat Composition: Stabilized Al ₂ O ₃		
Geometry: Corrugated Roll	Wash Coat Weight (g/m ²): --		
Surface/Volume (m ² /m ³): 4100	Active Materials:		
Percent Open Area: 93		<u>(kg/m³)</u>	<u>(g/m²)</u>
	Pt	<u>5.27</u>	<u>1.04</u>
		_____	_____
		_____	_____
		_____	_____

COMBUSTION SYSTEM ASSEMBLY

Length of catalytic segment (cm) : 7.55
Number of segments : 2
GAP between segments (cm) : 5
Total catalyst volume (cm³) : 308

REMARKS: Two segments of this catalyst were packed into the catalyst combustion chamber with a 5 cm gap between the segments.

CATALYST DESCRIPTION

IDENTIFICATION CODE (PC)

<u>SUPPORT</u>	<u>CATALYTIC COMPONENTS</u>		
Manufacturer: Matthey-Bishop	Manufacturer: Matthey-Bishop		
Material: Metal (Ni Alloy)	Wash Coat Composition: Al ₂ O ₃ + Stabilizer		
Geometry: Screens	Wash Coat Weight (g/m ²): Not Known		
Surface/Volume (m ² /m ³): Not Known	Active Materials:		
Percent Open Area: Not Known		<u>(kg/m³)</u>	<u>(g/m²)</u>
	Pt	Not Known	_____
		_____	_____
		_____	_____
		_____	_____

COMBUSTION SYSTEM ASSEMBLY

Length of catalytic segment (cm) : 10.16
Number of segments : 1
GAP between segments (cm) : 10.16
Total catalyst volume (cm³) : 205

REMARKS: The Matthey-Bishop metal substrate catalyst (PC) was located at the leading end of the catalyst chamber and a 5.08 cm. long segment of General Refractories Co. square hole monolith coated with Al₂O₃ and 5.5 g/l of (1/1) Pt/Pd (FL) was located at the exit end of the chamber. A 10.16 cm. gap existed between segments.

CATALYST DESCRIPTION

IDENTIFICATION CODE (FL)

<u>SUPPORT</u>	<u>CATALYTIC COMPONENTS</u>															
General Manufacturer: Refractories Co.	Manufacturer: Oxy-Catalyst, Inc.															
Material: Cordierite	Wash Coat Composition: Al ₂ O ₃ + SiO ₂															
Geometry: 0.16 cm. square	Wash Coat Weight (g/m ²): 47.6															
Surface/Volume (m ² /m ³): 1937	Active Materials:															
Percent Open Area: 73																
	<table><thead><tr><th></th><th>(kg/m³)</th><th>(g/m²)</th></tr></thead><tbody><tr><td>Pt</td><td><u>2.75</u></td><td><u>1.42</u></td></tr><tr><td>Pd</td><td><u>2.75</u></td><td><u>1.42</u></td></tr><tr><td></td><td>_____</td><td>_____</td></tr><tr><td></td><td>_____</td><td>_____</td></tr></tbody></table>		(kg/m ³)	(g/m ²)	Pt	<u>2.75</u>	<u>1.42</u>	Pd	<u>2.75</u>	<u>1.42</u>		_____	_____		_____	_____
	(kg/m ³)	(g/m ²)														
Pt	<u>2.75</u>	<u>1.42</u>														
Pd	<u>2.75</u>	<u>1.42</u>														
	_____	_____														
	_____	_____														

COMBUSTION SYSTEM ASSEMBLY

Length of catalytic segment (cm) : 5.08
Number of segments : 1
GAP between segments (cm) : 10.16
Total catalyst volume (cm³) : 105

REMARKS: One segment of this catalyst was used in combination with catalyst PC, which was located upstream.

CATALYST DESCRIPTION

IDENTIFICATION CODE (FF)

<u>SUPPORT</u>	<u>CATALYTIC COMPONENTS</u>															
General Manufacturer: Refractories Co.	Manufacturer: Oxy-Catalyst, Inc.															
Material: Cordierite	Wash Coat Composition: $Al_2O_3 + SiO_2$															
Geometry: 0.16 cm. square	Wash Coat Weight (g/m^2): 49.2															
Surface/Volume (m^2/m^3): 1937	Active Materials															
Percent Open Area: 73																
	<table><thead><tr><th></th><th>(kg/m^3)</th><th>(g/m^2)</th></tr></thead><tbody><tr><td>Pd</td><td><u>3.3</u></td><td><u>1.71</u></td></tr><tr><td>$Cr_2O_3 + MnO_2$</td><td><u>28</u></td><td><u>14.5</u></td></tr><tr><td></td><td><u> </u></td><td><u> </u></td></tr><tr><td></td><td><u> </u></td><td><u> </u></td></tr></tbody></table>		(kg/m^3)	(g/m^2)	Pd	<u>3.3</u>	<u>1.71</u>	$Cr_2O_3 + MnO_2$	<u>28</u>	<u>14.5</u>		<u> </u>	<u> </u>		<u> </u>	<u> </u>
	(kg/m^3)	(g/m^2)														
Pd	<u>3.3</u>	<u>1.71</u>														
$Cr_2O_3 + MnO_2$	<u>28</u>	<u>14.5</u>														
	<u> </u>	<u> </u>														
	<u> </u>	<u> </u>														

COMBUSTION SYSTEM ASSEMBLY

Length of catalytic segment (cm) : 5.08
Number of segments : 4
GAP between segments (cm) : 0
Total catalyst volume (cm^3) : 411

REMARKS: This catalyst was destroyed by a misfire in the primary combustor.
No data were obtained.

CATALYST DESCRIPTION

IDENTIFICATION CODE (FD)

<u>SUPPORT</u>	<u>CATALYTIC COMPONENTS</u>															
General Manufacturer: Refractories Co.	Manufacturer: Oxy-Catalyst, Inc.															
Material: Cordierite	Wash Coat Composition: Al ₂ O ₃ + SiO ₂															
Geometry: 0.16 cm. square	Wash Coat Weight (g/m ²): 49.2															
Surface/Volume (m ² /m ³): 1937	Active Materials:															
Percent Open Area: 73																
	<table><thead><tr><th></th><th>(kg/m³)</th><th>(g/m²)</th></tr></thead><tbody><tr><td>Ir</td><td>1.7</td><td>0.88</td></tr><tr><td></td><td>_____</td><td>_____</td></tr><tr><td></td><td>_____</td><td>_____</td></tr><tr><td></td><td>_____</td><td>_____</td></tr></tbody></table>		(kg/m ³)	(g/m ²)	Ir	1.7	0.88		_____	_____		_____	_____		_____	_____
	(kg/m ³)	(g/m ²)														
Ir	1.7	0.88														
	_____	_____														
	_____	_____														
	_____	_____														

COMBUSTION SYSTEM ASSEMBLY

Length of catalytic segment (cm) : 5.08
Number of segments : 4
GAP between segments (cm) : 0
Total catalyst volume (cm³) : 411

REMARKS: Two segments of this catalyst were tested with two segments of catalyst (FE). The different segments were alternated.

CATALYST DESCRIPTION

IDENTIFICATION CODE (FE)

<u>SUPPORT</u>	<u>CATALYTIC COMPONENTS</u>															
General Manufacturer: Refractories Co.	Manufacturer: Oxy-Catalyst, Inc.															
Material: Cordierite	Wash Coat Composition: $Al_2O_3 + SiO_2$															
Geometry: 0.16 cm. square	Wash Coat Weight (g/m^2): 46.5															
Surface/Volume (m^2/m^3): 1937	Active Materials:															
Percent Open Area: 73																
	<table><thead><tr><th></th><th style="text-align: center;"><u>(kg/m^3)</u></th><th style="text-align: center;"><u>(g/m^2)</u></th></tr></thead><tbody><tr><td style="text-align: center;">Pt</td><td style="text-align: center;"><u>.85</u></td><td style="text-align: center;"><u>.437</u></td></tr><tr><td style="text-align: center;">Ir</td><td style="text-align: center;"><u>.85</u></td><td style="text-align: center;"><u>.437</u></td></tr><tr><td></td><td style="text-align: center;">_____</td><td style="text-align: center;">_____</td></tr><tr><td></td><td style="text-align: center;">_____</td><td style="text-align: center;">_____</td></tr></tbody></table>		<u>(kg/m^3)</u>	<u>(g/m^2)</u>	Pt	<u>.85</u>	<u>.437</u>	Ir	<u>.85</u>	<u>.437</u>		_____	_____		_____	_____
	<u>(kg/m^3)</u>	<u>(g/m^2)</u>														
Pt	<u>.85</u>	<u>.437</u>														
Ir	<u>.85</u>	<u>.437</u>														
	_____	_____														
	_____	_____														

COMBUSTION SYSTEM ASSEMBLY

Length of catalytic segment (cm) : 5.08
Number of segments : 4
GAP between segments (cm) : 0
Total catalyst volume (cm^3) : 411

REMARKS: Two segments of this catalyst were tested with two segments of catalyst (FD). The different segments were alternated.

APPENDIX III

SUMMARY OF EMISSION INDEXES AND COMBUSTION EFFICIENCIES

The experimental results are tabulated in chronological order. The catalyst identification code letters appear in the heading for each run number. Since the primary and secondary air streams were preheated to 400 K, this fact was omitted from the tabulation. The column "LOC" indicates the location in the combustor where the data were taken. The data point locations are given in Figure 1 in the text. Under the column identified "TEMP", corresponding to a particular "LOC", zero (0) indicates that temperature was not measured at that location during that run. The data obtained at the catalyst bed inlet is identified under "LOC" by the number 1, and the data obtained at the exit of the catalyst bed is identified by number 2. The combustion efficiency and emission indexes were estimated for each "LOC" by solving the equations given in Section IV, Part 13 of the text. The remaining data columns are self-explanatory.

RUN NUMBER 128
CAT. I.D. KT

AIR/FUEL --RATIOS-- PRI ALL	CAT PRESS OROP (KPA)	BED INLET TEMP (K)	LOC	TEMP (K)	CO PPM	O2 VOL PCT	NO PPM	NOX PPM	UHC PPM	COMB EFF PCT	---EMISSION INDEXES--- ---G/KG FUEL---		
											CO	UHC	NO2
10.43	51.96	103.35	A	1972	0	0.0	0	0	0	0.0	0.00	0.00	0.00
10.43	51.96	103.35	H	1167	335	16.9	8	12	230	98.9	17.13	6.72	1.00
10.43	51.96	103.35	I	1161	318	16.3	12	14	150	99.1	16.26	4.38	1.34
10.43	51.96	103.35	J	0	260	15.5	16	20	70	99.4	13.29	2.04	1.68
10.43	51.96	103.35	K	0	195	14.7	22	24	80	99.5	9.97	2.33	2.01
10.43	51.96	103.35	D	0	100	15.5	28	29	33	99.7	5.11	0.96	2.43
10.43	51.96	103.35	I	0	280	15.5	17	21	110	99.3	14.31	3.21	1.76

RUN NUMBER 130
CAT. I.D. EH

AIR/FUEL --RATIOS-- PRI ALL	CAT PRESS OROP (KPA)	BED INLET TEMP (K)	LOC	TEMP (K)	CO PPM	O2 VOL PCT	NO PPM	NOX PPM	UHC PPM	COMB EFF PCT	---EMISSION INDEXES--- ---G/KG FUEL---		
											CO	UHC	NO2
10.13	50.47	51.67	A	1694	0	0.0	0	0	0	0.0	0.00	0.00	0.00
10.13	50.47	51.67	G	1267	200	15.0	30	34	41	99.6	9.94	1.16	2.77
10.13	50.47	51.67	H	1156	740	16.5	10	17	640	97.3	36.77	18.17	1.38
10.13	50.47	51.67	I	1228	750	16.5	10	17	670	97.2	37.27	19.02	1.38
10.13	50.47	51.67	J	0	665	16.6	12	20	510	97.7	33.05	14.48	1.63
10.13	50.47	51.67	K	0	415	14.9	24	30	130	99.1	20.62	3.69	2.44
10.13	50.47	51.67	L	0	170	15.1	32	35	22	99.7	8.44	0.62	2.85
10.13	50.47	51.67	M	0	263	16.8	21	24	330	98.7	13.07	9.37	1.95
10.13	50.47	51.67	O	0	185	14.6	24	29	68	99.5	9.19	1.71	2.36
10.13	50.47	51.67	I	0	665	15.7	14	20	530	97.7	33.05	15.05	1.63
10.13	50.47	51.67	Z	0	220	15.8	23	27	210	99.1	10.93	5.96	2.20

RUN NUMBER 131
CAT. I.D. UK

AIR/FUEL --RATIOS-- PRI ALL	CAT PRESS OROP (KPA)	BED INLET TEMP (K)	LOC	TEMP (K)	CO PPM	O2 VOL PCT	NO PPM	NOX PPM	UHC PPM	COMB EFF PCT	---EMISSION INDEXES--- ---G/KG FUEL---		
											CO	UHC	NO2
10.63	52.99	22.73	A	1692	0	0.0	0	0	0	0.0	0.00	0.00	0.00
10.63	52.99	22.73	G	1167	220	15.0	31	34	81	99.4	11.46	2.41	2.91
10.63	52.99	22.73	H	1056	535	15.6	10	17	480	97.9	27.86	14.29	1.45
10.63	52.99	22.73	I	1172	555	15.5	11	18	480	97.8	28.93	14.29	1.54
10.63	52.99	22.73	J	0	535	15.5	12	20	420	98.1	27.68	12.51	1.71
10.63	52.99	22.73	K	0	307	14.2	25	35	120	99.2	16.00	3.57	2.99
10.63	52.99	22.73	L	0	140	14.5	36	38	21	99.7	7.29	0.62	3.25
10.63	52.99	22.73	M	0	260	15.6	24	28	210	99.0	13.55	6.25	2.39
10.63	52.99	22.73	N	0	195	15.1	24	28	210	99.1	10.16	6.25	2.39
10.63	52.99	22.73	O	0	195	14.5	28	34	70	99.5	10.16	2.08	2.91
10.63	52.99	22.73	1	0	555	15.5	14	20	380	98.1	28.93	11.31	1.71
10.63	52.99	22.73	2	0	233	15.4	28	31	107	99.4	12.14	2.97	2.65
10.63	52.99	22.73	2	0	233	15.4	25	29	115	99.3	12.14	3.42	2.48

RUN NUMBER 132 CAT. I.D. FH															
AIR/FUEL ---RATIOS---		CAT PRESS DROP (KPA)	GED INLET TEMP (K)	LOC	TEMP (K)	CC PPH	O2 VOL PCT	MO PPH	NOX PPH	UMC PPH	COMB EFF PCT	---EMISSION INDEXES---			
PRI	ALL											CC	G/KG FUEL	UMC	NO2
11.26	56.10	24.11	1100	A	1673	0	0.0	0	0	0	0.0	0.0	0.00	0.00	0.00
11.26	56.10	24.11	1100	G	1100	75	1.2	29	32	77	99.6	4.13	2.42	2.42	2.85
11.26	56.10	24.11	1100	H	950	447	17.0	4	10	640	97.4	24.64	20.16	20.16	0.90
11.26	56.10	24.11	1100	I	1122	465	16.7	6	12	600	97.5	25.63	18.90	18.90	1.08
11.26	56.10	24.11	1100	J	0	415	15.0	11	18	430	98.1	22.68	13.54	13.54	1.63
11.26	56.10	24.11	1100	K	0	260	14.2	28	34	110	99.3	14.33	3.46	3.46	3.07
11.26	56.10	24.11	1100	L	0	75	15.5	28	31	88	99.6	4.13	2.77	2.77	2.80
11.26	56.10	24.11	1100	M	0	60	14.7	32	35	22	99.8	3.30	0.69	0.69	3.17
11.26	56.10	24.11	1100	N	0	70	14.9	30	32	40	99.7	3.85	1.26	1.26	2.8
11.26	56.10	24.11	1100	O	0	90	15.2	26	29	83	99.6	4.95	2.61	2.61	2.62
11.26	56.10	24.11	1100	1	0	400	16.0	13	19	440	98.1	22.05	13.86	13.86	1.72
11.26	56.10	24.11	1100	2	0	80	15.0	29	32	52	99.7	4.61	1.63	1.63	2.89

RUN NUMBER 133 CAT. I.D. FH															
AIR/FUEL ---RATIOS---		CAT PRESS DROP (KPA)	GED INLET TEMP (K)	LOC	TEMP (K)	CC PPH	O2 VOL PCT	MO PPH	NOX PPH	UMC PPH	COMB EFF PCT	---EMISSION INDEXES---			
PRI	ALL											CC	G/KG FUEL	UMC	NO2
14.16	70.54	17.22	978	A	1693	0	0.0	0	0	0	0.0	0.00	0.00	0.00	0.00
14.16	70.54	17.22	978	G	978	40	15.7	31	34	43	99.7	2.76	1.69	1.69	3.85
14.16	70.54	17.22	978	H	867	250	16.8	7	13	385	98.0	17.26	15.19	15.19	1.47
14.16	70.54	17.22	978	I	994	270	16.6	7	13	390	98.0	18.65	15.39	15.39	1.47
14.16	70.54	17.22	978	J	0	250	16.2	11	18	290	98.4	17.26	11.44	11.44	2.04
14.16	70.54	17.22	978	K	0	202	15.2	21	28	96	99.2	13.95	3.78	3.78	3.17
14.16	70.54	17.22	978	L	0	70	16.1	28	31	64	99.6	3.45	2.52	2.52	3.51
14.16	70.54	17.22	978	M	0	50	15.6	32	35	40	99.7	3.45	1.57	1.57	3.97
14.16	70.54	17.22	978	N	0	50	15.7	30	33	65	99.6	3.45	2.56	2.56	3.74
14.16	70.54	17.22	978	O	0	60	15.9	27	30	59	99.6	4.14	2.32	2.32	3.40
14.16	70.54	17.22	978	1	0	240	16.4	14	20	250	98.6	16.57	9.86	9.86	2.26
14.16	70.54	17.22	978	2	0	50	15.7	33	36	44	99.7	3.45	1.73	1.73	4.08

RUN NUMBER 134 CAT. I.D. FH															
AIR/FUEL ---RATIOS---		CAT PRESS DROP (KPA)	GED INLET TEMP (K)	LOC	TEMP (K)	CC PPH	O2 VOL PCT	MO PPH	NOX PPH	UMC PPH	COMB EFF PCT	---EMISSION INDEXES---			
PRI	ALL											CC	G/KG FUEL	UMC	NO2
18.17	90.54	13.78	844	A	1618	0	0.0	0	0	0	0.0	0.00	0.00	0.00	0.00
18.17	90.54	13.78	844	G	844	55	16.0	30	34	56	99.6	4.86	2.82	2.82	4.93
18.17	90.54	13.78	844	H	811	155	18.	3	10	500	97.1	13.69	25.25	25.25	1.45
18.17	90.54	13.78	844	I	883	178	17.5	6	13	390	97.6	15.73	19.69	19.69	1.88
18.17	90.54	13.78	844	J	0	178	16.7	11	19	245	98.3	15.73	12.37	12.37	2.75
18.17	90.54	13.78	844	K	0	150	15.9	24	33	74	99.3	13.25	3.73	3.73	4.79
18.17	90.54	13.78	844	L	0	40	16.5	29	34	50	99.6	3.53	2.52	2.52	4.93
18.17	90.54	13.78	844	M	0	40	16.6	27	32	62	99.6	3.53	3.13	3.13	4.64
18.17	90.54	13.78	844	N	0	40	16.7	25	30	72	99.5	3.53	3.63	3.63	4.35
18.17	90.54	13.78	844	O	0	45	16.5	28	32	55	99.6	3.97	2.82	2.82	4.64
18.17	90.54	13.78	844	1	0	168	17.0	11	18	270	98.2	14.84	13.63	13.63	2.61
18.17	90.54	13.78	844	2	0	40	16.4	30	34	53	99.6	3.53	2.67	2.67	4.93

RUN NUMBER 135
CAT. I.D. FH

AIR/FUEL RATIOS-- OVER PRI ALL	CAT PRESS DROP (KPA)	BED INLET TEMP (K)	LOC	TEMP (K)	CO PPH	O2 VOL PCT	NO PPH	NOX PPH	UHC PPH	COMB EFF PCT	EMISSION INDEXES-- G/KG FUEL		
											CO	UHC	NO2
25.37 126.41	13.78	756	A	1444	0	0.0	0	0	0	0.0	0.00	0.00	0.00
25.37 126.41	13.78	756	1	0	70	18.5	5	8	150	98.7	8.61	10.54	1.61
25.37 126.41	13.78	756	2	0	20	18.2	11	13	54	99.5	2.46	3.79	2.62

RUN NUMBER 136
CAT. I.D. FH

10.03 49.98	20.67	1189	A	1603	0	0.0	0	0	0	0.0	0.00	0.00	0.00
10.03 49.98	20.67	1189	G	1189	75	14.5	38	41	21	99.8	3.69	0.59	3.31
10.03 49.98	20.67	1189	H	1033	465	16.4	15	17	520	98.0	22.88	14.62	1.37
10.03 49.98	20.67	1189	I	1233	545	15.0	15	22	460	98.	26.92	12.93	1.77
10.03 49.98	20.67	1189	J	0	555	15.4	16	23	430	98.1	27.31	12.09	1.85
10.03 49.98	20.67	1189	K	0	300	13.2	38	46	75	99.4	14.76	2.10	3.71
10.03 49.98	20.67	1189	L	0	80	15.6	40	42	22	99.8	3.93	0.61	3.39
10.03 49.98	20.67	1189	M	0	40	14.2	38	42	6	99.9	1.96	0.16	3.39
10.03 49.98	20.67	1189	N	0	60	14.4	40	42	12	99.8	2.95	0.33	3.39
10.03 49.98	20.67	1189	O	0	80	14.6	35	40	19	99.8	3.93	0.53	3.23
10.03 49.98	20.67	1189	1	0	385	15.5	18	25	290	98.7	18.95	8.15	2.02
10.03 49.98	20.67	1189	2	0	75	14.7	34	39	10	99.8	3.69	0.28	3.15

RUN NUMBER 137
CAT. I.D. JH

10.17 50.69	17.22	1167	A	1523	0	0.0	0	0	0	0.0	0.00	0.00	0.00
10.17 50.69	17.22	1167	G	1167	155	14.7	34	37	80	99.5	7.73	2.28	3.03
10.17 50.69	17.22	1167	H	1000	475	16.5	9	15	520	97.9	23.70	14.83	1.22
10.17 50.69	17.22	1167	I	1206	555	16.3	10	17	570	97.8	27.70	14.83	1.39
10.17 50.69	17.22	1167	J	0	605	15.6	12	20	540	97.7	30.19	15.40	1.63
10.17 50.69	17.22	1167	K	0	385	13.5	28	34	110	99.1	19.21	3.99	2.78
10.17 50.69	17.22	1167	L	0	195	15.1	30	34	110	99.4	9.73	3.13	2.78
10.17 50.69	17.22	1167	M	0	70	14.6	31	36	5	99.9	3.49	0.14	2.95
10.17 50.69	17.22	1167	N	0	75	14.5	36	39	13	99.8	3.74	0.37	3.19
10.17 50.69	17.22	1167	O	0	168	15.0	29	32	72	99.6	8.38	2.05	2.62
10.17 50.69	17.22	1167	1	0	525	15.6	15	21	410	98.2	26.20	11.69	1.72
10.17 50.69	17.22	1167	2	0	130	15.0	29	35	32	99.7	6.48	0.91	2.86

RUN NUMBER 138
CAT. I.D. JH

AIR/FUEL --RATIOS-- PRI ALL	CAT PRESS DRGP (KPA)	BED IMLET TEMP (K)	LOC	TEMP (K)	CO PPH	O2 VOL PCT	NO PPH	NOX PPH	UMC PPH	COMB EFF PCT	---EMISSION INDEXES--- ---G/KG FUEL---	
											CO	UMC NO2
10.77	53.64	15.15	A	1543	0	0.0	0	0	0	0.0	0.00	0.00
10.77	53.64	15.15	G	1089	80	14.8	32	36	60	99.7	4.22	1.80
10.77	53.64	15.15	H	939	395	16.5	10	16	540	97.8	20.84	16.28
10.77	53.64	15.15	I	1122	415	16.0	12	20	480	98.0	21.89	14.47
10.77	53.64	15.15	J	0	0	15.0	23	28	400	98.3	20.31	12.05
10.77	53.64	15.15	K	0	240	13.6	28	36	60	99.4	12.56	2.41
10.77	53.64	15.15	L	0	120	15.4	26	32	120	99.4	6.33	3.61
10.77	53.64	15.15	M	0	60	14.9	29	34	24	99.8	3.16	0.87
10.77	53.64	15.15	N	0	70	14.9	30	34	33	99.8	3.69	0.99
10.77	53.64	15.15	O	0	110	15.4	24	29	100	99.5	5.80	3.01
10.77	53.64	15.15	1	0	375	15.9	15	22	380	98.3	19.78	11.45
10.77	53.64	15.15	2	0	100	15.0	24	32	40	99.7	5.27	1.20

RUN NUMBER 139
CAT. I.D. JH

AIR/FUEL --RATIOS-- PRI ALL	CAT PRESS DRGP (KPA)	BED IMLET TEMP (K)	LOC	TEMP (K)	CO PPH	O2 VOL PCT	NO PPH	NOX PPH	UMC PPH	COMB EFF PCT	---EMISSION INDEXES--- ---G/KG FUEL---	
											CO	UMC NO2
14.44	71.97	13.09	A	1463	0	0.0	0	0	0	0.0	0.00	0.00
14.44	71.97	13.09	G	967	50	15.4	34	38	35	99.7	3.52	1.40
14.44	71.97	13.09	H	889	250	16.2	10	16	410	97.9	17.61	16.50
14.44	71.97	13.09	I	989	270	17.0	8	14	380	98.0	19.02	15.29
14.44	71.97	13.09	J	0	250	16.4	10	17	260	98.5	17.61	10.46
14.44	71.97	13.09	K	0	210	15.4	15	24	82	99.3	14.79	3.30
14.44	71.97	13.09	L	0	110	15.6	22	26	130	99.2	7.75	5.23
14.44	71.97	13.09	M	0	75	15.9	24	30	70	99.5	5.28	2.81
14.44	71.97	13.09	N	0	80	15.7	26	32	100	99.4	4.02	3.70
14.44	71.97	13.09	O	0	80	16.0	26	29	120	99.3	5.63	4.83
14.44	71.97	13.09	1	0	220	15.4	15	22	240	98.6	15.50	9.66
14.44	71.97	13.09	2	0	60	15.7	31	35	52	99.6	4.22	2.09

RUN NUMBER 140
CAT. I.D. JH

AIR/FUEL --RATIOS-- PRI ALL	CAT PRESS DRGP (KPA)	BED IMLET TEMP (K)	LOC	TEMP (K)	CO PPH	O2 VOL PCT	NO PPH	NOX PPH	UMC PPH	COMB EFF PCT	---EMISSION INDEXES--- ---G/KG FUEL---	
											CO	UMC NO2
18.54	92.37	10.33	A	1313	0	0.0	0	0	0	0.0	0.00	0.00
18.54	92.37	10.33	G	856	50	16.4	25	33	60	99.5	4.50	3.09
18.54	92.37	10.33	H	617	185	17.7	8	15	500	97.0	16.67	25.75
18.54	92.37	10.33	I	872	178	17.3	12	19	430	97.4	16.04	22.15
18.54	92.37	10.33	J	0	168	16.4	20	27	240	98.4	15.14	12.36
18.54	92.37	10.33	K	0	168	15.9	26	32	100	99.1	15.14	5.15
18.54	92.37	10.33	L	0	50	16.8	24	29	100	99.3	4.50	5.15
18.54	92.37	10.33	M	0	50	16.9	24	30	80	99.4	4.50	4.12
18.54	92.37	10.33	N	0	50	16.7	26	30	90	99.4	4.50	4.63
18.54	92.37	10.33	O	0	60	16.8	28	32	90	99.4	5.40	4.63
18.54	92.37	10.33	1	0	140	17.0	14	20	190	98.7	12.62	9.78
18.54	92.37	10.33	2	0	60	16.5	24	30	59	99.5	5.40	3.03

RUN NUMBER 141
CAT. I.D. GH

AIR/FUEL RATIOS OVER PRI ALL	CAT PRESS DROP (KPA)	BED INLET TEMP (K)	LOC	TEMP (K)	CO PPM	O2 VOL PCT	NO PPM	NOX PPM	UMC PPM	COMB EFF PCT	EMISSION INDEXES		
											CO	G/KG FUEL	NO2
9.78	48.72	1233	A	0	0	0.0	0	0	0	0.0	0.00	0.00	0.00
9.78	48.72	1233	G	1233	70	15.1	35	38	26	99.8	3.36	0.71	2.99
9.78	48.72	1233	H	1096	500	17.4	7	13	760	97.3	24.00	20.85	1.02
9.78	48.72	1233	I	1278	625	16.5	15	21	610	97.6	30.00	16.73	1.05
9.78	48.72	1233	J	0	665	15.6	21	26	510	97.8	31.92	13.99	2.05
9.78	48.72	1233	K	0	328	13.4	42	46	70	99.4	15.74	1.92	3.62
9.78	48.72	1233	L	0	90	15.4	33	36	22	99.8	4.32	0.60	2.83
9.78	48.72	1233	M	0	130	15.4	34	36	ε	99.6	6.24	2.19	2.83
9.78	48.72	1233	N	0	30	15.0	36	40	2	99.9	1.44	0.05	3.15
9.78	48.72	1233	O	0	130	15.7	31	32	70	98.6	6.24	1.92	2.52
9.78	48.72	1233	1	0	565	16.4	17	24	500	97.9	27.12	13.71	1.89
9.78	48.72	1233	2	0	70	15.4	36	38	12	99.8	3.36	0.32	2.99

RUN NUMBER 142
CAT. I.D. GH

AIR/FUEL RATIOS OVER PRI ALL	CAT PRESS DROP (KPA)	BED INLET TEMP (K)	LOC	TEMP (K)	CO PPM	O2 VOL PCT	NO PPM	NOX PPM	UMC PPM	COMB EFF PCT	EMISSION INDEXES		
											CO	G/KG FUEL	NO2
10.97	54.68	1150	A	0	0	0.0	0	0	0	0.0	0.00	0.00	0.00
10.97	54.68	1150	G	1150	50	15.6	31	35	40	99.8	2.68	1.22	3.09
10.97	54.68	1150	H	983	395	17.5	10	17	550	97.8	21.23	16.89	1.32
10.97	54.68	1150	I	1200	455	16.5	15	21	460	98.0	24.46	14.13	1.85
10.97	54.68	1150	J	0	415	15.5	27	31	400	98.2	22.31	12.28	2.73
10.97	54.68	1150	K	0	250	13.7	38	42	70	99.4	13.44	2.15	3.70
10.97	54.68	1150	L	0	60	15.6	30	34	38	99.8	3.22	1.16	3.00
10.97	54.68	1150	M	0	90	15.6	32	34	89	99.6	4.83	2.73	3.00
10.97	54.68	1150	N	0	30	15.4	33	36	9	99.9	1.61	0.27	3.17
10.97	54.68	1150	O	0	80	15.8	29	32	64	99.7	4.30	1.96	2.82
10.97	54.68	1150	1	0	400	16.5	15	20	390	98.3	21.50	11.98	1.76
10.97	54.68	1150	2	0	60	15.5	30	34	28	99.8	3.22	0.86	3.00

RUN NUMBER 143
CAT. I.D. GH

AIR/FUEL RATIOS OVER PRI ALL	CAT PRESS DROP (KPA)	BED INLET TEMP (K)	LOC	TEMP (K)	CO PPM	O2 VOL PCT	NO PPM	NOX PPM	UMC PPM	COMB EFF PCT	EMISSION INDEXES		
											CO	G/KG FUEL	NO2
17.82	88.78	928	A	0	0	0.0	0	0	0	0.0	0.00	0.00	0.00
17.82	88.78	928	G	928	0	0.0	0	0	0	0.0	0.00	0.00	0.00
17.82	88.78	928	H	833	0	0.0	0	0	0	0.0	0.00	0.00	0.00
17.82	88.78	928	I	900	0	0.0	0	0	0	0.0	0.00	0.00	0.00
17.82	88.78	928	1	0	155	18.2	12	17	150	98.9	13.43	7.43	2.42
17.82	88.78	928	2	0	40	17.9	19	25	24	99.8	3.46	1.18	3.56

RUN NUMBER 144
CAT. I.D. RA

AIR/FUEL RATIOS-- OVER PRI ALL	CAT PRESS DRESS (KPA)	BED INLET TEMP (K)	LOC	YEAR (K)	CO PPM	O2 VOL PCT	NO PPM	NOX PPM	UHC PPM	COMB EFF PCT	EMISSION INDEXES-- G/KG FUEL		
											CO	UHC	NO2
9.97	49.69	30.31	1172	A	1618	0	0.0	0	0	0.0	0.00	0.00	0.00
9.97	49.69	30.31	1172	M	0	318	15.4	27	32	1.3	15.56	4.19	2.57
9.97	49.69	30.31	1172	N	0	326	15.4	24	30	59	16.05	1.65	2.41
9.97	49.69	30.31	1172	0	0	475	16.2	20	23	350	23.24	9.78	1.84
9.97	49.69	30.31	1172	1	0	490	15.9	17	24	430	23.98	12.02	1.92
9.97	49.69	30.31	1172	2	0	465	15.6	28	32	150	22.75	4.19	2.57

RUN NUMBER 145
CAT. I.D. RA

11.19	55.76	23.42	1117	A	1653	0	0.0	0	0	0.0	0.00	0.00	0.00
11.19	55.76	23.42	1117	1	0	400	15.4	16	21	410	21.92	12.84	1.89
11.19	55.76	23.42	1117	2	0	395	16.1	24	28	240	21.65	7.51	2.52

RUN NUMBER 146
CAT. I.D. RA

14.02	69.85	22.04	989	A	1658	0	0.0	0	0	0.0	0.00	0.00	0.00
14.02	69.85	22.04	989	1	0	270	17.1	15	20	270	18.47	10.55	2.24
14.02	69.85	22.04	989	2	0	250	16.9	23	26	180	17.10	7.03	2.92

RUN NUMBER 147
CAT. I.D. RA

17.99	89.65	19.98	844	A	1628	0	0.0	0	0	0.0	0.00	0.00	0.00
17.99	89.65	19.98	844	1	0	155	18.0	14	21	215	13.56	10.75	3.01
17.99	89.65	19.98	844	2	0	195	17.5	16	24	170	17.06	8.50	3.45

RUN NUMBER 148
CAT. I.D. RA

25.13	125.17	16.53	733	A	1458	0	0.0	0	0	0.0	0.00	0.00	0.00
25.13	125.17	16.53	733	1	0	80	18.5	7	12	190	9.74	13.22	2.40
25.13	125.17	16.53	733	2	0	70	18.5	8	14	170	8.52	11.83	2.80

RUN NUMBER 149
CAT. I.D. KR

9.68	48.25	74.41	1244	A	1563	0	0.0	0	0	0.0	0.00	0.00	0.00
9.68	48.25	74.41	1244	1	0	475	15.4	21	26	340	22.59	9.23	2.03
9.68	48.25	74.41	1244	2	0	415	15.0	26	32	170	19.73	4.61	2.50

AIR/FUEL --RATIOS-- OVER PRI ALL		CAT PRESS DROPP (KPA)		BED INLET TEMP (K)		LOC	TEMP (K)	CO PPM	O2 PCT	NO PPH	NOX PPH	UHC PPH	---EMISSION INDEXES--- -----G/KG FUEL----- CO UHC NO2		
RUN NUMBER 150 CAT. I.D. KR															
10.87	54.15	62.01	1178	A	1608	0	0.0	0	0	0	0	0	0.00	0.00	0.00
10.87	54.15	62.01	1178	1	0	400	16.0	15	20	360	98.4	98.4	21.30	10.95	1.74
10.87	54.15	62.01	1178	2	0	375	15.7	23	27	265	98.7	98.7	19.97	8.06	2.36
RUN NUMBER 151 CAT. I.D. KR															
13.62	67.85	52.36	1033	A	1643	0	0.0	0	0	0	0.0	0.00	0.00	0.00	0.00
13.62	67.85	52.36	1033	1	0	240	16.9	17	21	740	98.7	98.7	15.95	9.11	2.29
13.62	67.85	52.36	1033	2	0	290	16.4	17	24	110	99.1	99.1	19.28	4.17	2.62
RUN NUMBER 152 CAT. I.D. KR															
17.48	87.09	48.23	889	A	1578	0	0.0	0	0	0	0.0	0.00	0.00	0.00	0.00
17.48	87.09	48.23	889	1	0	185	17.5	12	20	190	98.7	98.7	15.73	9.23	2.79
17.48	87.09	48.23	889	2	0	202	17.0	21	28	80	99.2	99.2	17.18	3.88	3.91
RUN NUMBER 153 CAT. I.D. KR															
24.41	121.59	40.65	772	A	1438	0	0.0	0	0	0	0.0	0.00	0.00	0.00	0.00
24.41	121.59	40.65	772	1	0	80	18.3	10	16	160	98.6	98.6	9.46	10.82	3.11
24.41	121.59	40.65	772	2	0	110	18.0	10	17	140	98.7	98.7	13.02	9.46	3.30
RUN NUMBER 154 CAT. I.D. KR															
0.00	0.00	0.00	1200	A	1478	0	0.0	0	0	0	0.0	0.00	0.00	0.00	0.00
9.50	47.34	75.79	1200	1	0	445	15.2	21	26	335	98.6	98.6	20.77	8.93	1.99
9.50	47.34	75.79	1200	2	0	40	14.4	33	38	16	99.9	99.9	1.86	0.42	2.91
RUN NUMBER 155 CAT. I.D. KR															
0.00	0.00	0.00	1111	A	1548	0	0.0	0	0	0	0.0	0.00	0.00	0.00	0.00
10.66	53.13	80.61	1111	1	0	375	15.7	17	21	360	98.4	98.4	19.60	10.75	1.80
10.66	53.13	80.61	1111	2	0	20	14.8	34	36	23	99.9	99.9	1.04	0.68	3.09
RUN NUMBER 156 CAT. I.D. KR															
0.00	0.00	0.00	983	A	1648	0	0.0	0	0	0	0.0	0.00	0.00	0.00	0.00
13.49	67.21	63.38	983	1	0	233	16.7	15	20	250	98.7	98.7	15.34	9.40	2.16
13.49	67.21	63.38	983	2	0	40	16.0	27	31	28	99.8	99.8	2.63	1.05	3.35

RUN NUMBER 157													
CAT. I.D. KQ													
AIR/FUEL --RATIOS-- OVER	CAT PRESS DROP (KPA)	BED INLET TEMP (K)	LOC	TEMP (K)	CO PPM	O2 VOL PCT	NC PPM	NOX PPM	UHC PPM	COMB EFF PCT	---EMISSION INDEXES---		
PR1 ALL											CO	UHC	NO2
0.00	0.00	844	A	1638	0	0.0	0	0	0	0.0	0.00	0.00	0.00
17.32	86.27	844	1	0	168	17.5	14	19	210	98.6	14.15	10.11	2.63
17.32	86.27	844	2	0	30	17.0	32	34	35	99.7	2.52	1.68	4.70
RUN NUMBER 158													
CAT. I.D. KQ													
0.00	0.00	717	A	1488	0	0.0	0	0	0	0.0	0.00	0.00	0.00
24.16	120.45	717	1	0	80	18.3	8	14	190	98.5	9.38	12.73	2.69
24.16	120.45	717	2	0	40	18.0	20	22	70	99.4	4.69	4.69	4.23
RUN NUMBER 159													
CAT. I.D. KU													
9.87	49.20	1200	A	1553	0	0.0	0	0	0	0.0	0.00	0.00	0.00
9.87	49.20	1200	1	0	475	15.6	20	25	350	98.4	23.02	9.69	1.99
9.87	49.20	1200	2	0	80	15.4	30	33	28	99.8	3.87	0.77	2.62
RUN NUMBER 160													
CAT. I.D. KU													
0.00	0.00	1122	A	1583	0	0.0	0	0	0	0.0	0.00	0.00	0.00
11.08	55.22	1122	1	0	365	15.6	15	20	345	98.4	19.81	10.70	1.78
11.08	55.22	1122	2	0	80	15.2	30	32	40	99.7	4.34	1.24	2.85
RUN NUMBER 161													
CAT. I.D. KU													
0.00	0.00	944	A	1638	0	0.0	0	0	0	0.0	0.00	0.00	0.00
14.02	69.85	944	1	0	270	16.2	14	19	210	98.7	18.47	8.20	2.13
14.02	69.85	944	2	0	210	15.5	27	29	91	99.3	14.36	3.55	3.25
RUN NUMBER 162													
CAT. I.D. KU													
0.00	0.00	833	A	1613	0	0.0	0	0	0	0.0	0.00	0.00	0.00
17.99	89.65	833	1	0	168	16.4	14	18	230	98.5	14.70	11.50	2.58
17.99	89.65	833	2	0	195	16.2	7	8	110	99.0	17.06	5.50	1.15
RUN NUMBER 163													
CAT. I.D. KU													
0.00	0.00	722	A	1468	0	0.0	0	0	0	0.0	0.00	0.00	0.00
25.13	125.17	722	1	0	70	17.0	6	10	235	98.1	8.52	16.35	2.00
25.13	125.17	722	2	0	100	16.8	14	17	200	98.3	12.18	13.92	3.40

RUN NUMBER 164												
CAT. I.D. XU												
AIR/FUEL	CAT	RED	LOC	TEMP	CO	O2	NO	NOX	UMC	EMISSION INDEXES		
---RATIO---	PRESS	INLET		(K)	PPM	%OL	PPM	PPM	PPM	CO	UMC	NO2
PRI ALL	(KPA)	TEMP								G/KG	FUEL	
0.00 0.00	0.00	1211	A	1539	0	0.0	0	0	0	0.00	0.00	0.00
9.97 49.69	73.72	1211	1	0	335	15.3	26	28	210	16.39	5.87	2.25
9.97 49.65	73.72	1211	2	0	75	15.9	30	34	18	3.67	0.50	2.73
RUN NUMBER 165												
CAT. I.D. KU												
0.00 0.00	0.00	1144	A	1583	0	0.0	0	0	0	0.00	0.00	0.00
11.08 55.22	68.90	1144	1	0	260	16.4	20	24	270	14.11	8.37	2.11
11.08 55.22	68.90	1144	2	0	80	15.9	31	32	22	4.34	0.68	2.85
RUN NUMBER 166												
CAT. I.D. KU												
0.00 0.00	0.00	1000	A	1658	0	0.0	0	0	0	0.00	0.00	0.00
14.02 69.85	57.18	1000	1	0	220	17.0	17	22	160	15.05	6.25	2.47
14.02 69.85	57.18	1000	2	0	168	16.4	28	31	48	11.49	1.87	3.48
RUN NUMBER 167												
CAT. I.D. KU												
0.00 0.00	0.00	867	A	1636	0	0.0	0	0	0	0.00	0.00	0.00
17.99 89.65	48.23	867	1	0	140	17.0	17	23	150	12.25	7.50	3.30
17.99 89.65	48.23	867	2	0	168	15.9	31	34	78	14.70	3.90	4.88
RUN NUMBER 168												
CAT. I.D. KU												
0.00 0.00	0.00	744	A	1498	0	0.0	0	0	0	0.00	0.00	0.00
25.13 125.17	1.34	744	1	0	70	17.4	7	12	150	8.52	10.44	2.40
25.13 125.17	41.34	744	2	0	80	17.4	14	17	140	9.74	9.74	3.40
RUN NUMBER 169												
CAT. I.D. KU												
0.00 0.00	0.00	711	A	1463	0	0.0	0	0	0	0.00	0.00	0.00
27.89 138.95	39.27	711	1	0	60	17.4	4	8	170	8.10	13.12	1.77
27.89 138.95	39.27	711	2	0	75	17.4	10	10	150	10.13	12.35	2.21
RUN NUMBER 170												
CAT. I.D. KU												
0.00 0.00	0.00	767	A	1548	0	0.0	0	0	0	0.00	0.00	0.00
22.86 113.88	44.78	767	1	0	80	17.2	8	15	170	8.87	10.77	2.73
22.86 113.88	44.78	767	2	0	100	17.1	18	22	140	11.09	8.87	4.00

RUN NUMBER 171													
CAT. I.D. KU													
AIR/FUEL	CAT	SED	LDC	TEMP	CO	O2	NO	NOX	UMC	COMB	EMISSION INDEXES		
---RATIOS---	PRESS	INLET		(K)	PPM	VOL	PPM	PPM	PPM	EFF	---G/KG FUEL---		
PRI ALL	(RPA)	TEMP				PCT				PCT	CO	UMC	NO2
0.00 0.00	0.00	833	A	1623	0	0.0	0	0	0	0.0	0.00	0.00	0.00
19.37 96.49	45.47	833	1	0	120	16.9	14	.2	180	98.7	11.29	9.68	3.60
19.37 96.49	45.47	833	2	0	150	16.7	31	33	110	99.0	14.12	5.91	5.10
RUN NUMBER 172													
CAT. I.D. KU													
0.00 0.00	0.00	694	A	1408	0	0.0	0	0	0	0.0	0.00	0.00	0.00
31.04 154.63	37.89	694	1	0	40	20.0	3	6	140	98.6	6.01	12.02	1.48
31.04 154.63	37.89	694	2	0	50	20.2	7	9	140	98.6	7.51	12.02	2.22
RUN NUMBER 173													
CAT. I.D. KU													
0.00 0.00	0.00	661	A	1348	0	0.0	0	0	0	0.0	0.00	0.00	0.00
35.43 176.50	37.20	661	1	0	50	19.9	2	4	160	98.2	8.56	15.66	1.12
35.43 176.50	37.20	661	2	0	50	20.0	4	5	170	98.1	8.56	16.64	1.40
RUN NUMBER 174													
CAT. I.D. KU													
0.00 0.00	0.00	644	A	1267	0	0.0	0	0	0	0.0	0.00	0.00	0.00
41.27 203.59	35.82	644	1	0	90	19.6	1	3	180	97.5	17.95	20.51	0.98
41.27 203.59	35.82	644	2	0	100	19.8	3	4	220	97.0	19.94	25.07	1.31
RUN NUMBER 175													
CAT. I.D. MQ													
0.00 0.00	0.00	1178	A	1558	0	0.0	0	0	0	0.0	0.00	0.00	0.00
9.59 47.79	125.39	1178	1	0	400	0.0	23	27	130	99.2	18.84	3.49	2.08
9.59 47.79	125.39	1178	2	0	150	0.0	32	34	50	99.7	7.06	1.34	2.63
RUN NUMBER 176													
CAT. I.D. MQ													
0.00 0.00	0.00	1089	A	1633	0	0.0	0	0	0	0.0	0.00	0.00	0.00
10.77 53.64	106.79	1089	1	0	365	0.0	20	23	220	98.8	19.25	6.63	1.99
10.77 53.64	106.79	1089	2	0	150	0.0	30	32	100	99.5	7.91	3.01	2.77
RUN NUMBER 177													
CAT. I.D. MQ													
0.00 0.00	0.00	956	A	1663	0	0.0	0	0	0	0.0	0.00	0.00	0.00
13.62 67.85	88.19	956	1	0	250	0.0	16	20	140	99.0	16.62	5.31	2.18
13.62 67.85	88.19	956	2	0	210	0.0	18	24	62	99.3	13.96	3.11	2.62

RUN NUMBER 179													
CAT. I.D. HQ													
AIR/FUEL	CAT	LOC	LOC	TEMP	CO	O2	NO	NOX	UHC	COMB EFF PCT	EMISSION INDEXES		
--RATIOS--	PRESS DROP (KPA)	INLET TEMP (K)	TEMP (K)	(K)	PPH	V/L PLT	PPH	PPH	PPH		CO	G/KG FUEL	UHC
PRI	ALL												
0.00	0.00	0.00	A	1583	0	0.0	0	0	0	0.0	0.00	0.00	0.00
24.41	121.59	64.76	1	0	110	0.0	12	16	84	99.1	13.02	5.68	3.11
24.41	121.59	64.76	2	0	90	0.0	11	16	50	99.4	10.65	3.38	3.11
RUN NUMBER 180													
CAT. I.D. KQ													
0.00	0.00	0.00	A	1629	0	0.0	0	0	0	0.0	0.00	0.00	0.00
9.59	47.79	37.89	1	0	365	15.2	26	31	110	99.3	17.19	2.96	2.39
9.59	47.79	37.89	2	0	120	14.9	31	33	36	99.7	5.65	0.96	2.55
RUN NUMBER 181													
CAT. I.D. KQ													
0.00	0.00	0.00	A	1573	0	0.0	0	0	0	0.0	0.00	0.00	0.00
10.77	53.64	34.45	1	0	335	14.8	20	24	170	99.0	17.67	5.12	2.08
10.77	53.64	34.45	2	0	120	15.1	27	30	70	99.6	6.33	2.11	2.60
RUN NUMBER 182													
CAT. I.D. KQ													
0.00	0.00	0.00	A	1618	0	0.0	0	0	0	0.0	0.00	0.00	0.00
13.62	67.85	30.31	1	0	250	15.2	16	21	130	99.1	16.62	4.93	2.29
13.62	67.85	30.31	2	0	130	15.0	21	25	68	99.5	8.64	2.58	2.13
RUN NUMBER 183													
CAT. I.D. KQ													
0.00	0.00	0.00	A	1613	0	0.0	0	0	0	0.0	0.00	0.00	0.00
17.48	87.09	26.87	1	0	130	15.3	15	20	62	99.4	11.05	3.01	2.79
17.48	87.09	26.87	2	0	60	15.4	22	25	38	99.6	6.80	1.84	3.49
RUN NUMBER 184													
CAT. I.D. KQ													
0.00	0.00	0.00	A	1503	0	0.0	0	0	0	0.0	0.00	0.00	0.00
24.41	121.59	23.42	1	0	70	15.6	10	15	63	99.3	8.28	4.26	2.91
24.41	121.59	23.42	2	0	60	15.5	15	19	42	99.5	7.10	2.84	3.69
RUN NUMBER 185													
CAT. I.D. YY													
0.00	0.00	0.00	A	1528	0	0.0	0	0	0	0.0	0.00	0.00	0.00
0.00	0.00	0.00	0	0	0	0.0	0	0	0	0.0	0.00	0.00	0.00
0.00	0.00	0.00	0	0	0	0.0	0	0	0	0.0	0.00	0.00	0.00
0.00	0.00	0.00	H	1117	0	0.0	0	0	0	0.0	0.00	0.00	0.00
0.00	0.00	0.00	I	1200	0	0.0	0	0	0	0.0	0.00	0.00	0.00
3.59	47.79	44.78	1	0	280	14.9	28	30	64	99.5	13.19	1.72	2.32
3.59	47.79	44.78	2	0	20	14.9	31	33	5	99.9	0.94	0.13	2.55

AIR/FUEL --RATIOS-- PRI ALL		CAT PRESS DROP (KPA)	RED I-LET TEMP (K)	LOC	TEMP (K)	CO PPH	O2 VOL PCT	NO PPH	NOX PPH	UHC PPM	COMB EFF PCT	---EMISSION INDEXES---		
												CO	UHC	NO2
0.60	0.00	0.00	0	A	1543	0	0.0	0	0	0	0.0	0.00	0.00	0.00
0.00	0.00	0.00	0	B	1344	0	0.0	0	0	0	0.0	0.00	0.00	0.00
0.00	0.00	0.00	0	G	1122	0	0.0	0	0	0	0.0	0.00	0.00	0.00
0.00	0.00	0.00	0	H	1011	0	0.0	0	0	0	0.0	0.00	0.00	0.00
0.00	0.00	0.00	0	I	1122	0	0.0	0	0	0	0.0	0.00	0.00	0.00
0.77	53.64	37.89	1122	1	0	280	14.4	21	25	92	99.3	14.77	2.77	2.16
10.77	53.64	37.89	1122	2	0	40	14.5	28	29	15	99.9	2.11	0.45	2.51

RUN NUMBER 186 CAT. I.D. YY		RUN NUMBER 187 CAT. I.D. YY													
0.00	0.00	0.00	0	A	1616	0	0.0	0	0	0	0.0	0.00	0.00	0.00	
0.00	0.00	0.00	0	B	1500	0	0.0	0	0	0	0.0	0.00	0.00	0.00	
0.00	0.00	0.00	0	G	967	0	0.0	0	0	0	0.0	0.00	0.00	0.00	
0.00	0.00	0.00	0	H	869	0	0.0	0	0	0	0.0	0.00	0.00	0.00	
0.00	0.00	0.00	0	I	989	0	0.0	0	0	0	0.0	0.00	0.00	0.00	
13.62	67.85	34.45	967	1	0	185	14.5	18	22	36	99.5	12.29	1.36	2.40	
13.62	67.85	34.45	967	2	0	40	14.0	25	28	8	99.9	2.65	0.30	3.95	

RUN NUMBER 188 CAT. I.D. YY		RUN NUMBER 189 CAT. I.D. YY													
0.00	0.00	0.00	0	A	1628	0	0.0	0	0	0	0.0	0.00	0.00	0.00	
0.00	0.00	0.00	0	B	1411	0	0.0	0	0	0	0.0	0.00	0.00	0.00	
0.00	0.00	0.00	0	G	844	0	0.0	0	0	0	0.0	0.00	0.00	0.00	
0.00	0.00	0.00	0	H	811	0	0.0	0	0	0	0.0	0.00	0.00	0.00	
0.00	0.00	0.00	0	I	878	0	0.0	0	0	0	0.0	0.00	0.00	0.00	
17.48	87.09	28.24	844	1	0	130	14.5	15	19	38	99.5	11.05	1.84	2.65	
17.48	87.09	28.24	844	2	0	40	14.4	24	27	9	99.8	3.40	0.43	3.77	

RUN NUMBER 189 CAT. I.D. YY		RUN NUMBER 190 CAT. I.D. YY													
0.00	0.00	0.00	0	A	1533	0	0.0	0	0	0	0.0	0.00	0.00	0.00	
0.00	0.00	0.00	0	B	1211	0	0.0	0	0	0	0.0	0.00	0.00	0.00	
0.00	0.00	0.00	0	G	711	0	0.0	0	0	0	0.0	0.00	0.00	0.00	
0.00	0.00	0.00	0	H	733	0	0.0	0	0	0	0.0	0.00	0.00	0.00	
0.00	0.00	0.00	0	I	756	0	0.0	0	0	0	0.0	0.00	0.00	0.00	
24.41	121.59	24.80	711	1	0	70	15.0	11	15	43	99.5	8.28	2.90	2.91	
24.41	121.59	24.80	711	2	0	40	14.7	17	20	20	99.7	4.73	1.35	3.88	

AIR/FUEL --RATIOS-- PRI ALL		CAT PRESS DRCP (KPA)	BED INLET TEMP (K)	LOC	TEMP (K)	CO PPM	O2 VCL PCT	NO PPM	NOX PPM	UHC PPM	COMB EFF PCT	---EMISSION INDEXES--- -----G/KG FUEL----- CO UHC NO2		
0.00	0.00	0.00	0	A	1543	0	0.0	0	0	0	0.0	0.00	0.00	0.00
0.00	0.00	0.00	0	B	1644	0	0.0	0	0	0	0.0	0.00	0.00	0.00
0.00	0.00	0.00	0	G	1178	0	0.0	0	0	0	0.0	0.00	0.00	0.00
0.00	0.00	0.00	0	H	1089	0	0.0	0	0	0	0.0	0.00	0.00	0.00
0.00	0.00	0.00	0	I	1144	0	0.0	0	0	0	0.0	0.00	0.00	0.00
9.78	48.72	34.45	1178	1	0	290	15.0	26	29	100	99.4	13.92	2.74	2.28
9.78	48.72	34.45	1178	2	0	75	15.4	29	30	38	99.8	3.60	1.04	2.36

AIR/FUEL --RATIOS-- PRI ALL		CAT PRESS DRCP (KPA)	BED INLET TEMP (K)	LOC	TEMP (K)	CO PPM	O2 VCL PCT	NO PPM	NOX PPM	UHC PPM	COMB EFF PCT	---EMISSION INDEXES--- -----G/KG FUEL----- CO UHC NO2		
0.00	0.00	0.00	0	A	1593	0	0.0	0	0	0	0.0	0.00	0.00	0.00
0.00	0.00	0.00	0	B	1644	0	0.0	0	0	0	0.0	0.00	0.00	0.00
0.00	0.00	0.00	0	G	1078	0	0.0	0	0	0	0.0	0.00	0.00	0.00
0.00	0.00	0.00	0	H	1000	0	0.0	0	0	0	0.0	0.00	0.00	0.00
0.00	0.00	0.00	0	I	1067	0	0.0	0	0	0	0.0	0.00	0.00	0.00
10.97	54.68	30.31	1078	1	0	233	15.0	22	26	88	99.4	12.52	2.70	2.29
10.97	54.68	30.31	1078	2	0	75	15.5	25	26	40	99.7	4.03	1.22	2.29

AIR/FUEL --RATIOS-- PRI ALL		CAT PRESS DRCP (KPA)	BED INLET TEMP (K)	LOC	TEMP (K)	CO PPM	O2 VCL PCT	NO PPM	NOX PPM	UHC PPM	COMB EFF PCT	---EMISSION INDEXES--- -----G/KG FUEL----- CO UHC NO2		
0.00	0.00	0.00	0	A	1638	0	0.0	0	0	0	0.0	0.00	0.00	0.00
0.00	0.00	0.00	0	B	1511	0	0.0	0	0	0	0.0	0.00	0.00	0.00
0.00	0.00	0.00	0	G	939	0	0.0	0	0	0	0.0	0.00	0.00	0.00
0.00	0.00	0.00	0	H	883	0	0.0	0	0	0	0.0	0.00	0.00	0.00
0.00	0.00	0.00	0	I	939	0	0.0	0	0	0	0.0	0.00	0.00	0.00
13.88	69.17	27.56	939	1	0	168	15.4	17	22	60	99.4	11.38	2.53	2.44
13.88	69.17	27.56	939	2	0	100	15.2	22	25	44	99.6	6.77	1.70	2.78

AIR/FUEL --RATIOS-- PRI ALL		CAT PRESS DRCP (KPA)	BED INLET TEMP (K)	LOC	TEMP (K)	CO PPM	O2 VCL PCT	NO PPM	NOX PPM	UHC PPM	COMB EFF PCT	---EMISSION INDEXES--- -----G/KG FUEL----- CO UHC NO2		
0.00	0.00	0.00	0	A	1638	0	0.0	0	0	0	0.0	0.00	0.00	0.00
0.00	0.00	0.00	0	B	1400	0	0.0	0	0	0	0.0	0.00	0.00	0.00
0.00	0.00	0.00	0	G	822	0	0.0	0	0	0	0.0	0.00	0.00	0.00
0.00	0.00	0.00	0	H	789	0	0.0	0	0	0	0.0	0.00	0.00	0.00
0.00	0.00	0.00	0	I	822	0	0.0	0	0	0	0.0	0.00	0.00	0.00
17.82	88.78	24.11	822	1	0	100	15.4	15	20	68	99.4	8.66	3.36	2.84
17.82	88.78	24.11	822	2	0	80	15.5	21	24	47	99.6	6.93	2.32	3.41

AIR/FUEL --RATIOS-- PRI ALL	CAT PRESS DROP (KPA)	BED INLET TEMP (K)	LOC	TEMP (K)	CO		O2		NO		NOX		UHC		---EMISSION INDEXES---		
					PPM	PCT	PPM	PCT	PPM	PCT	PPM	PCT	PPM	PCT	CO	UHC	NO2
0.00	0.00	0	A	1548	0	0.0	0	0.0	0	0	0	0	0	0	0.00	0.00	0.00
0.00	0.00	0	B	1200	0	0.0	0	0.0	0	0	0	0	0	0	0.00	0.00	0.00
0.00	0.00	0	G	706	0	0.0	0	0.0	0	0	0	0	0	0	0.00	0.00	0.00
0.00	0.00	0	H	711	0	0.0	0	0.0	0	0	0	0	0	0	0.00	0.00	0.00
0.00	0.00	0	I	711	0	0.0	0	0.0	0	0	0	0	0	0	0.00	0.00	0.00
24.88	123.95	20.67	1	0	60	15.7	10	15.7	10	15	15	15	80	99.2	7.23	5.51	2.97
24.88	123.95	20.67	2	0	70	15.6	14	15.6	14	16	16	16	64	99.3	8.44	4.41	3.17

RUN NUMBER 194 CAT. I.D. FV		RUN NUMBER 195 CAT. I.D. FY	
0.00	0.00	0.00	0.00
0.00	0.00	0.00	0.00
0.00	0.00	0.00	0.00
0.00	0.00	0.00	0.00
0.00	0.00	0.00	0.00
9.74	48.55	30.31	1211
9.74	48.55	30.31	1211

RUN NUMBER 196 CAT. I.D. FY		RUN NUMBER 197 CAT. I.D. FY	
0.00	0.00	0.00	0.00
0.00	0.00	0.00	0.00
0.00	0.00	0.00	0.00
0.00	0.00	0.00	0.00
0.00	0.00	0.00	0.00
10.77	53.64	24.80	1111
10.77	53.64	24.80	1111

RUN NUMBER 194 CAT. I.D. FV		RUN NUMBER 195 CAT. I.D. FY		RUN NUMBER 196 CAT. I.D. FY		RUN NUMBER 197 CAT. I.D. FY	
0.00	0.00	0.00	0.00	0.00	0.00	0.00	0.00
0.00	0.00	0.00	0.00	0.00	0.00	0.00	0.00
0.00	0.00	0.00	0.00	0.00	0.00	0.00	0.00
0.00	0.00	0.00	0.00	0.00	0.00	0.00	0.00
0.00	0.00	0.00	0.00	0.00	0.00	0.00	0.00
13.36	66.59	23.42	978	17	24	94	99.3
13.36	66.59	23.42	978	14.9	24	29	99.8

AIR/FUEL --RATIO-- PRI ALL		CAT PRESS DROP (MPA)	BED INLET TEMP (K)	LOC	TEMP (K)	CO PPM	O2 VOL PCT	NO PPM	NOX PPM	UHC PPM	COMB EFF PCT	---EMISSION INDEXES--- ---G/KG FUEL---		
												CO	UHC	NO2
0.00	0.00	0.00	0	A	1648	0	0.0	0	0	0	0.0	0.00	0.00	0.00
0.00	0.00	0.00	0	B	1533	0	0.0	0	0	0	0.0	0.00	0.00	0.00
0.00	0.00	0.00	0	C	844	0	0.0	0	0	0	0.0	0.00	0.00	0.00
0.00	0.00	0.00	0	H	811	0	0.0	0	0	0	0.0	0.00	0.00	0.00
0.00	0.00	0.00	0	I	867	0	0.0	0	0	0	0.0	0.00	0.00	0.00
17.15	85.46	20.67	844	1	0	120	15.0	15	20	68	99.4	10.01	3.24	2.74
17.15	85.46	20.67	844	2	0	35	15.3	20	24	17	99.8	3.00	0.81	3.29

RUI: NUMBER CAT. I.D.		199 FY												
0.00	0.00	0	0.0	0	0	0	0.0	0	0	0	0.0	0.00	0.00	0.00
0.00	0.00	0	0.0	0	0	0	0.0	0	0	0	0.0	0.00	0.00	0.00
0.00	0.00	0.00	0	G	722	0	0.0	0	0	0	0.0	0.00	0.00	0.00
0.00	0.00	0.00	0	H	744	0	0.0	0	0	0	0.0	0.00	0.00	0.00
0.00	0.00	0.00	0	I	744	0	0.0	0	0	0	0.0	0.00	0.00	0.00
23.95	119.32	17.22	722	1	0	60	15.4	12	17	62	99.4	6.97	4.11	3.24
23.95	119.32	17.22	722	2	0	30	15.3	16	20	26	99.7	3.48	1.72	3.81

RUN NUMBER CAT. I.D.		200 FZ												
0.00	0.00	0	0.0	0	0	0	0.0	0	0	0	0.0	0.00	0.00	0.00
0.00	0.00	0.00	0	B	1644	0	0.0	0	0	0	0.0	0.00	0.00	0.00
0.00	0.00	0.00	0	G	1244	0	0.0	0	0	0	0.0	0.00	0.00	0.00
0.00	0.00	0.00	0	H	1111	0	0.0	0	0	0	0.0	0.00	0.00	0.00
0.00	0.00	0.00	0	I	1189	0	0.0	0	0	0	0.0	0.00	0.00	0.00
9.68	48.25	25.49	1244	1	0	318	15.4	24	28	100	99.2	15.12	4.34	2.18
9.68	48.25	25.49	1244	2	0	80	15.6	26	28	42	99.7	3.80	1.14	2.18

RUN NUMBER CAT. I.D.		201 FZ												
0.00	0.00	0	0.0	0	0	0	0.0	0	0	0	0.0	0.00	0.00	0.00
0.00	0.00	0.00	0	B	1644	0	0.0	0	0	0	0.0	0.00	0.00	0.00
0.00	0.00	0.00	0	G	1100	0	0.0	0	0	0	0.0	0.00	0.00	0.00
0.00	0.00	0.00	0	H	989	0	0.0	0	0	0	0.0	0.00	0.00	0.00
0.00	0.00	0.00	0	I	1089	0	0.0	0	0	0	0.0	0.00	0.00	0.00
10.87	54.15	23.42	1100	1	0	260	15.6	17	23	140	99.2	13.84	4.26	2.01
10.87	54.15	23.42	1100	2	0	70	16.0	24	25	50	99.7	3.72	1.52	2.18

RUN NUMBER 202
CAT. I.D. FZ

AIR/FUEL RATIOS-- OVER PRI ALL	CAT PRESS DROP (KPA)	BED INLET TEMP (K)	LOC	TEMP (K)	CO PPM	O2 VOL PCT	NO PPM	NOX PPM	UHC PPM	COMB EFF PCT	---EMISSION INDEXES--- ---G/KG FUEL--- CO UHC NO2		
0.60	0.00	0	A	1453	0	0.0	0	0	0	0.0	0.00	0.00	0.00
0.00	0.00	0	B	1578	0	0.0	0	0	0	0.0	0.00	0.00	0.00
0.00	0.00	0	G	967	0	0.0	0	0	0	0.0	0.00	0.00	0.00
0.00	0.00	0	H	889	0	0.0	0	0	0	0.0	0.00	0.00	0.00
0.00	0.00	0	I	967	0	0.0	0	0	0	0.0	0.00	0.00	0.00
13.62	67.85	967	1	0	178	15.8	15	20	82	99.4	11.83	3.11	2.18
13.62	67.85	967	2	0	70	15.5	21	24	40	99.7	4.65	1.51	2.62

RUN NUMBER 203
CAT. I.D. FZ

0.00	0.00	0	A	1426	0	0.0	0	0	0	0.0	0.00	0.00	0.00
0.00	0.00	0	B	1400	0	0.0	0	0	0	0.0	0.00	0.00	0.00
0.00	0.00	0	G	833	0	0.0	0	0	0	0.0	0.00	0.00	0.00
0.00	0.00	0	H	789	0	0.0	0	0	0	0.0	0.00	0.00	0.00
0.00	0.00	0	I	833	0	0.0	0	0	0	0.0	0.00	0.00	0.00
17.48	87.09	833	1	0	110	15.7	12	17	68	99.4	9.35	3.30	2.37
17.48	87.09	833	2	0	70	15.9	20	22	38	99.6	5.95	1.84	3.07

RUN NUMBER 204
CAT. I.D. FZ

0.00	0.00	0	A	1348	0	0.0	0	0	0	0.0	0.00	0.00	0.00
0.00	0.00	0	B	1233	0	0.0	0	0	0	0.0	0.00	0.00	0.00
0.00	0.00	0	G	722	0	0.0	0	0	0	0.0	0.00	0.00	0.00
0.00	0.00	0	H	722	0	0.0	0	0	0	0.0	0.00	0.00	0.00
0.00	0.00	0	I	722	0	0.0	0	0	0	0.0	0.00	0.00	0.00
24.41	121.59	722	1	0	75	16.1	10	14	82	99.2	8.87	5.54	2.72
24.41	121.59	722	2	0	70	16.0	14	17	55	99.4	8.28	3.72	3.30

RUN NUMBER 205
CAT. I.D. FG

0.00	0.00	0	A	1313	0	0.0	0	0	0	0.0	0.00	0.00	0.00
0.00	0.00	0	B	1644	0	0.0	0	0	0	0.0	0.00	0.00	0.00
0.00	0.00	0	G	1244	0	0.0	0	0	0	0.0	0.00	0.00	0.00
0.00	0.00	0	H	1111	0	0.0	0	0	0	0.0	0.00	0.00	0.00
0.00	0.00	C	I	1233	0	0.0	0	0	0	0.0	0.00	0.00	0.00
9.27	46.18	1244	1	0	110	15.0	32	34	130	99.5	5.01	3.38	2.5
9.27	46.18	1244	2	0	30	15.2	31	32	15	99.9	1.36	0.39	2.39

AIR/FUEL --RATIOS-- OVER PRI ALL		CAT PRESS DROP (KPA)	BED INLET TEMP (K)	LOC	TEMP (K)	CO PPH	O ₂ VOL PCT	NO PPH	NOX PPH	UHC PPM	COMB EFF PCT	---EMISSION INDEXES--- -----G/KG FUEL----- CO UHC NO ₂		
RUN NUMBER 206 CAT. I.D. FG														
0.00	0.00	0.00	0	A	1283	0	0.0	0	0	0	0.0	0.00	0.00	0.00
0.00	0.00	0.00	0	B	1644	0	0.0	0	0	0	0.0	0.00	0.00	0.00
0.00	0.00	0.00	0	G	1200	0	0.0	0	0	0	0.0	0.00	0.00	0.00
0.00	0.00	0.00	0	M	1089	0	0.0	0	0	0	0.0	0.00	0.00	0.00
0.00	0.00	0.00	0	I	1200	0	0.0	0	0	0	0.0	0.00	0.00	0.00
9.41	46.90	44.78	1200	1	0	110	13.6	22	28	150	99.4	5.08	3.96	2.12
9.41	46.90	44.78	1200	2	0	40	14.3	29	30	22	99.8	1.85	0.58	2.27
RUN NUMBER 207 CAT. I.D. FG														
0.00	0.00	0.00	0	A	1283	0	0.0	0	0	0	0.0	0.00	0.00	0.00
0.00	0.00	0.00	0	B	1644	0	0.0	0	0	0	0.0	0.00	0.00	0.00
0.00	0.00	0.00	0	G	1089	0	0.0	0	0	0	0.0	0.00	0.00	0.00
0.00	0.00	0.00	0	H	1000	0	0.0	0	0	0	0.0	0.00	0.00	0.00
0.00	0.00	0.00	0	I	1111	0	0.0	0	0	0	0.0	0.00	0.00	0.00
10.36	52.64	43.40	1089	1	0	100	13.6	21	26	160	99.4	5.17	4.73	2.21
10.56	52.64	43.40	1089	2	0	40	13.6	25	28	40	99.8	2.07	1.18	2.38
RUN NUMBER 208 CAT. I.D. FG														
0.00	0.00	0.00	0	A	1278	0	0.0	0	0	0	0.0	0.00	0.00	0.00
0.00	0.00	0.00	0	B	1611	0	0.0	0	0	0	0.0	0.00	0.00	0.00
0.00	0.00	0.00	0	G	956	0	0.0	0	0	0	0.0	0.00	0.00	0.00
0.00	0.00	0.00	0	H	889	0	0.0	0	0	0	0.0	0.00	0.00	0.00
0.00	0.00	0.00	0	I	978	0	0.0	0	0	0	0.0	0.00	0.00	0.00
13.36	66.59	38.58	956	1	0	75	13.6	15	21	110	99.4	4.89	4.10	2.25
13.36	66.59	38.58	956	2	0	50	13.9	23	24	31	99.8	3.26	1.15	2.57
RUN NUMBER 209 CAT. I.D. FG														
0.00	0.00	0.00	0	A	1268	0	0.0	0	0	0	0.0	0.00	0.00	0.00
0.00	0.00	0.00	0	B	1411	0	0.0	0	0	0	0.0	0.00	0.00	0.00
0.00	0.00	0.00	0	G	833	0	0.0	0	0	0	0.0	0.00	0.00	0.00
0.00	0.00	0.00	0	H	811	0	0.0	0	0	0	0.0	0.00	0.00	0.00
0.00	0.00	0.00	0	I	856	0	0.0	0	0	0	0.0	0.00	0.00	0.00
17.15	85.46	34.45	833	1	0	50	14.3	12	19	48	99.6	4.17	2.28	2.60
17.15	85.46	34.45	833	2	0	40	14.2	20	22	21	99.8	3.33	1.00	3.01

AIR/FUEL RATIO PRI ALL	CAT PRESS DROP (KPA)	BED INLET TEMP (K)	LOC	TEMP (K)	CO		O2		NO		NOX		UHC		EMISSION INDEXES		
					PPM	PCT	PPM	PCT	PPM	PCT	PPM	PCT	PPM	PCT	PPM	PCT	CO
0.00	0.00	0	A	1183	0	0.0	0	0.0	0	0	0	0	0	0	0.00	0.00	0.00
0.00	0.00	0	B	1233	0	0.0	0	0.0	0	0	0	0	0	0	0.00	0.00	0.00
0.00	0.00	0	C	711	0	0.0	0	0.0	0	0	0	0	0	0	0.00	0.00	0.00
0.00	0.00	0	H	756	0	0.0	0	0.0	0	0	0	0	0	0	0.00	0.00	0.00
0.00	0.00	0	I	733	0	0.0	0	0.0	0	0	0	0	0	0	0.00	0.00	0.00
23.95	31.00	711	1	0	30	14.8	11	15	60	3.48	3.98	2.86	99.5	3.48	3.98	2.86	
23.95	31.00	711	2	0	30	14.9	16	17	44	3.48	2.92	3.24	99.6	3.48	2.92	3.24	

RUN NUMBER 210 CAT. I.D. FG		RUN NUMBER 211 CAT. I.D. JG	
0.00	0.00	0.00	0.00
0.00	0.00	0.00	0.00
0.00	0.00	0.00	0.00
0.00	0.00	0.00	0.00
0.00	0.00	0.00	0.00
9.50	47.34	27.56	1256
9.50	47.34	27.56	1256

RUN NUMBER 212 CAT. I.D. JG		RUN NUMBER 213 CAT. I.D. JG	
0.00	0.00	0.00	0.00
0.00	0.00	0.00	0.00
0.00	0.00	0.00	0.00
0.00	0.00	0.00	0.00
0.00	0.00	0.00	0.00
10.66	53.13	20.67	1111
10.66	53.13	20.67	1111

RUN NUMBER 210 CAT. I.D. FG		RUN NUMBER 211 CAT. I.D. JG		RUN NUMBER 212 CAT. I.D. JG		RUN NUMBER 213 CAT. I.D. JG	
0.00	0.00	0.00	0.00	0.00	0.00	0.00	0.00
0.00	0.00	0.00	0.00	0.00	0.00	0.00	0.00
0.00	0.00	0.00	0.00	0.00	0.00	0.00	0.00
0.00	0.00	0.00	0.00	0.00	0.00	0.00	0.00
0.00	0.00	0.00	0.00	0.00	0.00	0.00	0.00
13.49	67.21	19.29	978	16	22	100	99.5
13.49	67.21	19.29	978	16	22	100	99.7

AIR/FUEL --RATIOS--		CAT PRESS DROP (KPA)		SEO INLET TEMP (K)		LOC		TEMP (K)		CO		NO		NOX		UHC		---EMISSION INDEXES---		
PMI	ALL							(K)		PPM	PCT	PPM	PCT	PPM	PPM	PPM	PPM	CO	UHC	NO2
0.00	0.00	0.00	0.00	0	0	A	1223	0	0.0	0	0.0	0	0	0	0	0	0.00	0.00	0.00	
0.00	0.00	0.00	0.00	0	0	B	1089	0	0.0	0	0.0	0	0	0	0	0	0.00	0.00	0.00	
0.00	0.00	0.00	0.00	0	0	C	856	0	0.0	0	0.0	0	0	0	0	0	0.00	0.00	0.00	
0.00	0.00	0.00	0.00	0	0	H	889	0	0.0	0	0.0	0	0	0	0	0	0.00	0.00	0.00	
0.00	0.00	0.00	0.00	0	0	I	867	0	0.0	0	0.0	0	0	0	0	0	0.00	0.00	0.00	
17.32	86.27	17.22	856	1	0	1	0	40	15.8	14	20	50	99.6	0.00	0.00	0.00	3.37	2.40	2.76	
17.32	86.27	17.22	856	2	0	2	0	40	15.6	24	27	38	99.7	0.00	0.00	0.00	3.37	1.82	3.73	

AIR/FUEL --RATIOS--		CAT PRESS DROP (KPA)		SEO INLET TEMP (K)		LOC		TEMP (K)		CO		NO		NOX		UHC		---EMISSION INDEXES---		
PMI	ALL							(K)		PPM	PCT	PPM	PCT	PPM	PPM	PPM	PPM	CO	UHC	NO2
0.00	0.00	0.00	0.00	0	0	A	1098	0	0.0	0	0.0	0	0	0	0	0	0.00	0.00	0.00	
0.00	0.00	0.00	0.00	0	0	B	1644	0	0.0	0	0.0	0	0	0	0	0	0.00	0.00	0.00	
0.00	0.00	0.00	0.00	0	0	G	733	0	0.0	0	0.0	0	0	0	0	0	0.00	0.00	0.00	
0.00	0.00	0.00	0.00	0	0	H	811	0	0.0	0	0.0	0	0	0	0	0	0.00	0.00	0.00	
0.00	0.00	0.00	0.00	0	0	I	756	0	0.0	0	0.0	0	0	0	0	0	0.00	0.00	0.00	
24.18	120.45	13.78	733	1	0	1	0	20	16.2	12	17	48	99.6	0.00	0.00	0.00	2.34	3.21	3.27	
24.18	120.45	13.78	733	2	0	2	0	20	15.7	17	22	30	99.7	0.00	0.00	0.00	2.34	2.01	4.23	

AIR/FUEL --RATIOS--		CAT PRESS DROP (KPA)		SEO INLET TEMP (K)		LOC		TEMP (K)		CO		NO		NOX		UHC		---EMISSION INDEXES---		
PMI	ALL							(K)		PPM	PCT	PPM	PCT	PPM	PPM	PPM	PPM	CO	UHC	NO2
0.00	0.00	0.00	0.00	0	0	A	1573	0	0.0	0	0.0	0	0	0	0	0	0.00	0.00	0.00	
0.00	0.00	0.00	0.00	0	0	B	1644	0	0.0	0	0.0	0	0	0	0	0	0.00	0.00	0.00	
0.00	0.00	0.00	0.00	0	0	C	1218	0	0.0	0	0.0	0	0	0	0	0	0.00	0.00	0.00	
0.00	0.00	0.00	0.00	0	0	D	1173	0	0.0	0	0.0	0	0	0	0	0	0.00	0.00	0.00	
0.00	0.00	0.00	0.00	0	0	E	791	0	0.0	0	0.0	0	0	0	0	0	0.00	0.00	0.00	
9.71	48.41	88.19	1256	F	0	F	0	168	15.8	24	26	230	99.1	0.00	0.00	0.00	8.01	6.27	2.33	
9.71	48.41	88.19	1256	G	0	G	1256	70	15.3	28	31	110	99.6	0.00	0.00	0.00	3.33	2.99	2.42	
9.71	48.41	88.19	1256	H	0	H	1144	40	15.0	30	32	70	99.7	0.00	0.00	0.00	1.90	1.90	2.50	
9.71	48.41	88.19	1256	I	0	I	1167	40	15.0	26	29	68	99.7	0.00	0.00	0.00	1.90	1.85	2.27	
9.71	48.41	88.19	1256	J	0	J	1222	30	14.8	27	29	68	99.7	0.00	0.00	0.00	1.43	1.85	2.27	
9.71	48.41	88.19	1256	K	0	K	1144	30	14.6	27	29	58	99.8	0.00	0.00	0.00	1.43	1.58	2.27	
9.71	48.41	88.19	1256	L	0	L	1133	40	14.5	25	27	72	99.7	0.00	0.00	0.00	1.90	1.58	2.27	
9.71	48.41	88.19	1256	M	0	M	1172	30	14.3	26	29	58	99.8	0.00	0.00	0.00	1.43	1.58	2.27	
9.71	48.41	88.19	1256	N	0	N	1076	70	13.9	27	29	100	99.6	0.00	0.00	0.00	1.43	1.58	2.27	

1 14 1

AIR/FUEL ---RATIOS---		CAT PRESS DROP (KPA)	GED INLET TEMP (K)	LOC	TEMP (K)	CO		O2		NO		NOX		UHC		---EMISSION INDEXES---		
PRI	ALL					PPM	PCT	PPM	PCT	PPM	PCT	PPM	PCT	PPM	PCT	CO	UHC	NO2
0.00	0.00	0.00	0	A	1478	0	0.0	0.0	0	0	0	0	0	0	0.00	0.00	0.00	
0.00	0.00	0.00	0	B	1644	0	0.0	0.0	0	0	0	0	0	0	0.00	0.00	0.00	
0.00	0.00	0.00	0	C	1233	0	0.0	0.0	0	0	0	0	0	0	0.00	0.00	0.00	
0.00	0.00	0.00	0	D	1173	0	0.0	0.0	0	0	0	0	0	0	0.00	0.00	0.00	
0.00	0.00	0.00	0	E	498	0	0.0	0.0	0	0	0	0	0	0	0.00	0.00	0.00	
10.47	52.15	79.92	1256	F	0	150	12.5	16	21	16	21	300	98.9	8.79	1.77	2.19		
10.47	52.15	79.92	1256	G	1256	70	12.2	20	26	20	26	90	99.6	2.63	2.27	2.19		
10.47	52.15	79.92	1256	H	1122	50	12.2	23	27	23	27	80	99.7	2.34	2.27	2.19		
10.47	52.15	79.92	1256	I	1167	40	12.2	23	26	23	26	80	99.7	2.34	2.27	2.19		
10.47	52.15	79.92	1256	J	1200	40	12.0	25	27	25	27	70	99.7	2.05	2.27	2.19		
10.47	52.15	79.92	1256	K	1133	30	12.0	24	26	24	26	70	99.7	1.53	2.05	2.19		
10.47	52.15	79.92	1256	L	1133	50	12.2	21	24	21	24	120	99.5	3.51	2.02	2.19		
10.47	52.15	79.92	1256	M	1256	30	11.9	24	27	24	27	85	99.7	2.49	2.27	2.19		
10.47	52.15	79.92	1256	N	1089	70	11.8	25	27	25	27	120	99.5	3.51	2.27	2.19		

AIR/FUEL ---RATIOS---		CAT PRESS DROP (KPA)	GED INLET TEMP (K)	LOC	TEMP (K)	CO		O2		NO		NOX		UHC		---EMISSION INDEXES---		
PRI	ALL					PPM	PCT	PPM	PCT	PPM	PCT	PPM	PCT	PPM	PCT	CO	UHC	NO2
0.00	0.00	0.00	0	A	1668	0	0.0	0.0	0	0	0	0	0	0	0.00	0.00	0.00	
0.00	0.00	0.00	0	B	1450	0	0.0	0.0	0	0	0	0	0	0	0.00	0.00	0.00	
0.00	0.00	0.00	0	C	963	0	0.0	0.0	0	0	0	0	0	0	0.00	0.00	0.00	
0.00	0.00	0.00	0	D	943	0	0.0	0.0	0	0	0	0	0	0	0.00	0.00	0.00	
0.00	0.00	0.00	0	E	473	0	0.0	0.0	0	0	0	0	0	0	0.00	0.00	0.00	
13.75	68.51	71.65	989	F	0	40	18.7	15	20	15	20	52	99.7	1.99	2.20	2.64		
13.75	68.51	71.65	989	G	989	30	18.0	21	24	21	24	20	99.8	0.76	2.64	2.64		
13.75	68.51	71.65	989	H	944	30	17.9	23	28	23	28	16	99.8	0.61	3.08	3.08		
13.75	68.51	71.65	989	I	978	20	17.5	24	27	24	27	12	99.9	0.46	2.97	2.97		
13.75	68.51	71.65	989	J	978	20	17.4	24	28	24	28	9	99.9	0.34	3.06	3.06		
13.75	68.51	71.65	989	K	933	10	17.0	25	28	25	28	6	99.9	0.23	3.08	3.08		
13.75	68.51	71.65	989	L	922	10	17.0	24	26	24	26	6	99.9	0.67	2.86	2.86		
13.75	68.51	71.65	989	M	839	10	16.6	26	29	26	29	4	99.9	0.15	3.19	3.19		
13.75	68.51	71.65	989	N	839	10	16.4	26	28	26	28	5	99.9	0.19	3.08	3.08		

AIR/FUEL RATIOS-- OVER ALL		CAT PRESS DROPS (KPA)	BED INLET TEMP (K)	LOC	TEMP (K)	CO PPH	O2 VOL PCT	NO PPH	NOX PPH	UHC PPM	COMB EFF PCT	EMISSION INDEXES-- G/KG FUEL--		
PRI	ALL		(K)		(K)	PPH	PCT	PPH	PPH	PPM		CO	UHC	NO2
0.00	0.00	0.00	0	A	1608	0	0.0	0	0	0	0.0	0.00	0.00	0.00
0.00	0.00	0.00	0	B	1622	0	0.0	0	0	0	0.0	0.00	0.00	0.00
0.00	0.00	0.00	0	C	828	0	0.0	0	0	0	0.0	0.00	0.00	0.00
0.00	0.00	0.00	0	D	816	0	0.0	0	0	0	0.0	0.00	0.00	0.00
0.00	0.00	0.00	0	E	498	0	0.0	0	0	0	0.0	0.00	0.00	0.00
17.48	87.09	0.00	867	F	0	20	16.5	12	19	44	99.7	1.70	2.13	2.65
17.48	87.09	0.00	867	G	867	20	16.2	16	23	24	99.8	1.70	1.16	3.21
17.48	87.09	0.00	867	H	867	20	16.0	20	25	22	99.8	1.70	1.06	3.49
17.48	87.09	0.00	867	I	867	20	16.0	21	25	30	99.8	1.70	1.45	3.49
17.48	87.09	0.00	867	J	833	20	16.0	20	24	28	99.8	1.70	1.36	3.35
17.48	87.09	0.00	867	K	833	20	16.0	21	24	28	99.8	1.70	1.36	3.35
17.48	87.09	0.00	867	L	811	20	15.9	21	24	24	99.8	1.70	1.16	3.35
17.48	87.09	0.00	867	M	722	10	15.8	21	24	22	99.8	0.85	1.06	3.35
17.48	87.09	0.00	867	N	722	10	15.8	22	25	25	99.8	0.85	1.21	3.49

AIR/FUEL RATIOS-- OVER ALL		CAT PRESS DROPS (KPA)	BED INLET TEMP (K)	LOC	TEMP (K)	CO PPH	O2 VOL PCT	NO PPH	NOX PPH	UHC PPM	COMB EFF PCT	EMISSION INDEXES-- G/KG FUEL--		
PRI	ALL		(K)		(K)	PPH	PCT	PPH	PPH	PPM		CO	UHC	NO2
0.00	0.00	0.00	0	A	1463	0	0.0	0	0	0	0.0	0.00	0.00	0.00
0.00	0.00	0.00	0	B	856	0	0.0	0	0	0	0.0	0.00	0.00	0.00
0.00	0.00	0.00	0	C	703	0	0.0	0	0	0	0.0	0.00	0.00	0.00
0.00	0.00	0.00	0	D	693	0	0.0	0	0	0	0.0	0.00	0.00	0.00
0.00	0.00	0.00	0	E	511	0	0.0	0	0	0	0.0	0.00	0.00	0.00
24.64	122.76	49.60	728	F	0	20	20.0	6	10	72	99.4	2.38	4.91	1.96
24.64	122.76	49.60	728	G	728	20	20.0	7	11	52	99.5	2.38	3.55	2.15
24.64	122.76	49.60	728	H	756	20	20.0	9	12	46	99.6	2.38	3.14	2.35
24.64	122.76	49.60	728	I	756	20	20.0	9	12	43	99.6	2.38	2.93	2.35
24.64	122.76	49.60	728	J	700	20	20.0	10	12	4	99.6	2.38	2.73	2.35
24.64	122.76	49.60	728	K	700	20	19.8	11	12	8	99.6	2.38	2.59	2.55
24.64	122.76	49.60	728	L	689	20	19.8	11	13	38	99.6	2.38	2.59	2.55
24.64	122.76	49.60	728	M	633	20	19.6	12	14	34	99.7	2.38	2.32	2.74
24.64	122.76	49.60	728	N	633	20	19.5	12	14	32	99.7	2.38	2.18	2.74

AIR/FUEL --RATIOS-- OVER PRI ALL		CAT PRESS DROP (KPA)	BED INLET TEMP (K)	LOC	TEMP (K)	CO PPM	O2 VOL PCT	NO PPM	NOX PPM	UHC PPM	COMB EFF PCT	---EMISSION INDEXES--- -----G/KG FUEL----- CO UHC NO2		
9.71	48.41	86.12	1233	M	0	50	13.6	22	27	44	99.8	2.38	1.19	2.11
9.71	48.41	86.12	1233	O	0	140	14.3	19	24	21C	99.2	6.67	5.72	1.88
9.71	48.41	86.12	1233	M	0	90	14.0	21	27	50	99.7	4.29	1.36	2.11
9.71	48.41	86.12	1233	O	0	130	12.0	20	25	230	99.2	6.20	6.27	1.95
9.71	48.41	86.12	1233	N	0	110	11.8	21	27	60	99.7	5.24	1.63	2.11
9.71	48.41	86.12	1233	O	1233	130	13.6	15	20	250	99.1	6.20	6.81	1.56
9.71	48.41	86.12	1233	N	1200	60	12.9	27	30	55	99.7	2.86	1.49	2.35
9.71	48.41	86.12	1256	O	1256	140	12.0	19	25	270	99.2	6.67	5.99	1.95
9.71	48.41	86.12	1256	N	1200	60	11.5	26	33	65	99.6	3.81	2.31	2.52
9.71	48.41	86.12	1244	O	1244	155	13.2	19	25	110	98.9	7.39	8.45	1.95
9.71	48.41	86.12	1244	N	1189	75	12.9	32	35	130	99.5	3.57	3.54	2.74
9.71	48.41	86.12	1267	O	1267	168	11.6	20	25	310	98.9	8.01	8.45	1.95
9.71	48.41	86.12	1267	N	1200	80	12.0	30	33	140	99.5	3.81	3.81	2.58
9.71	48.41	88.88	1244	O	1244	155	13.9	17	22	200	99.2	7.39	5.45	1.72
9.71	48.41	85.43	1244	N	1161	80	13.8	26	30	75	99.7	3.81	2.04	2.35
9.71	48.41	85.43	1233	O	1233	178	12.0	17	21	250	99.1	8.49	6.81	1.64
9.71	48.41	86.19	1233	N	1167	75	12.4	25	27	110	99.6	3.57	2.99	2.11

AIR/FUEL --RATIOS-- OVER PRI ALL		CAT PRESS DROP (KPA)	BED INLET TEMP (K)	LOC	TEMP (K)	CO PPM	O2 VOL PCT	NO PPM	NOX PPM	UHC PPM	COMB EFF PCT	---EMISSION INDEXES--- -----G/KG FUEL----- CO UHC NO2		
9.71	48.41	86.88	1222	O	1222	168	13.7	15	20	300	98.9	8.01	6.17	1.56
9.71	48.41	86.12	1222	N	1161	90	13.4	24	28	90	99.6	4.29	2.45	2.19
9.71	48.41	86.81	1256	O	1256	140	12.5	15	19	290	99.0	6.57	7.90	1.48
9.71	48.41	86.12	1256	M	1233	70	12.4	28	30	85	99.6	3.33	2.31	2.35
9.71	48.41	88.88	1194	O	1194	150	14.0	14	19	330	98.9	7.15	8.99	1.48
9.71	48.41	86.12	1194	M	1159	70	13.2	27	31	65	99.7	3.33	1.77	2.42
9.71	48.41	85.43	1189	O	1189	150	12.5	15	19	281	99.0	7.15	7.63	1.48
9.71	48.41	87.30	1189	N	1144	70	12.4	27	30	50	99.7	3.33	1.36	2.35
9.71	48.41	83.36	1156	O	1156	140	16.2	14	19	300	99.0	6.67	8.17	1.48
9.71	48.41	81.30	1156	O	1122	60	15.3	26	30	110	99.6	3.81	2.99	2.35
9.71	48.41	83.36	1200	O	1200	168	12.7	16	20	280	99.0	8.01	7.63	1.56
9.71	48.41	82.88	1200	N	1144	80	13.0	28	30	95	99.6	3.81	2.58	2.35
9.71	48.41	151.58	1067	O	1067	0	0.0	0	0	0	0.0	0.00	0.00	0.00
9.71	48.41	154.33	1067	N	1094	0	0.0	0	0	0	0.0	0.00	0.00	0.00

AIR/FUEL ---RATIOS---		CAT DROPP (KPA)		BED INLET TEMP (K)		LOC	TEMP (K)	CO PPM	O2 VOL PCT	NO PPM	NOX PPM	UNC PPM	---EMISSION INDEXES---		
PRI	ALL	OVER	ALL	YEMP	(K)		(K)	PPM	PCT	PPM	PPM	PPM	CO	UHC	NO2
9.30	46.34	27.56	27.56	1244	1558	A	1558	0	0.0	0	0	0	0.00	0.00	0.00
9.30	46.34	27.56	27.56	1244	1600	B	1622	0	0.0	0	0	0	0.00	0.00	0.00
9.30	46.34	27.56	27.56	1244	1144	G	1244	0	0.0	0	0	0	0.00	0.00	0.00
9.30	46.34	27.56	27.56	1244	956	H	1033	0	0.0	0	0	0	0.00	0.00	0.00
9.30	46.34	27.56	27.56	1244	1089	I	1044	0	0.0	0	0	0	0.00	0.00	0.00
9.30	46.34	27.56	27.56	1244	978	J	1050	0	0.0	0	0	0	0.00	0.00	0.00
9.30	46.34	27.56	27.56	1244	0	1	0	168	15.6	17	22	220	7.67	5.74	1.65
9.30	46.34	27.56	27.56	1244	0	2	0	30	14.8	35	38	14	1.37	0.36	2.85

AIR/FUEL ---RATIOS---		CAT DROPP (KPA)		BED INLET TEMP (K)		LOC	TEMP (K)	CO PPM	O2 VOL PCT	NO PPM	NOX PPM	UNC PPM	---EMISSION INDEXES---		
PRI	ALL	OVER	ALL	YEMP	(K)		(K)	PPM	PCT	PPM	PPM	PPM	CO	UHC	NO2
10.28	51.20	22.73	22.73	1144	1553	A	1553	0	0.0	0	0	0	0.00	0.00	0.00
10.28	51.20	22.73	22.73	1144	1600	B	1600	0	0.0	0	0	0	0.00	0.00	0.00
10.28	51.20	22.73	22.73	1144	1144	G	1144	0	0.0	0	0	0	0.00	0.00	0.00
10.28	51.20	22.73	22.73	1144	956	H	956	0	0.0	0	0	0	0.00	0.00	0.00
10.28	51.20	22.73	22.73	1144	1089	I	1089	0	0.0	0	0	0	0.00	0.00	0.00
10.28	51.20	22.73	22.73	1144	978	J	978	0	0.0	0	0	0	0.00	0.00	0.00
10.28	51.20	22.73	22.73	1144	0	1	0	140	14.4	14	18	240	7.05	6.91	1.49
10.28	51.20	22.73	22.73	1144	0	2	0	20	14.2	30	32	21	1.00	0.60	2.64

AIR/FUEL ---RATIOS---		CAT DROPP (KPA)		BED INLET TEMP (K)		LOC	TEMP (K)	CO PPM	O2 VOL PCT	NO PPM	NOX PPM	UNC PPM	---EMISSION INDEXES---		
PRI	ALL	OVER	ALL	YEMP	(K)		(K)	PPM	PCT	PPM	PPM	PPM	CO	UHC	NO2
13.00	64.77	17.91	17.91	989	1643	A	1643	0	0.0	0	0	0	0.00	0.00	0.00
13.00	64.77	17.91	17.91	989	1450	B	1450	0	0.0	0	0	0	0.00	0.00	0.00
13.00	64.77	17.91	17.91	989	989	G	989	0	0.0	0	0	0	0.00	0.00	0.00
13.00	64.77	17.91	17.91	989	856	H	856	0	0.0	0	0	0	0.00	0.00	0.00
13.00	64.77	17.91	17.91	989	944	I	944	0	0.0	0	0	0	0.00	0.00	0.00
13.00	64.77	17.91	17.91	989	856	J	856	0	0.0	0	0	0	0.00	0.00	0.00
13.00	64.77	17.91	17.91	989	0	1	0	90	14.4	9	15	175	5.71	6.35	1.56
13.00	64.77	17.91	17.91	989	0	2	0	20	13.8	25	29	30	1.27	1.08	3.02

AIR/FUEL ---RATIOS---		CAT DROPP (KPA)		BED INLET TEMP (K)		LOC	TEMP (K)	CO PPM	O2 VOL PCT	NO PPM	NOX PPM	UNC PPM	---EMISSION INDEXES---		
PRI	ALL	OVER	ALL	YEMP	(K)		(K)	PPM	PCT	PPM	PPM	PPM	CO	UHC	NO2
16.69	83.13	16.53	16.53	844	1638	A	1638	0	0.0	0	0	0	0.00	0.00	0.00
16.69	83.13	16.53	16.53	844	1256	B	1256	0	0.0	0	0	0	0.00	0.00	0.00
16.69	83.13	16.53	16.53	844	844	G	844	0	0.0	0	0	0	0.00	0.00	0.00
16.69	83.13	16.53	16.53	844	822	H	822	0	0.0	0	0	0	0.00	0.00	0.00
16.69	83.13	16.53	16.53	844	811	I	811	0	0.0	0	0	0	0.00	0.00	0.00
16.69	83.13	16.53	16.53	844	750	J	750	0	0.0	0	0	0	0.00	0.00	0.00
16.69	83.13	16.53	16.53	844	0	1	0	40	14.6	12	16	42	3.24	1.94	2.13
16.69	83.13	16.53	16.53	844	0	2	0	20	14.4	22	25	4	1.62	0.18	3.33

AIR/FUEL --RATIOS-- PRI ALL		CAT PRESS DRGP (KPA)	SED INLET TEMP (K)	LOC	TEMP (K)	CO PPM	O2 VOL PCT	NO PPM	NOX PPM	UHC PPM	COMB EFF PCT	---EMISSION INDEXES---		
												CO	G/KG FUEL	UHC NO2
23.30	116.07	13.78	744	A	1588	0	0.0	0	0	0	0.0	0.00	0.00	0.00
23.30	116.07	13.78	744	S	1133	0	0.0	0	0	0	0.0	0.00	0.00	0.00
23.30	116.07	13.78	744	G	744	0	0.0	0	0	0	0.0	0.00	0.00	0.00
23.30	116.07	13.78	744	H	800	0	0.0	0	0	0	0.0	0.00	0.00	0.00
23.30	116.07	13.78	744	I	722	0	0.0	0	0	0	0.0	0.00	0.00	0.00
23.30	116.07	13.78	744	J	722	0	0.0	0	0	0	0.0	0.00	0.00	0.00
23.30	116.07	13.78	744	1	0	20	15.0	12	17	23	99.7	2.26	1.48	3.15
23.30	116.07	13.78	744	2	0	10	14.8	18	22	4	99.9	1.13	0.25	4.08
9.30	46.34	27.56	1200	1	0	178	14.6	12	18	850	97.5	8.13	22.20	1.35
9.30	46.34	28.24	1200	2	0	10	13.3	33	36	50	99.8	0.45	1.30	2.70
9.45	47.09	26.87	1200	1	0	100	14.2	14	20	360	98.9	4.64	9.55	1.52
9.45	47.09	27.56	1200	2	0	10	13.9	35	37	13	99.9	0.46	0.34	2.82
9.81	48.86	29.62	1156	1	0	155	14.4	9	11	280	99.0	7.46	7.70	0.87
9.81	48.86	27.56	1156	2	0	10	13.4	25	27	14	99.9	0.48	0.38	2.13
9.81	48.86	28.93	1189	1	0	150	15.0	9	10	230	99.1	7.22	6.32	0.79
9.81	48.86	28.24	1189	2	0	50	14.2	22	24	4	99.9	2.40	0.11	1.89
9.71	48.41	26.18	1200	1	0	140	15.9	18	20	150	99.4	6.67	4.08	1.56
9.71	48.41	26.87	1200	2	0	20	13.4	29	32	10	99.9	0.95	0.27	2.50
9.71	48.41	26.18	1222	1	0	150	14.4	20	22	120	99.5	7.15	3.27	1.72
9.71	48.41	27.56	1222	2	0	20	14.6	34	36	2	99.9	0.95	0.05	2.82

AIR/FUEL RATIO OVER ALL	CAT PRESS INLET TEMP (KPa)	BED INLET TEMP (K)	LOC	TEMP (K)	CO PPM	O2 VOL PCT	NO PPM	MOX PPM	UHC PPM	COMB EFF PCT	EMISSION INDEXES G/KG FUEL		
											CO	UHC	NO2
RUN NUMBER 233 CAT. I.D. OF													
9.71 48.41	31.69	1189	1	0	140	17.2	7	6	160	99.3	6.67	4.90	0.52
9.71 48.41	32.38	1189	2	0	30	16.3	9	10	26	99.8	1.43	0.70	0.78
RUN NUMBER 234 CAT. I.D. OF													
9.71 48.41	30.31	1189	1	0	140	17.5	9	10	175	99.3	6.67	4.77	0.78
9.71 48.41	31.69	1189	2	0	30	16.8	11	12	6	99.5	1.43	0.21	0.94
RUN NUMBER 235 CAT. I.D. OF													
9.71 48.41	29.62	1178	1	0	130	17.5	11	12	170	99.3	6.20	4.63	0.94
9.71 48.41	30.31	1178	2	0	10	16.5	12	13	6	99.9	0.47	0.21	1.01
RUN NUMBER 236 CAT. I.D. OF													
9.71 48.41	27.96	1133	1	0	140	17.8	7	6	220	99.2	6.67	5.99	0.62
9.71 48.41	28.24	1133	2	0	10	14.5	6	7	26	99.9	0.47	0.70	0.54
RUN NUMBER 238 CAT. I.D. OF													
10.74 49.38	28.93	1211	1	0	150	14.2	20	28	220	99.2	7.20	6.11	2.23
10.74 49.38	27.96	1211	2	0	60	15.7	24	27	75	99.7	3.89	2.08	2.15
RUN NUMBER 239 CAT. I.D. OF													
12.05 55.62	25.49	1133	1	0	120	14.2	15	24	175	99.3	6.53	5.44	2.14
12.05 55.62	26.18	1133	2	0	70	13.9	19	25	60	99.6	3.81	2.49	2.23
RUN NUMBER 246 CAT. I.D. OF													
9.16 45.62	30.31	1278	1	0	40	14.4	28	36	20	99.9	1.60	0.51	2.66
9.16 45.62	31.00	1278	2	0	20	14.5	33	38	6	99.9	0.90	0.20	2.81
RUN NUMBER 247 CAT. I.D. OF													
10.28 51.20	27.96	1133	1	0	40	14.6	22	28	42	99.8	2.01	1.20	2.31
10.28 51.20	28.24	1133	2	0	2	14.9	25	31	30	99.6	1.00	0.86	2.56

AIR/FUEL --RATIOS--		CAT		BED		LOC		TEMP		CO		O2		NO		NOX		UHC		---EMISSION INDEXES---		
PRI	ALL	PRESS DROP (KPA)	INLET TEMP (K)	INLET TEMP (K)	(K)	(K)	PPM	PCT	PPM	PPM	PPM	PPM	PPM	PPM	PPM	PPM	PPM	PPM	PPM	CO	UHC	NO2
13.00	64.77	24.11	1022	1022	1	0	30	15.4	20	30	44	99.7	1.90	1.59	3.12					1.90	1.59	3.12
13.00	64.77	24.80	1022	1022	2	0	30	15.0	24	32	60	99.7	1.90	2.17	3.33					1.90	2.17	3.33
RUN NUMBER 248 CAT. I.D. FE																						
16.69	83.13	20.67	922	922	1	0	20	15.2	22	34	30	99.8	1.62	1.39	4.53					1.62	1.39	4.53
16.69	83.13	20.57	922	922	2	0	10	15.4	21	32	75	99.8	0.81	1.20	4.27					0.81	1.20	4.27
RUN NUMBER 249 CAT. I.D. FE																						
23.30	116.07	17.51	778	778	1	0	10	15.9	17	25	34	99.1	1.13	2.19	4.64					1.13	2.19	4.64
23.30	116.07	18.53	778	778	2	0	0	15.4	17	26	30	0.0	0.00	1.93	4.82					0.00	1.93	4.82
RUN NUMBER 250 CAT. I.D. FE																						
9.24	46.04	41.34	0	0	1	0	90	13.4	33	37	35	99.8	4.08	0.90	2.76					4.08	0.90	2.76
9.24	46.04	42.02	0	0	2	0	30	13.7	30	33	10	99.9	1.36	0.25	2.46					1.36	0.25	2.46
RUN NUMBER 251 CAT. I.D. PC																						
10.37	51.67	39.96	0	0	1	0	50	14.4	20	23	17	99.8	2.54	0.47	2.08					2.54	0.47	2.08
10.37	51.67	40.65	0	0	2	0	20	14.9	22	24	10	99.9	1.01	0.29	2.00					1.01	0.29	2.00
RUN NUMBER 252 CAT. I.D. PC																						
13.12	65.36	34.45	0	0	1	0	50	15.6	15	20	18	75.0	3.20	0.65	2.10					3.20	0.65	2.10
13.12	65.36	33.76	0	0	2	0	30	15.5	17	20	16	99.8	1.92	0.58	2.10					1.92	0.58	2.10
RUN NUMBER 253 CAT. I.D. PC																						
16.84	83.89	31.00	0	0	1	0	30	15.7	17	25	22	99.8	2.45	1.03	3.36					2.45	1.03	3.36
16.84	83.89	31.00	0	0	2	0	20	16.0	18	25	18	99.8	1.63	0.84	3.36					1.63	0.84	3.36
RUN NUMBER 254 CAT. I.D. PC																						
23.51	117.13	27.56	0	0	1	0	10	16.3	13	20	28	99.7	1.14	1.82	3.74					1.14	1.82	3.74
23.51	117.13	27.56	0	0	2	0	10	16.2	13	20	24	99.8	1.14	1.56	3.74					1.14	1.56	3.74
RUN NUMBER 255 CAT. I.D. PC																						

REFERENCES

1. Environmental Protection Agency Regulations on Control of Air Pollution from Aircraft and Aircraft Engines, 40CFR87-38FR 19088, July 17, 1973; 38 FR 34734, December 18, 1973; 38 FR 35000, December 31, 1973.
2. Jones, R. E., "Advanced Technology for Reducing Aircraft Engine Pollution", ASME Paper No. 73-WA/Aero-2.
3. Blazowski, W. S. and Bresowar, G. E., "Preliminary Study of the Catalytic Combustor Concept as Applied to Aircraft Gas Turbines", AFAPL-TR-74-32, May, 1974.
4. Anderson, D. N., "Preliminary Results from Screening Tests of Commercial Catalysts with Potential Use in Gas Turbine Combustors - Part II. Combustion Test Rig Evaluation", NASA TMX-73412, May, 1976.
5. Shaw, H., "Fuel Modification for Abatement of Aircraft Turbine Engine Oxides of Nitrogen Emissions", U. S. Dept. Commer., Nat'l. Tech. Info. Serv. AD #752,581 (October, 1972), 122 p. (Also AFAPL-TR-72-80.)
6. Weast, R. C., Handbook of Chemistry and Physics, 55th ed., CRC Press (1974).
7. Fleet, B. and Von Storp, H., "Analytical Evaluation of a Cyanide-Ion Selective Membrane Electrode Under Flow-Stream Conditions", Anal. Chem. Vol. 43, October, 1971, pp. 1575-1581.
8. Grenleski, S. and Falk, F., "An Investigation of Catalytic Ignition of JP-5/Air Mixtures", SAE Paper 918C, October, 1964.
9. Siminski, V. J., "Research on Methods of Improving the Combustion Characteristics of Liquid Hydrocarbon Fuels", AFAPL-TR-72-74.
10. Margolis, L., "Catalytic Oxidation of Hydrocarbons", Advances in Catalysis, Vol. 14, 429-501, 1963.
11. Hawthorne, R. D., "Afterburner Catalysts - Effects of Heat and Mass Transfer Between Gas and Catalyst Surface", AIChE Symposium Series No. 137, 1974, pp. 428-438.
12. Gordon, S., and McBride, B., NASA-Lewis Research Center, Chemical Equilibrium Program, Nov. 6, 1970.
13. Siminski, V. J. and Cerkancwicz, A., "Compilation of Literature and Patents Relating to Catalytic Combustion Modeling and Process Design Studies", October, 1975, Exxon Research and Engineering Company, Linden, New Jersey.

REFERENCES (CONT'D.)

14. Siminski, V. J., "Catalytic Combustion of Jet-A in a Gas Turbine Burner", Project 773310, September, 1973, Exxon Research and Engineering Company, Linden, New Jersey.
15. Bernstein, L. S., Lang, R. J., Lunt, R. S., and Musser, G. D., "Nickel-Copper Alloy NO_x Reduction Catalysts for Dual Catalyst Systems", SAE Paper No. 730567, May, 1973.
16. Doelp, L., Koester, D. W., and Mitchell, M. M. Jr., "Oxidative Automotive Emission Control Catalysts. Selected Factors Affecting Catalyst Activity", Adv. Chem. Ser., Vol. 143, 1974, pp. 133-146.
17. Cerkanowicz, A. E., Cole, R. B., and Stevens, J. G., "Catalytic Combustion Modeling; Comparisons with Experimental Data", ASME Paper No. 77-GT-85.
18. Hill, T. L., "Introduction to Statistical Thermodynamics", Addison-Wesley, Reading, Massachusetts, 1960, pp. 134.
19. Retallick, W., Private Communications (Oxy-Catalyst, Inc., West Chester, Pennsylvania).
20. Shaw, H., "The Effects of Water, Pressure and Equivalence Ratio on NO Production in Gas Turbines", Transactions of the ASME, Journal of Engineering for Power, Vol. 96, Series A, No. 3, July, 1974, pp. 240-246.
21. Blazowski, W. S. and Henderson, R. E., "Aircraft Exhaust Pollution and Its Effect on the U. S. Air Force", AFAPL-TR-74-64.
22. Zeldovich, J., "The Oxidation of Nitrogen in Combustion and Explosives", Acta Physicochimica U.S.S.R., Vol. 21, 1946, p. 577.
23. Fenimore, C. P., "Formation of Nitric Oxide in Premixed Hydrocarbon Flames", 13th International Symposium on Combustion, Salt Lake City, 1970.
24. Gott, P. G. and Bastress, E. K., "Performance Criteria for Aircraft Turbine Engine Emission Control Methods", Presented at the 69th Annual Meeting of the Air Pollution Control Association, Portland, Oregon, June 27-July 1, 1976, Paper No. 76-8.3.
25. Roberts, R., Fiorentino, A. J., and Diehl, L., "The Pollution Reduction Technology Program for Can Annular Combustor Engines - Description and Results", Presented at the 12th Propulsion Conference, July 26-29, 1976, AIAA Paper No. 76-761.

REFERENCES (CONT'D.)

26. Sawyer, R. F., et al., "The Formation of Nitrogen Oxides from Fuel Nitrogen", EPRI 223-1, Final Report, March, 1976.
27. Kalfadelis, C. D. and Shaw, H., "A Pilot Plant Study of Jet Fuel Production from Coal and Shale-Derived Oils", Presented at the 82nd AIChE National Meeting, Atlantic City, New Jersey, September, 1976.
28. Longwell, J. P., private communication.
29. Martin, G. B., "NO_x Considerations in Alternate Fuel Combustion" Presented at Environmental Aspects of Fuel Conversion Processes Symposium sponsored by EPA at Hollywood, Florida, December 14-18, 1975.
30. Rosfjord, T., private communication.